DISSERTATION

OPTIMAL STOCHASTIC SCHEDULING OF RESTORATION OF INFRASTRUCTURE SYSTEMS FROM HAZARDS: AN APPROXIMATE DYNAMIC PROGRAMMING APPROACH

Submitted by

Saeed Nozhati

Department of Civil and Environmental Engineering

In partial fulfillment of the requirements

For the Degree of Doctor of Philosophy

Colorado State University

Fort Collins, Colorado

Summer 2019

Doctoral Committee:

Advisor: Bruce R. Ellingwood
Co-advisor: Hussam N. Mahmoud

Edwin K.P. Chong
John W. van de Lindt

ABSTRACT

OPTIMAL STOCHASTIC SCHEDULING OF RESTORATION OF INFRASTRUCTURE SYSTEMS FROM HAZARDS: AN APPROXIMATE DYNAMIC PROGRAMMING APPROACH

This dissertation introduces approximate dynamic programming (ADP) techniques to identify near-optimal recovery strategies following extreme natural hazards. The proposed techniques are intended to support policymakers, community stakeholders, and public or private entities to manage the restoration of critical infrastructure of a community following disasters. The computation of optimal scheduling schemes in this study employs the rollout algorithm, which provides an effective computational tool for optimization problems dealing with real-world large-scale networks and communities. The Markov decision process (MDP)-based optimization approach incorporates different sources of uncertainties to compute the restoration policies. The fusion of the proposed rollout method with metaheuristic algorithms and optimal learning techniques to overcome the computational intractability of large-scale, multi-state communities is probed in detail. Different risk attitudes of policymakers, which include risk-neutral and risk-averse attitudes in community recovery management, are taken into account.

The context for the proposed framework is provided by objectives related to minimizing food-insecurity issues and impacts within a small community in California following an extreme earthquake. Probabilistic food security metrics, including food *availability*, *accessibility*, and *affordability*, are defined and quantified to provide risk-informed decision support to policymakers in the aftermath of an extreme natural hazard. The proposed ADP-based approach

then is applied to identify practical policy interventions to hasten the recovery of food systems and reduce the adverse impacts of food insecurity on a community.

All proposed methods in this study are applied on a testbed community modeled after Gilroy, California, United States, which is impacted by earthquakes on the San Andreas Fault. Different infrastructure systems, along with their spatial distributions, are modeled as part of the evaluation of the restoration of food security within that community. The methods introduced are completely independent of the initial condition of a community following disasters and type of community (network) simulation. They treat the built environment like a black box, which means the simulation and consideration of any arbitrary network and/or sector of a community do not affect the applicability and quality of the framework. Therefore, the proposed methodologies are believed to be adaptable to any infrastructure systems, hazards, and policymakers' preferences.

ACKNOWLEDGEMENTS

This work was funded by the National Science Foundation under CRISP Collaborative Research Grant CMMI-1638284. This support is gratefully acknowledged. Moreover, I was honored to be a recipient of the 2017-2018 Sally & Thomas Keefer Award and 2016-2017 Anthony P. Chrest Memorial Award and would like to take this opportunity to thank the selection committee for choosing me for these prestigious awards.

I am sincerely grateful to my advisor, Professor Bruce R. Ellingwood for his guidance – for giving me the freedom and support to explore and develop my research. His patience, guidance, instruction intellectual challenges, care, and enthusiasm have made the research process continuously rewarding. He is truly an inspiration and I am honored to be his student.

Thank you to Professor Edwin Chong for so generously advising me on various aspects of my research and for being a consummate researcher. I have been extremely fortunate to study under his tutelage.

Thank you to Dr. Hussam Mahmoud who has provided support and helped me to shape my ambitions. Collaborating on projects with Dr. Mahmoud has been a pleasure.

Thank you to Professor John van de Lindt for supporting my desire to join the CSU civil engineering program and for advocating on my behalf as I pursued my doctorate.

Although the way to this Ph.D. has been lightened by countless people, I would like to express my gratitude to my friends Hassan Masoomi, Yugandhar Sarkale, and Pamela Orin. Hassan (now Dr. Masoomi!) has been a steadfast friend and bright colleague ever since I started my college life. I look forward to our continued friendship. My conversations with Pam and Yugandhar on life have been the source of new visions, meditation, and continuous enjoyment!

My acknowledgments cannot possibly be complete without thanks to my family, especially Baba-Joon, Maman-Joon, Rahil, Masoud, and Setareh for their constant encouragement and guidance which they have generously bestowed on me throughout my life.

DEDICATION

I dedicate this dissertation to my mother and father for their endless support.

TABLE OF CONTENTS

LIST OF TABLES

LIST OF FIGURES

CHAPTER 1: INTRODUCTION

1.1. Community Resilience

Household well-being relies on interdependent critical infrastructure systems (ICISs) such as transportation, energy, water, and food distribution. While ICISs shape the ability of our communities to meet everyday household needs, the level to which these needs are met can be quite variable across households through time and space and there may well be acute periods of disruption due to events such as natural hazards.

A disruption to ICISs, whether the result of a natural catastrophe (e.g., Hurricane Maria in 2017 or the Japan Earthquake and Tsunami of 2011), a terrorist attack (e.g., the 2001 World Trade Center Attack), or an accident (e.g., the 2003 North America Blackout), could potentially lead to extensive losses of functionality that influence not only the infrastructure but also all the entities depending on them. Therefore, an interdependent network is more vulnerable to disasters with large geographic footprints. In this regard, the functionality of ICISs has recently gained attention with a particular emphasis on analyzing their risk and improving their resilience.

The term resilience has frequently been used in the research literature because of the role in mitigating the disruption of ICISs. The word resilience derives from the Latin word “resiliere” which means “to bounce back”.

Hosseini et al. (2016) studied the definition of resilience throughout studies published from 2000 to 2015 in different domains. They categorized the definitions of resilience into four domains: organizational (e.g., Vogus and Sutcliffe, 2007), social (e.g., Keck and Sakdapolrak, 2013; Pfefferbaum et al., 2008), economic (e.g., Rose and Liao, 2005; Martin, 2011), and engineering (e.g., Bruneau et al., 2003; Youn et al., 2011). They also classified resilience assessment methodologies into qualitative (e.g., Kahan et al., 2009; Vlacheas et al., 2013) and quantitative (e.g., Ayyub, 2014; Bruneau et al., 2003; Chang and Shinozuka, 2004; Henry and Ramirez-Marquez, 2012) methodologies, each of which was classified into several sub-categories.

In the realm of ICISs, the concept of system resilience has been advanced over the last few years. A resilient community has been described as a community that has prepared for potential hazards to be able to resist, absorb, and adjust to changing conditions as well as to return to a level of normalcy within a reasonable time following a disaster (Alexander, 2013; Bruneau et al., 2003; PPD-21, 2013).

Bruneau et al. (2003) proposed a community resilience framework and a quantitative index, known as the resilience triangle model. They recommended four attributes of resilience: (i) Robustness: the strength or ability of a system to resist any disruptive event or accident to prevent losing functionality, (ii) Redundancy: the extent of substitutable components or systems that are capable of satisfying functionality requirements in the presence of disruption, (iii) Resourcefulness: the ability to recognize and manage problems in a case of emergency or disaster by defining priorities and allocating material and human resources to achieve predefined goals, and (iv) Rapidity: the speed or rate of system restoration to meet an acceptable level of functionality in the aftermath of a disaster.

A probabilistic seismic approach to measure community resilience by analyzing original performance loss in a system and the recovery period was introduced by Chang and Shinozuka (2004). They defined standards with respect to four dimensions of community resilience of the Bruneau et al. (2003) model: technical, organizational, social, and economic dimensions. Chang and Shinozuka (2004) demonstrated their proposed measurement framework by evaluating the resilience of the water distribution system in Memphis, Tennessee, for two retrofit plans.

Another conceptual framework of community resilience and recovery under disasters was introduced by Miles and Chang (2003, 2004, and 2006). The relationships among a community's households, businesses, critical infrastructure, and neighborhoods are the cornerstone of their proposed framework. Five factors - time, space, agents' attributes, interactions, and policy - were suggested to establish the model. Spatiotemporal effects describe the importance of the topology and evolution of the community with the passage of time.

Lin et al. (2016) proposed a disaggregation framework by means of an optimization problem. The study explored design performance purposes for single structures that enabled a community-level goal to be achieved. The framework motivates an advance from current performance-based design (PBD) methods for individual facilities and sites (e.g., Hemmati and Mahmoud, 2019; Asteris et al. 2018; Karami Mohammadi and Hemmati, 2013; Khayat at al., 2016; Karimi Askarani and Pakbaz, 2016; Khaloo et al. 2016a, 2016b; Seyyed Alangi et al. 2018) to a community-level performance-based design (e.g., Masoomi and van de Lindt, 2018a, 2018b, 2019; Masoomi, 2018; Masoomi et al. 2018; Nozhati et al. 2019a). The resilience assessment can also play a significant role in monitoring essential factors at petroleum facilities (Karimi Askarani et al. 2018).

Resilience-based design (RBD) was suggested by Cimellaro et al. (2015) as a continuation of PBD. RBD reflects the interdependencies of all structures and infrastructure systems within a community to evaluate a community-level resilience metric. Mieler et al. (2015) also proposed a conceptual framework that is consistent with broad, community-level goals instead of the consideration of the structures (i.e., components) individually.

Lin and Wang (2017) proposed a building portfolio recovery model (BPRM) to predict the stochastic recovery process of building portfolios in the aftermath of a hazard. The BPRM models recovery of each building-level functionalities as a discrete state, continuous time Markov Chain, while the portfolio-level recovery can be computed by aggregating spatiotemporally the building-level recovery processes.

Masoomi et al. (2018) proposed a population outmigration framework to estimate the number of displaced people after a tornado event as a metric that is helpful to administrators for planning an emergency response after a disruption. The representation examines the interdependence of residential buildings, the electrical power network, the potable water network, and business sectors to study the post-hazard population outmigration.

A comprehensive review of the effects of natural hazards on the built environment, social and economic systems is provided by Koliou et al. (2018).

In this study, all methodologies include the spatiotemporal interactions between the components and networks within a community in addressing the four properties of the resilience assessment identified by Bruneau et al (2003) (i.e., robustness, redundancy, resourcefulness, and rapidity). However, the decision-making methodologies, introduced in the next section, emphasize particularly resourcefulness and rapidity.

1.2. Risk-Informed Decision-Making Framework

The absence of a comprehensive risk-informed decision-making framework at the community level presents a challenge to post-disaster risk management. Network-level decision-making algorithms must address large-scale optimization problems that pose computational challenges. The complexity of these optimization problems increases when various sources of uncertainty are considered. During the past decade, researchers have proposed different methods to extend decision formulations regarding risk mitigation, response, and recovery from individual facilities or networks to a community.

Ji et al., (2016) suggested scheduling repair of a network based on the importance values of its components. Components with larger importance values have higher priority to be repaired. For example, the restoration of electrical transmission substations, transmission lines, critical facilities, and the distribution components is a restoration plan that can return electricity to the greatest number of clients. Some researchers found more efficient factors to prioritize damaged components. For example, the largest ratio of the functionality increase to a damaged component required repair time (Nojima and Kameda, 1992), components degree (Sun and Zeng, 2017), or betweenness (Ulusan and Ergun, 2018). Different heuristic algorithms have also been applied to solve complicated restoration scheduling problems, such as genetic algorithms (Ozdamar, 1999; Xu et al., 2007), simulated annealing algorithms (Boctor, 1996; Bouleimen and Lecocq, 2003), and binary particle swarm optimization (Zhang and Wang, 2017). Some researchers have assumed that the operation model of the ICISs is linear, and utilized the mathematical programming approaches like a mixed integer linear programming (MILP) model (Ouyang and Fang, 2017).

The recovery process of ICISs includes multiple phases in which decisions must be made at specific stages to satisfy the policymakers' preferences. With this in mind, many researchers in various fields have utilized powerful sequential decision methodologies, such as dynamic programming (DP) and Markov decision processes (MDP). In the realm of civil infrastructure management, several studies have used MDPs to optimize the repair and maintenance of infrastructure (Ellis et. al, 1995; Frangopol et. al, 2004; Corotis et. al, 2005). Madanat (1993) introduced Latent MDP (LMDP) at the component level to recognize the random errors in the measurements of the conditions of infrastructure. Subsequently, Smilowitz and Madanat (2000) extended LMDP to system-level maintenance scheduling, where they considered condition state and budgetary constraints. Medury and Madanat (2013) used Approximate Dynamic Programming (ADP) with MDP for pavement management systems. Papakonstantinou and Shinozuka (2014) reviewed the literature on optimal maintenance planning using Dynamic Programming (DP) and MDPs. Meidani and Ghanem (2015) studied the problem of maintenance of pavement using DP and MDP with random transitions.

This dissertation introduces various scheduling formulations based on approximate dynamic programming (ADP) to identify near-optimal recovery actions following extreme natural hazards. This approach can support rational risk-informed decision making at the community level.

The proposed methodology has the following key properties (hereinafter referred to as "paramount properties"):

i. It balances the reluctance for low immediate reward with the desire of high future rewards (also referred as “non-myopic” or look-ahead property);
ii. It considers different sources of uncertainties;
iii. It makes decisions periodically to not only take advantage of information that becomes available when recovery actions are in progress but also to adapt to disturbances over the recovery process;
iv. It manages a large decision-making space, which is typical for the problems at the community level;

v. It can handle multi-objective decisions, which are common in real-world domains, especially in community resilience applications. The interconnectedness among networks and probable conflicts among competing objectives complicate the decision-making procedure;

vi. It considers different constraints, such as time constraints, limited budget and repair crew, and current regional entities' policies;

vii. It can address different risk behaviors of policymakers from risk-neutral to risk-averse behaviors.

1.3. FOOD SECURITY

The food and agriculture sector has been identified as one of sixteen critical infrastructure sectors by Presidential Policy Directive 21 (PPD, 2013). For households at all income levels, and especially for those that are food-insecure, food access can be threatened by natural hazards. Extreme natural hazards can disrupt critical infrastructure systems, such as transportation or electrical power systems, damaging roads and bridges critical for maintaining food supply chains and electrical transmission lines needed for providing electricity for food refrigeration. Maintaining food security in the aftermath of a natural hazard challenges a community's resilience, recovery, and social well-being. The functionality of food retailers in terms of availability and accessibility must be returned to pre-disaster levels quickly and predictably in the aftermath of an extreme environmental event. Their ability to play this role in maintaining the security of the food chain depends on the vulnerability of utility networks (e.g., power, potable water, and wastewater), transportation systems, and building structures within the community to severe natural hazards. Problems in food access and affordability are greatly exacerbated following disasters when food distribution networks are compromised due to damage to facilities and damage and disruption to the critical infrastructure systems upon which they depend. For example, disaster-related food programs served 2.4 million households and distributed $928 million in benefits to households impacted by Hurricanes Katrina, Rita, and Wilma in 2005 (Food Research and Action Center, 2017). In 2008, similar programs issued $447 million in benefits to 1.2 million households impacted by wildfires in California and hurricanes making landfall on the Gulf Coast (United States Department of Agriculture, 2010). The human and economic losses and social disruption caused by failure of infrastructure systems are disproportionately high in relation to the actual physical damage to such systems, and the potential exists for even larger losses in the future, given that population and economic development in hazard-prone coastal areas of the United States has increased dramatically in the past two decades while investments in resilient infrastructure systems are lagging.

This study introduces a methodology to consider how the interconnectedness among civil infrastructure systems impacts food-security of urban inhabitants. To this end, different infrastructure systems along with their spatial distribution are modeled to evaluate the restoration of food security within a community. Food security metrics, including food *availability*, *accessibility*, and *affordability*, are defined in Chapter 6 and quantified to provide risk-informed decision support to policymakers in the aftermath of an extreme natural hazard. A decision-making framework based on ADP techniques is employed to provide the optimal strategies to identify practical policy interventions to hasten the recovery of food systems and reduce the adverse impacts of food insecurity on a community.

1.4. ORGANIZATION

This dissertation addresses several important issues related to risk and resilience assessment and introduces several methodologies for decision-making under uncertainty to address these issues. Chapter 2 introduce a testbed community, which provides a context for the numerical algorithms and models that are used for the decision problems considered in this dissertation. Chapters 3 and 4 describe decision-making methodologies for post-disaster community recovery management, both deterministically and stochastically. Chapter 5 introduces several methods to address large-scale communities, where the number of decision variables becomes extremely large. Chapter 6 deals with the definition of food security metrics and utilizes the methods, presented in Chapters 3-5 and the entire community, presented in Chapter 2.

Chapter 2 describes the different sectors and networks of the testbed community modeled and utilized in this dissertation, discussing the topology and structure of each layer and explaining how the dependencies and interdependencies within and between networks are modeled. The electrical power network, potable water network, highway bridges, main food retailers, and household units are modeled. The future chapters use the testbed community introduced in this chapter.

Chapter 3 introduces a sequential discrete optimization approach as a decision-making framework at the community level by starting from first principles of dynamic programming. The needs for dynamic optimization algorithms and approximate dynamic programming methods to address the community resilience problem are explained in this chapter.

Chapter 4 discusses a stochastic scheduling formulation based on a Markov Decision Process. The MDP-based optimization approach proposed in this chapter incorporates different sources of uncertainties to determine optimal restoration policies. The computation of optimal scheduling schemes using the method provides an effective computational tool for problems that are confronted by real-world communities. This chapter also studies the applicability of the method to address different risk attitudes of policymakers, which include risk-neutral and risk-averse attitudes in community recovery management.

Chapter 5 offers several methods to enrich the methodologies, introduced in Chapters 3 and 4 and to enhance their computational efficiencies. This chapter mainly discusses the applicability of meta-heuristic, optimal learning, and linear belief models in large-scale problems.

Chapter 6 presents the food security issues in the aftermath of an extreme natural hazard. This chapter utilizes the proposed methods in the previous chapters to compute the near-optimal recovery decisions for a dysfunctional community, with an emphasis on food security issues. Food security metrics based on food availability, accessibility, and affordability are defined and quantified probabilistically either at the grid level or at the community level.

Chapter 7 summarizes the important contributions, limitations and future extensions of this research.

Lastly, every chapter is presented with a quotation to join the dissertation with a touch of literature, of philosophy and of joyfulness.

CHAPTER 2: TESTBED COMMUNITY MODELING

—*The greatest enemy of knowledge is not ignorance, it is the illusion of knowledge*."
Stephen Hawking

2.1. Introduction

Household well-being depends on the services provided by critical infrastructure systems (ICISs) such as transportation, energy, water, and food distribution, which are interdependent in their functioning. While ICISs shape the ability of communities to meet everyday household needs, the level to which these needs are met can be quite variable across households through time and space and there may well be acute periods of service disruption due to events such as natural disasters. Unexpected damages due to unpredictable cascading failures can become regional disasters when the interdependencies in infrastructure systems are not well-understood (Zimmerman et al., 2016). Hence, the performance of such systems has recently garnered attention in resilience research, with an emphasis on improving the resilience of communities in the aftermath of severe hazards (McAllister, 2013). Predictable functioning of these systems is a cornerstone of a resilient community, one that is able to resist, absorb, and adapt to variable circumstances and *bounce back* to its initial state, or *bounce forward* to a more robust state following a disturbance (Vale, 2014).

The ICISs within a community are a system of systems (SoS) with highly coupled networks. Large-scale cascading effects can be potentially triggered by a malfunction of one or few components. Thus, the assessment of risk and resilience at the community level must consider the topology of the community and interdependencies among networks. In this dissertation, a testbed community was modeled, including interdependent utility networks, to provide a context for the decision algorithms that are the main goal of this research.

2.2. The Role of Network Interdependencies in Community Functionality

Understanding dependencies and interdependencies among critical civil infrastructure systems (networks[1]) and different critical sectors within a system is essential for quantifying reliability, vulnerability, survivability (robustness), and recoverability (rapidity) of such systems (Bruneau and Reinhorn, 2007). Further, metrics for measuring the resilience of communities and the performance of systems and components to support risk management and decision-making requires the consideration of the consequences of system interdependencies. Numerous sources of uncertainty propagate through the phases of transition of a system, from its initial condition prior to a disruptive event to a stable condition of normalcy following a period of recovery. The study of metrics along with uncertainties permits the effect of external disruptive events on systems and their corresponding recovery activities to be quantified from a stochastic viewpoint.

Interdependencies can be categorized by four basic types: physical, cyber, geographic, and logical (Rinaldi et al., 2001). In this study, physical interdependency of networks are modeled by graph theory with an augmented adjacency matrix, denoted as $\mathbf{A}$.

Consider a directed network $G(N, E)$, where N denotes the set of nodes, and E represents the set of edges in G. The adjacency matrix of $\mathbf{A}$ is a square matrix of dimension N in which element $\mathbf{A}_{ij}$ represents the dependency of two nodes of i and j. Matrix $\mathbf{A}$ is symmetric for undirected graphs, but not necessarily symmetric for directed graphs (networks). In order to consider uncertainty in

[1] The term network is regularly used to model a system in which the links between components, as opposed to the components themselves, are unreliable (Aslett, 2012). In this study, however, the terms network and system, as well as the terms of nodes and components, are used interchangeably.

the strength of coupling between nodes over time, one can model dependency by different time-dependent distributions, such as uniform, triangular, and pert-beta. Therefore, in the general case, **A** can be a time-dependent stochastic matrix that describes the interdependencies between nodes i and j over a period of recovery. Defining $x_i(t)$ as the state of the node i, the network state vector at time t, $\mathbf{x}(t) = (x_1(t); x_2(t); ...; x_N(t))$, denotes the state of all nodes at time t. The system function $\varphi(\mathbf{x}(t))$, which can be assessed for any likely realization of $\mathbf{x}(t)$, maps the network state vector into a network performance at time t.

The system performance function $\varphi(\mathbf{x}(t))$ represents the system behavior at time t and quantifies system resilience. Figure 2-1 shows stages that characterize the system the transition over time:

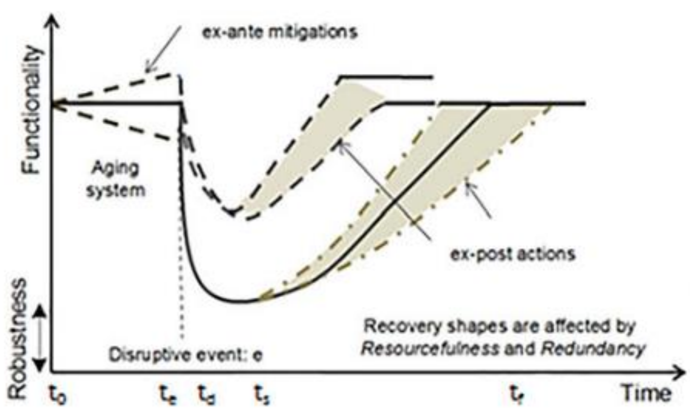

Figure 2-1. Concept of System Resilience (Adopted from McAllister, 2013)

- Prior to the disruptive event, the original system is in state S_0. Proactive activities during this period can improve the performance of the built environment at this stage as well as shorten the time to full or partial recovery. On the other hand, aging and temporary malfunctions can degrade system performance. These factors introduce uncertainties in the initial conditions prior to disruption.

- Following the disruptive event e at time t_e, system degradation initiates due to the loss of functionality of system components. Interdependencies contribute to this degradation significantly due to the cascading failures. Uncertainties in the hazard modeling and interdependencies propagate in this stage. Degradation continues to a maximum disrupted state φ (S_d). The degradation period for certain hazards such as earthquakes can be virtually instantaneous, representing a sudden reduction in functionality ($t_d - t_e \sim 0$), while it occurs more gradually for other hazards.
- Following the disruptive event, a period of time (preparation time) is required for the community to take stock of what has occurred and to inspect damage, secure funding for repair, obtain permits, hire contractors, and prepare construction drawings.
- Recovery from the disturbance, following initiation of repair of damage, follows the preparation time. Depending on the degree of interdependency among buildings and infrastructure systems, recovery paths can be highly uncertain (McAllister, 2013).

The system performance function, $\varphi(\mathbf{x}(t))$, can be assumed to be a non-decreasing function, under the assumption that the resilience is defined as uncoupled from the next event (Cimellaro et al., 2013), in which any further drop in functionality due to a future shock occurs after the recovery process from the current shock has been completed. The non-decreasing assumption for $\varphi(\mathbf{x}(t))$ implies that:

$$\varphi(\mathbf{x}(t_1)) \leq \varphi(\mathbf{x}(t_2)) \qquad \forall t_1 \leq t_2 \qquad \textit{Equation 2-1}$$

The system resilience given the disruptive event e at time t is (Barker et al., 2013):

$$R_{\varphi}(t_r|e) = \frac{\varphi(t_r|e)-\varphi(t_d|e)}{\varphi(t_0)-\varphi(t_r|e)} \quad t_r \in (t_s, t_f) \qquad \textit{Equation 2-2}$$

Pant et al. (2014) defined other temporal resilience metrics along with the stochastic ratio of the resilience defined by Equation 2-2. The metric "time to full network service resilience, $T_{\varphi(\mathbf{x}(t))(e)}$" and the metric "time to α ×100% resilience," $T_{\alpha}(e)$ shows the entire time taken from the time when recovery activities commence, at time t_s, up to the time, t_{α}, when the system service is restored to $\alpha \times \varphi(\mathbf{x}(t_0))$. Different recovery strategies can be commensurable in favor of temporal metrics.

2.3. TESTBED COMMUNITY- GILROY, CA

The testbed community considered in this study is Gilroy, CA, located in Santa Clara County, CA, approximately 50 kilometers (km) south of the city of San Jose (see Figure 2-2). Gilroy is at the intersection of two main highways, U.S. 101, which extends through the City in the north-south route and SR 152, which extends in an east and west direction (Gilroy Annex, 2011). As a result, damage to the highway bridges disrupts accessibility to critical facilities, like main food retailers, in the aftermath of an extreme earthquake event on the San Andreas Fault which runs approximately 12 km to the southwest from the center of Gilroy. The area of Gilroy is approximately 41.91 km^2 with a population of 48,821 in 14,175 household units at the time of the 2010 Census. While not all characteristics of Gilroy are covered in this study, our model of the community maintains adequate detail to study the dependency of food retailers on the availability and functioning of water, power, structure and transportation networks following an earthquake on the San Andreas Fault.

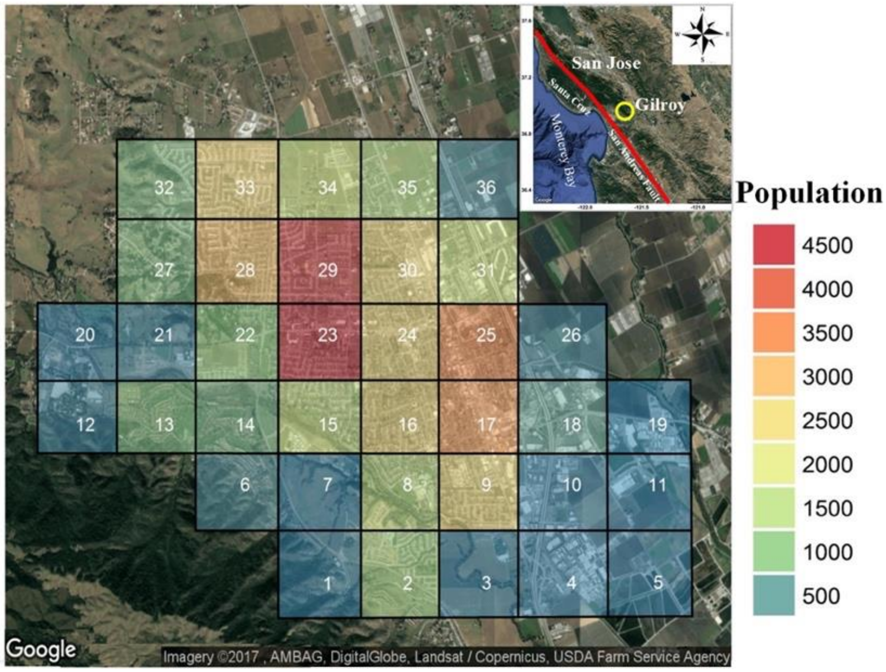

Figure 2-2. Gilroy Position along with the Population Heat Map over the Defined Grids

2.4. Urban Grids

The study area is divided into 36 grids (about 1.0-1.14 km^2 on a side) to define the properties of infrastructure systems, residential buildings, and the population in sufficient detail. Figure 2-2 shows a population heat map distributed over the defined grids. Other population qualities, such as racial and ethnic composition and age distribution are tabulated in Tables 2-1 and 2-2, respectively.

Table 2-1. Racial and Ethnic Composition of Gilroy (United States Census Bureau, 2010a)

Subject	Number	Percent
Total Population	48,821	100
Hispanic or Latino	28,214	57.8
Not Hispanic or Latino	20,607	42.2
White alone	15,335	31.4
Black or African American alone	709	1.5

American Indian and Alaska Native alone	180	0.4
Asian alone	3,265	6.7
Native Hawaiian and Other Pacific Islander alone	86	0.2
Some Other Race alone	58	0.1
Two or More Races	974	2

Table 2-2. Age Distribution of Gilroy (United States Census Bureau, 2010b)

Age Group	Number	Percent
Preschool (0-4 years)	4,144	8.4
School (5-17 years)	10,839	22.2
Young Adult (18-24 years)	4,514	9.2
Prime Working (25-54 years)	20,717	42.4
Retirement (55-64 years)	4,509	9.25
Senior Citizen (65+ years)	4,098	8.4

Household units are increasing at a faster pace in Gilroy than in Santa Clara County or the State of California (Harnish, 2014). In 2010, the average number of persons per household in Gilroy was 3.4, higher than the state and county average. 95.4% of Gilroy's housing units are occupied. A heat map of household units over the defined grids is shown in Figure 2-3. Table 2-3 shows the age of the housing stock of Gilroy.

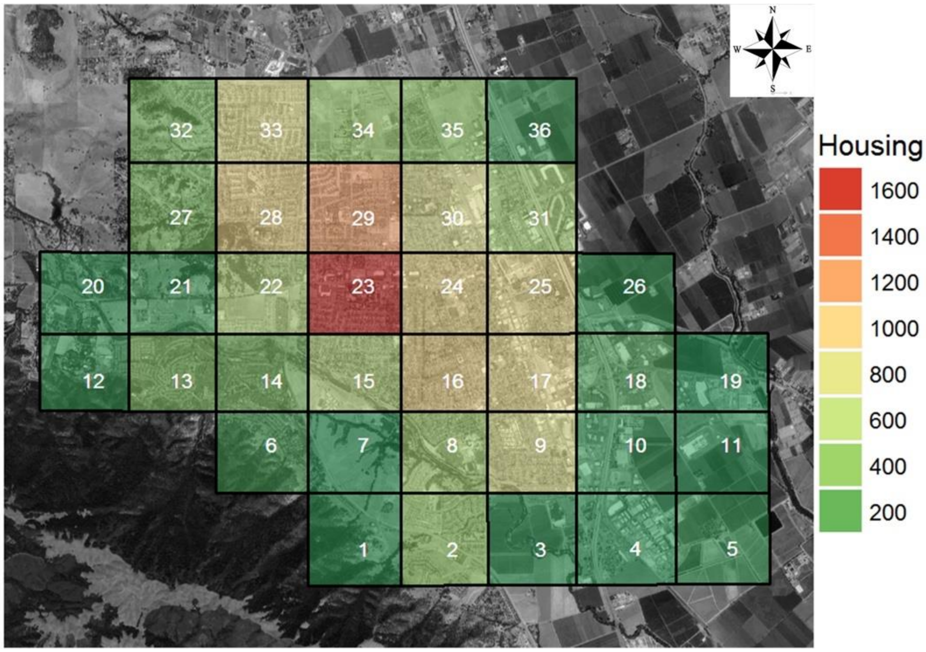

Figure 2-3. Household Units over the Defined Grids

Table 2-3. Age of Housing Stock of Gilroy (Harnish, 2014)

Year Built	2000-2009	1990-1999	1980-1989	1970-1979	1969 or earlier
Percent (%)	21	18	18	21	22

For each urban grid the total population and population in three age categories (child ages 0-17, adult ages 18-64, and senior ages 65+) were estimated using 2010 Census block data (United States Census Bureau, 2010a). The 2010 Block data provides the smallest level of geography for population counts with detailed characteristics such as age groups. For the data used in the models the total population was 47,905, the population for children ages 0-17 was 14,674, the population for adults ages 18-64 was 29,163, and the population for seniors ages 65+ was 4,068. Grids 11 and 21 both had the smallest population with 21 persons, and grid 23 had the largest population with 4,390 persons.

2.5. Description of Infrastructure Systems in Gilroy City

An 115kV power transmission line provides the electricity to the Llagas substation, the only transmission substation within the defined boundary of Gilroy. Twenty-eight steel lattice transmission towers are located within the community boundary, so that if any one of the towers supplying the substation fails, the city will not have external electric power. The series arrangement of overhead distribution lines without any redundancy makes the Electrical Power Network (EPN) more vulnerable when subjected to a severe earthquake or other natural hazard event. Distribution lines components are spaced 100 m from the substation to the centers of urban grids, food retailers, and water pumps, as shown in Figure 2-4.

The EPN does not depend on any other network; hence, we only need to consider the dependency within the network. The probability that a critical facility like a water pump or a food retailer *G* has electricity is:

$$P(EG) := P\left(\bigcap_{l=1}^{\hat{n}} EE_l\right) \qquad \textit{Equation 2-3}$$

where *EG* is the event that *G* has electricity, EE_l is the event that the l^{th} EPN component is functional, and $\hat{n}$ is the minimum number of EPN components required to supply electricity to *G*. The sample space is a singleton set that has the outcome, “is functional and nonfunctional.” The l^{th} EPN component is functional when it is undamaged or completely repaired *and* all the EPN components serving that EPN component are functional.

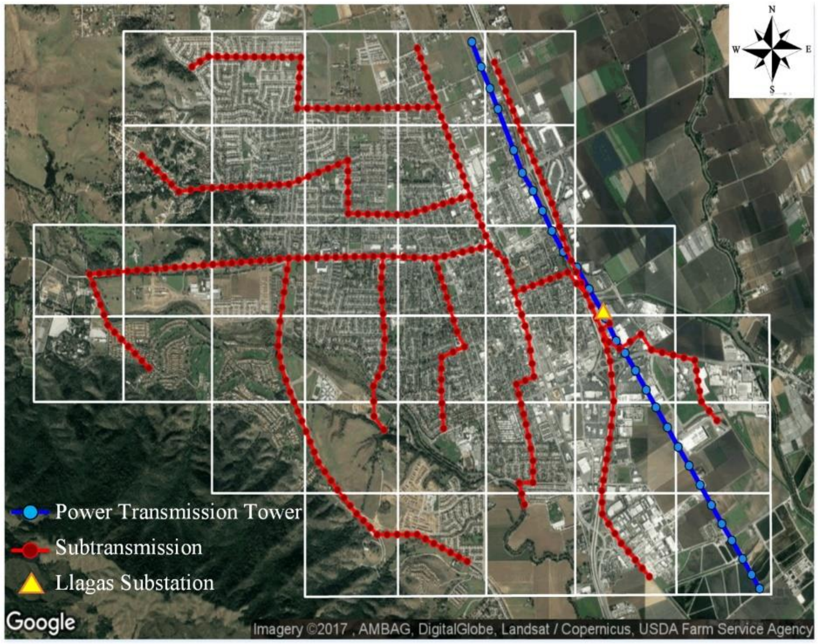

Figure 2-4. The Modeled Electrical Power Network

The city's Water Master Plan (Smelser and Akel, 2011) indicates that the Llagas sub-basin is the only source of domestic water in Gilroy. The Llagas sub-basin is approximately 24 km long, 4.8 km wide and located below the City of Gilroy. It is recharged by Llagas and Uvas Creeks from the basin's western side. Gilroy operates water wells, which are situated in wood-frame buildings, to provide water to the city inhabitants. Potable water is pumped directly into the distribution system; extra water is used to fill reservoirs. The various elevation levels necessitate the use of booster pumping stations in addition to well pumps. The potable water is distributed to the urban grids through pipes ranging between 102 mm and 610 mm in diameter. This study models the main 610 mm potable water pipelines along with wells (W), water tanks (WT), and booster pump stations (BPS). The locations of water network components of Gilroy, shown in Figure 2-5, are obtained from a database, maintained by the city's Water Master Plan.

The functionality of the WN depends on not only the functionality of its components but also the availability of electricity following the extreme hazard for water pump operation. Therefore, the dependency between the WN and EPN systems must be considered. The probability that a critical facility like an urban grid rectangle or a food retailer *G* has potable water is

$$P(WG) := P\left(\bigcap_{l'=1}^{\hat{k}} EW_{l'}\right) \qquad \textit{Equation 2-4}$$

where *WG* is the event that *G* has water, $\hat{k}$ is the minimum number of WN components (which could be BPS, wells, water tanks, or pipelines) required to supply water to *G*, and EW_i is the event that the l'^{th} WN component is functional. Again, the sample space here is a singleton set that has the outcome, "is functional and nonfunctional." If the l'^{th} WN component is a pipeline, then it is said to be functional when it is undamaged or completely repaired *and* all the WN components serving that pipeline are functional.

In addition, if the l'^{th} WN component is a BPS, well, or water tank, then it is said to be functional when it is undamaged or completely repaired *and* all the EPN components serving the l'^{th} WN component are functional. While the pipelines are not directly dependent on the EPN, they are indirectly dependent on the EPN through the other WN components. The variables $\hat{n}$ and $\hat{k}$ accommodate any potential redundancy in the EPN and WN.

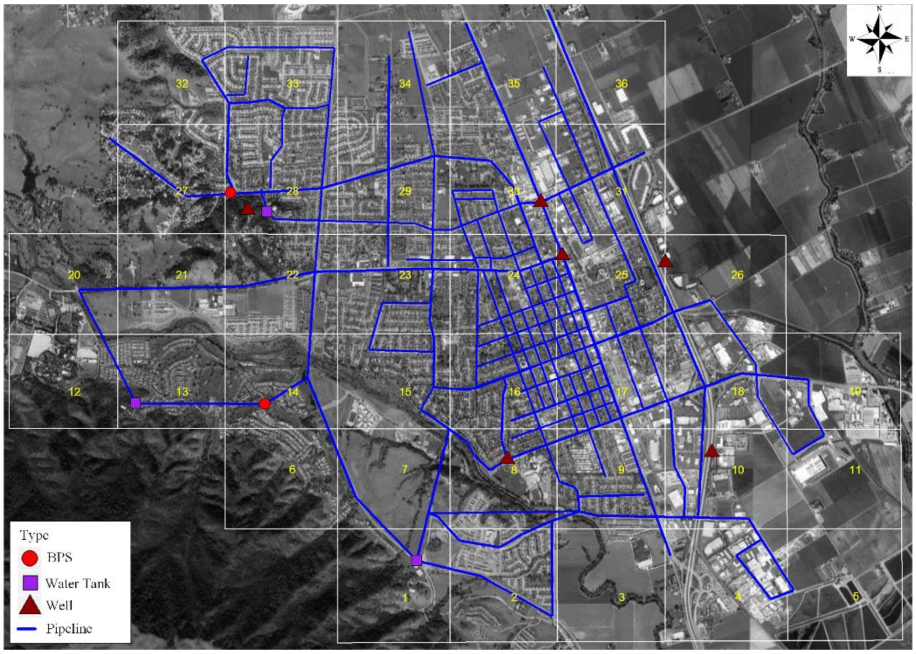

Figure 2-5. The Modeled Potable Water Network

2.6. FOOD RETAILERS

The majority of the food requirements of the city inhabitants is supplied by six main food retailers, summarized in Table 2-4, each of which has more than 100 employees. In this study, the availability of each food retailer depends on the physical structure that houses the food retailer as well as the availability of electricity and potable water. Figure 2-6 shows the locations of all main food retailers within the study area.

Table 2-4. The Number of Employees of Main Food Retailers (Harnish, 2014)

Food Retailer	Walmart	Costco	Target	Mi Pueblo Food	Nob Hill Foods	Safeway
No. Employees	395	220	130	106	100	130

Figure 2-6. Main Food Retailers in Gilroy

To assign the probabilities of shopping activity to each urban grid rectangle, the gravity model proposed by Adigaa et al. (2015) is used. The gravity model identifies the shopping location probabilistically, given the location of residences. These probabilities are assigned to be proportional to food retailers' capacities and inversely corresponding to retailers' distances from centers of urban grid rectangles. Consequently, distant small locations are less likely to be selected than close large locations. If the center of an urban grid is *c*, then food retailer *r* is chosen according to the following distribution:

$$P(r \mid c) \propto w_r e^{bT_{cr}} \qquad \textit{Equation 2-5}$$

where w_r is the capacity of food retailer *r*, determined by Harnish (2014), *b* is a negative constant, and T_{cr} is the travel time from urban grid *c* to food retailer *r*. Google's Distance Matrix API was called from within R by using the *ggmap* package (Kahle and Wickham, 2018) to provide distances and travel times for the assumed transportation mode of driving.

2.7. HAZARD SIMULATION

Gilroy has experienced several strong earthquakes over the past century, most recently the 1989 Loma Prieta earthquake, with moment magnitude, M_w=6.9, and an epicenter located approximately 27 km (16 mi) northwest of Gilroy on a section of the San Andreas Fault System. The Loma Prieta Earthquake caused an estimated $6 billion in property damages, 63 fatalities, and 3,757 injuries (National Research Council, 1994). In this study, an earthquake scenario similar to Loma Prieta is simulated, in which M_w=6.9 and the epicenter is located approximately 12 km (7 mi) southwest of downtown Gilroy, approximately the closest distance from the San Andreas Fault to the city.

The spatial estimation of earthquake ground-motion amplitudes is an essential element of seismic risk assessment of a community, and is typically characterized by ground-motion prediction equations (GMPEs). GMPEs require several parameters, such as earthquake magnitude M_w, fault properties (F_p), soil conditions (i.e., the average shear-wave velocity in the top 30 m of soil, V_{s30}, shown in Figure 2-7), and epicentral distances (R) to compute the seismic intensity measure (IM) at any point. Modern GMPEs typically take the form

$$\ln(IM) = f(M_w, R, V_{s30}, F_p) + \varepsilon_1\sigma + \varepsilon_2\tau \qquad \textit{Equation 2-6}$$

$$\ln(IM) = \ln(\bar{IM}) + \varepsilon_1\sigma + \varepsilon_2\tau \qquad \textit{Equation 2-7}$$

where σ and τ are period dependent and reflect the intra-event (within event) and inter-event (event-to-event) uncertainty respectively. The intra-event term $\varepsilon\sigma$ is spatially correlated, while the event-to-event term $\varepsilon\tau$ is perfectly correlated for any given data-set from a single earthquake.

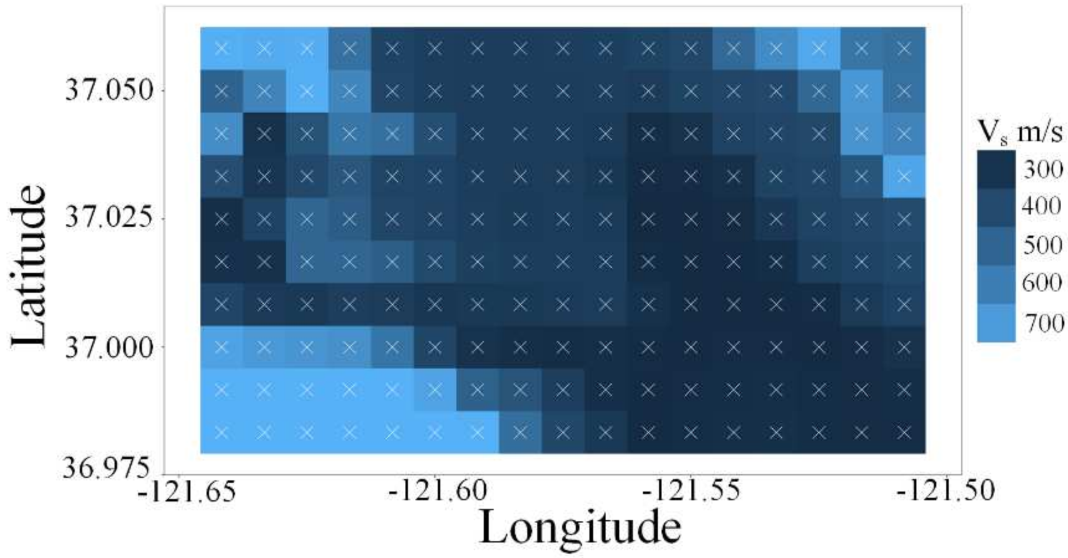

Figure 2-7. Heat Map of Shear Velocity, V_{s30}, at Gilroy Area

In this study, we use the Abrahamson et al. (2013) GMPE with epicenter approximately 12 km of Gilroy downtown on the San Andreas Fault projection. The histograms of IMs at selected locations in Gilroy are presented in Figure 2-8. Figure 2-9a and 2-9b show the map of ground motion field for Peak Ground Acceleration (PGA) and Peak Ground Velocity (PGV), respectively.

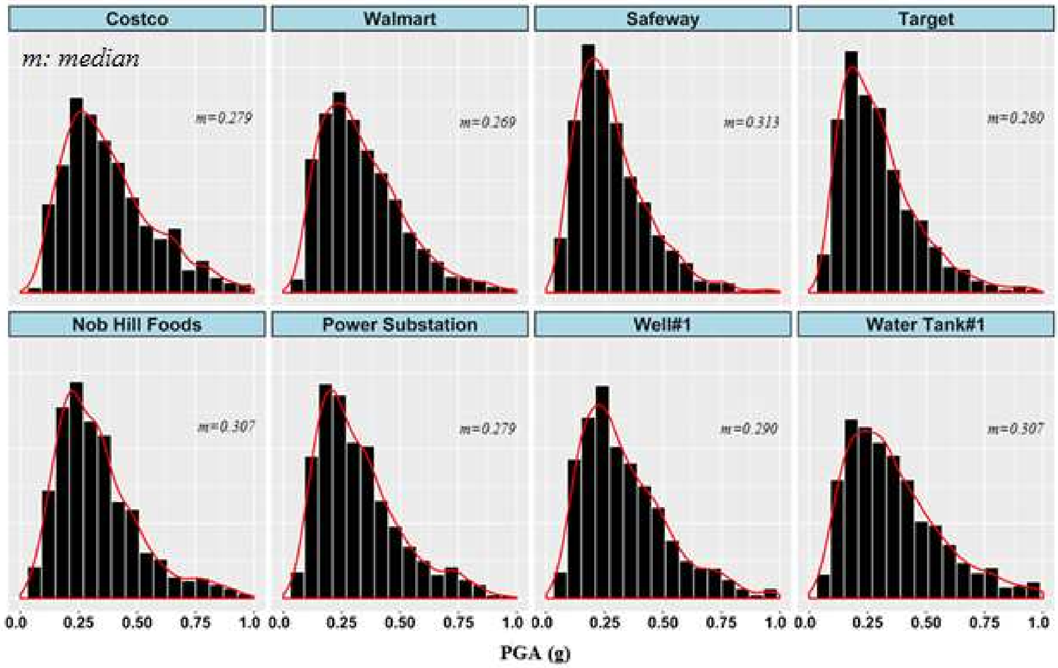

Figure 2-8. The Histograms of IM at Some Selected Locations in Gilroy and the Medians

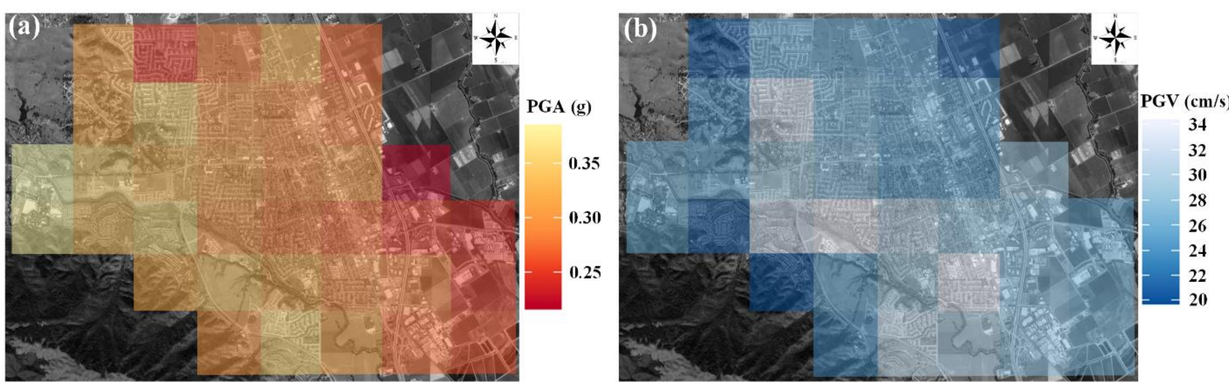

Figure 2-9. The Simulations of Median of Spatially Correlated PGA (a) and PGV (b) Fields over the Defined Grids

Permanent ground displacements (PGD) due to liquefaction occur only in zones where the PGV exceeds 75 cm/s (30 in/s) (O'Rourke and Jeon, 2000). As Figure 2-9b indicates, the PGV within the Gilroy area does not exceed roughly 35 cm/s; thus, the likelihood of pipe breakage by PGD due to liquefaction is negligible.

2.8. Damage and Restoration Assessment of Facilities

Food retailer establishments, power transmission towers, power substation, water tanks, wells, pipelines, household units, and bridges must function as an integrated system to provide the needed food and services to urban inhabitants. The performance of these engineered components when subjected to an earthquake is defined by seismic fragility curves. The relations between ground-motion intensities and earthquake damage are pivotal elements in seismic loss estimation and risk analysis of a community. The fragility of a component in this study is defined as the probability that it equals or exceeds a given damage state, conditioned on a level of an Intensity Measure (IM), such as peak ground displacement, velocity, acceleration, or spectral acceleration. HAZUS-MH (FEMA, 2003) is one nonproprietary source of the seismic fragilities used herein. In the present study, the seismic fragility curves of EPN components included in HAZUS-MH and Xie et al. (2012) are used for illustration. It is customary [Ellingwood 1991] to model component fragilities with lognormal distributions. The conditional probability of being in or exceeding a particular damage state (*ds*), conditioned on a particular level of intensity measure *IM*= *im*, is defined by

$$P(DS \geq ds \,|\, IM = im) = \Phi\left(\frac{\ln(im) - \lambda}{\xi}\right) \qquad \textit{Equation 2-8}$$

where Φ is the standard normal distribution and λ and ξ are the mean and standard deviation of $\ln(im)$.

Regarding the water network, this study will follow the assumptions in the study by Adachi and Ellingwood (2009), in which the components are assumed to be either fully functional or nonfunctional. The failure probability of a pipe is bounded as:

$$1-G_{\varepsilon PGV}\left(-CL\mu_{PGV}\right)\leq E\left[P_f\right]\leq 1-E\left[\exp\left(-CL\mu_{PGV}\right)\right] \qquad \textit{Equation 2-9}$$

in which $G_{\varepsilon PGV}(.)$ is the moment-generating function of εPGV (the residual of the PGV), P_f is the failure probability of a pipe, L is the length of the pipe, and μ_{PGV} is the average PGV for the entire length of the pipe. The term C for water pipe segment i is $C = K \times 0.00187 \times PGV_i$, where K is a coefficient determined by the pipe material, diameter, joint type, and soil condition based on the guidelines prepared by the American Lifeline Alliance (ALA) (2001). The Upper Bound (UB) and exact solutions in Equation 2-9 are close enough that in practical applications, the UB assessment (conservative evaluation) can be used (Adachi and Ellingwood, 2009).

Restoration quantification suffers from the lack of documented data on delay and repair time for different components of a network. The analysis of uncertainties in component restoration is an interdisciplinary endeavor. HAZUS-MH (FEMA, 2003) has restoration curves primarily based on expert judgment and available empirical data. The HAZUS-MH restoration curves are based on the assumption that restoration can be modeled by a normal distribution, which admits the possibility that restoration times can be negative. Accordingly, this study utilizes exponential distributions to model the repair times.

In summary, five networks were modeled for Gilroy in this dissertation—the household units, the food retailers, the electric power network, the water supply network, and the highway-bridges. The dependencies among the components of each network as well as among networks were modeled to capture the effects of cascading failure, as shown in Figure 2-10. The algorithms developed in the following chapter are applied to modeling recovery following a severe earthquake in Gilroy to provide context for the analysis.

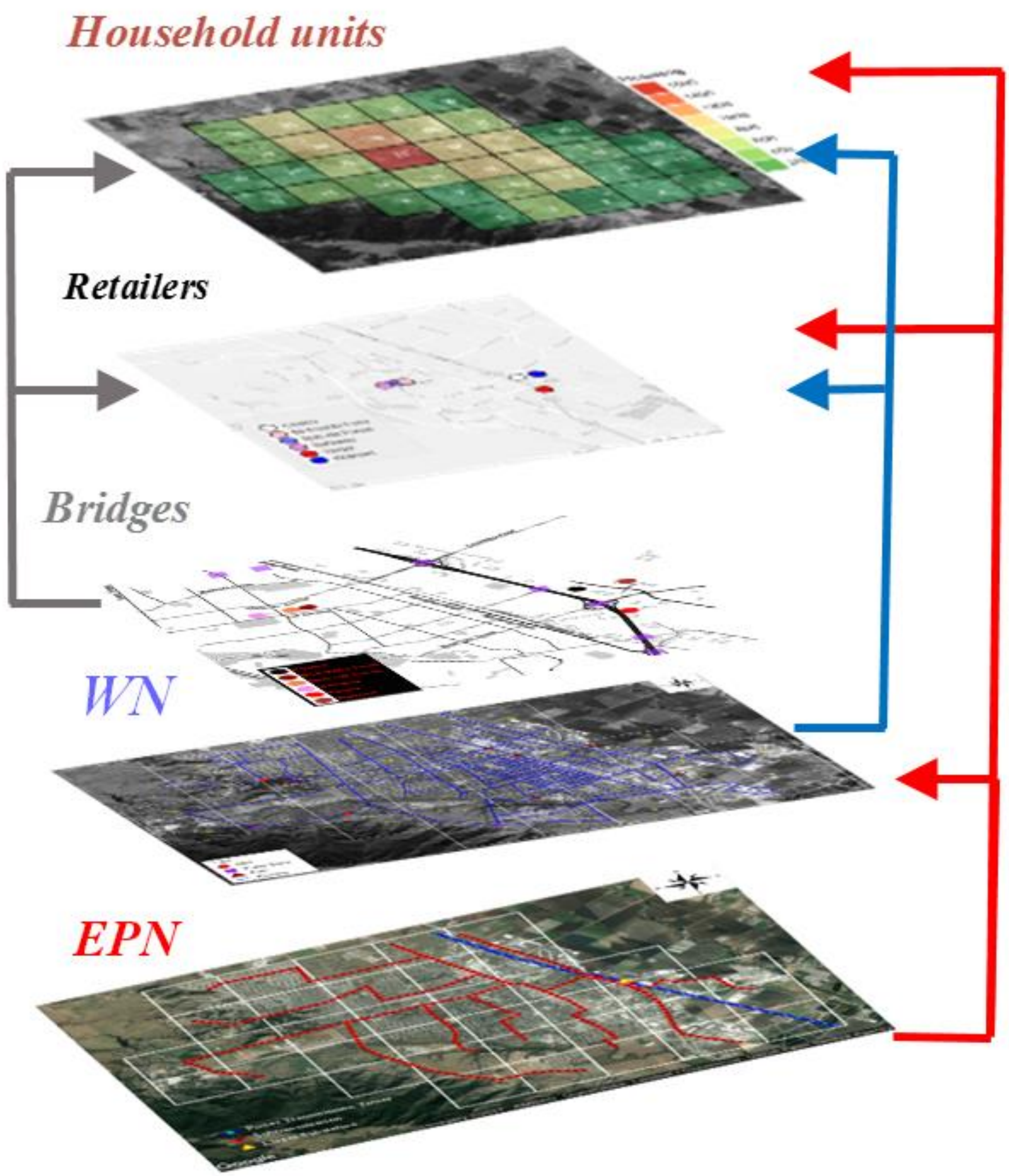

Figure 2-10. Gilroy Networks and the Corresponding Interdependencies

CHAPTER 3: NEAR-OPTIMAL RECOVERY PLANNING USING APPROXIMATE DYNAMIC PROGRAMMING

—Life can only be understood going backwards, but it must be lived going forwards."

Kierkegaard

3.1. Introduction

The functionality of modern infrastructure systems is essential for providing continuous services to communities and in supporting their public health and safety. Natural and anthropogenic hazards pose significant challenges to infrastructure systems and cause undesirable system malfunctions and consequences. Past experiences show that these malfunctions are not always inevitable despite design strategies like increasing system redundancy and component reliability (Nachlas, 2017). Therefore, a sequential rational decision-making framework should enable malfunctioning systems to be restored in a timely manner after the hazards. Post-event stressors and chaotic circumstances, time limitations, budget and resource constraints, and complexities in the community recovery process, highlight the necessity for a comprehensive risk-informed decision-making framework for recovery management at the community level. This decision-making framework must take into account indirect and delayed consequences of decisions (also called the post-effect property of decisions), which requires foresight or planning. Such a comprehensive decision-making system must also be able to handle large-scale scheduling problems that encompass large combinatorial decision spaces to make the most rational plans at the community level.

Generally speaking, optimization problems in large-scale systems belong to two main branches of operations research (Gosavi, 2015):

1. **Parametric** optimization (also referred to as **static** optimization).
2. **Control** optimization (also referred to as **dynamic** optimization).

Parametric optimization deals with finding values of decision variables (or set of parameters) that optimize some performance measure (objective function). Parametric optimization customarily is implemented using mathematical programming, e.g., linear, non-linear, and integer programming.

Conversely, control optimization refers to computing a set of actions (decisions) to be taken in the different states that a system reaches, such that the decisions selected optimize some performance measure of the system. Since the solution of the problem relies on a dynamic state control optimization is also called a *dynamic* optimization. Control optimization is generally implemented by means of dynamic programming, but sometimes via mathematical programming as well.

In the context of civil engineering, several studies have utilized the framework of dynamic programming for management of bridges and pavement maintenance (e.g., Ellis et al., 1995; Corotis et al., 2005). Typical methodological formulations employ principles of dynamic programming that utilize state-action pairs. These types of formulations are especially powerful when the outcome of each action is not fully predictable, as discussed in Chapter 4. In this chapter, it is assumed that the outcome of the decision maker is fully predictable, enabling the development of a powerful and relatively unexplored methodological framework of formulating large infrastructure problems as string-actions. The formulation does not require an explicit state-space model; therefore, it is shielded against the common problem of state explosion when such methodologies are employed. The sequential decision-making methodology presented here not only manages network-level infrastructure but also considers the interconnectedness and cascading effects in the entire recovery process that have not been addressed in past studies.

Dynamic programming formulations frequently suffer from the *curse of dimensionality*. This problem is further aggravated when dealing with large combinatorial decision spaces, which are characteristic of community recovery assessment. Therefore, using approximation techniques in conjunction with the dynamic programming formalism is essential for the solution of realistic decision problems, several of which are available in the literature (Kochenderfer, 2015). Here, a promising class of approximation techniques called rollout algorithms is employed, which blend naturally with our string-action formulation. Together, they form a robust tool to overcome some of the limitations faced in the application of dynamic programming techniques to massive real-world problems. The proposed approach is able to handle the curse of dimensionality in its analysis and management of multi-state, large-scale infrastructure systems and data sources. The proposed methodology is also able to consider and improve the current recovery policies of responsible public and private entities within the community. The proposed methodology is first applied to the modeled EPN, discussed in Chapter 2.

3.2. Optimization Problem Statement

After a severe earthquake event occurs, each component (e.g., home, water pump, power substation, bridge, etc.) within the community ends up in one of the damage states based on the fragility curves for that component. Let the total number of damaged components be M. To restore a network, a number of available resource units, N, as a generic single number, including equipment, replacement components, and repair crews are considered for assignment to damaged components, and each damaged component is assumed to require only one unit of resource (also called as resource units, RUs) (Ouyang et al., 2012). M and N are non-negative integers, and following severe earthquakes, like those considered in this study, $N << M$. This assumption is justified by the availability of limited resources to the planner when a large number of components are damaged in the aftermath of a hazard event. A decision maker or planner has the task of assigning resource units to repair these damaged components. Often, the decision maker has a heuristic or judgment-based policy on the basis of which he can make his decisions to optimize multiple objectives. The precise nature of the objective of the planner can vary. At the beginning of the first decision epoch, the decision maker deploys N unit of resources at N out of M damaged components. Each unit of resource is assigned to a distinct damaged component. At every subsequent decision epoch, the planner has the option of reassigning some or all of the resources to new locations based on his heuristics and objectives. He must have the flexibility of such a reassignment even if the repair work at the currently assigned locations is not complete. At every decision epoch, it is possible to forestall the reassignment of the units of resource that have not completed the repair work; however, we choose to solve the more general problem of preemptive assignment, where non-preemption at a few or all the locations is a special case of our problem. The preemptive assignment problem is a richer decision problem than the non-preemptive case in the sense that the process of optimizing the decision actions is a more complex task because the size of the decision space is bigger. Nevertheless, our goal is to address both preemptive and non-preemptive scheduling in this dissertation.

Two different scheduling schemes are proposed herein. In the first, which will be addressed in this chapter, outcomes of the decisions are fully predictable to the decision maker. In the second, which will be addressed in Chapter 4, the outcomes of decisions are not fully predictable (stochastic scheduling), but can be anticipated to some level of statistical regularity before the next action is determined.

3.3. Optimization Problem Formulation

Suppose that the decision maker begins by assigning repair locations to different resource units. The number of such non-trivial decisions to be made is less than or equal to $M-N$. When M becomes less than or equal to N (because of sequential application of repair actions to the damaged components), the assignment of units of resource becomes a trivial problem in our setting because each unit can simply be assigned one to one, in any order, to the damaged components. Consequently, a strict optimal assignment can be achieved in the trivial case. The size of this trivial assignment problem reduces by one at every new decision epoch until all the remaining damaged components are repaired. The additional resource units are retired rather than redeployed because deploying more than one unit of resource to the same location does not decrease the repair time associated with that damaged component. Henceforth, we focus on the non-trivial assignment problem.

Let D_t be the set of all damaged components at time, t, before a repair action x_t is performed. Let t_{end} denote the decision epoch at which repair action $x_{t_{end}}$ is selected so that $\left|D_{t_{end}}+1\right| \le N$. Note that $t \in A := (1, 2, ..., t_{end})$. Let $X = (x_1, x_2, ..., x_{t_{end}})$ represent the string of actions resulting from the non- trivial assignment. A repair action is said to be completed when at least 1 out of the N damaged components is repaired. Let $\mathbf{P}(D_t)$ be the powerset[2] of D_t.

[2] The powerset (or power set) of any set D is the set of all subsets of D.

$$\mathbf{P}_N(D_t) := \{C \in \mathbf{P}(D_t) : |C| = N\} \qquad \textit{Equation 3-1}$$

so that $x_t \in \mathbf{P}_N(D_t)$. C represents the number of element of the subsets that should be equal to the number of N (RUs). Let R_t be the set of all repaired components after the repair action x_t is completed. Note that $1 \leq |D_{t_{end}+1}| \leq N$, and the decision-making problem moves into the trivial assignment problem previously discussed. The objective is a string X of repair actions that optimizes objective functions $F(X)$, denoted by F_1 and F_2 and defined as follows:

- **Objective 1:** Let the variable p represent the population of Gilroy and γ represent a fraction of its population. Let $X_1 = (x_1, \ldots, x_i)$ be the string of repair actions that results in restoration of a system or a system of systems to $\gamma \times p$ number of people. Here, $x_i \in \mathbf{P}_N(D_t)$, where D_i is the number of damaged components at the i^{th} decision epoch. Let n represent the number of days required to restore the system or community to $\gamma \times p$ number of people as a result of repair actions X_1. Formally,

$$F_1(X_1) = n \qquad \textit{Equation 3-2}$$

The optimal solution X_1^* for Objective 1 is:

$$X_1^* := \arg\min_{X_1} F_1(X_1) \qquad \textit{Equation 3-3}$$

In objective 1, the aim is to find the string of actions that minimizes the number of days needed to restore the community to a certain fraction (γ) of the pre-event population of Gilroy.

- **Objective 2:** Objective F_2 is defined in terms of the number of people who have benefited from a specific system or several interdependent systems per unit of time; an example might be to restore power service to the maximum number per unit of time. The goal is to maximize this objective over a string of repair actions. Let the variable k_t denote the total time elapsed between the completion of repair action x_{t-1} and x_t, in which k_1 is the time elapsed between the start and completion of repair action x_1. Let h_t be the total number of people who have benefited after the repair action x_t is complete. Then,

$$F_2(X) = \frac{1}{k_{t_{end}}} \sum_{t=1}^{t_{end}} h_t \times k_t \qquad \textit{Equation 3-4}$$

The optimal solution X^* given by

$$X_2^* := \arg\min_X F_2(X_2) \qquad \textit{Equation 3-5}$$

3.4. The Proposed Optimization Solution

Calculating X^* is a sequential optimization problem. The decision maker applies the repair action x_t at the decision epoch t to maximize or minimize an objective function. The string of actions, as represented by X, are an outcome of this sequential decision-making process. This is particularly relevant in the context of dynamic programming where numerous solution techniques are available for the sequential optimization problem. Rollout is one such solution technique. It is possible to use the dynamic programming formalism to describe the method of rollout, but here the rollout concept is explained by starting from first principles (Bertsekas, 2013). The description of the rollout algorithm is inherently tied with the notion of approximate dynamic programming.

3.4.1. Approximate Dynamic Programming

Objective 1 can be optimized as described below. (The extension of this methodology to objective 2 is straightforward, using adapting notation used for objective 2 to the methodology presented below, and replacing the maximization problem by a minimization problem.) Objective 1 is optimized in the following manner: First calculate x_1^* as follows:

$$x_1^* \in \arg\min_{x_1} J_1(x_1) \qquad \textit{Equation 3-6}$$

where the function J_1 is defined as:

$$J_1(x_1) = \min_{x_2,\ldots,x_i} F_1(X_1) \qquad \textit{Equation 3-7}$$

Next, calculate x_2^* as:

$$x_2^* \in \arg\min_{x_2} J_2(x_1^*, x_2) \qquad \textit{Equation 3-8}$$

where the function J_2 is defined by

$$J_2(x_1, x_2) = \min_{x_3,\ldots,x_i} F_1(X_1) \qquad \textit{Equation 3-9}$$

Proceeding similarly in a step-wise fashion, we calculate the α-solution (at the α^{th} step) as follows:

$$x_\alpha^* \in \arg\min J_\alpha(x_1^*,\ldots,x_{\alpha-1}^*, x_\alpha) \qquad \textit{Equation 3-10}$$

where the function J_α is defined by

$$J_\alpha(x_1,\ldots,x_\alpha) = \min_{x_{\alpha+1},\ldots,x_i} F_1(X_1) \qquad \textit{Equation 3-11}$$

Functions J_α in Eqs (3-6) – (3-11) are called the *optimal cost-to-go* functions and are defined by the following recursion:

$$J_\alpha(x_1,\ldots,x_\alpha) = \min_{x_{\alpha+1}} J_{\alpha+1}(x_1,\ldots,x_{\alpha+1}) \qquad \textit{Equation 3-12}$$

J is standard notation used to represent *cost-to-go* functions in the dynamic programming literature.

The approach discussed above to calculate the optimal solutions is typical of the dynamic programming formulation. However, except for very special problems, such a formulation cannot be solved exactly because calculating and storing the optimal cost-to-go functions J_α can be numerically intensive.

In the problem at hand, let $\left|\mathbf{P}_N(D_t)\right| = \beta_t$; then the storage of J_α requires a table of size

$$S_\alpha = \prod_{t=1}^{\alpha} \beta_t \qquad \textit{Equation 3-13}$$

where $\alpha \le i$ for objective 1, and $\alpha \le t_{end}$ for objective 2. In the dynamic programming literature, this is referred to as the *curse of dimensionality*. If we consider objective 2 and wish to calculate J_α such that $\alpha = M\text{-}N$ (we assume for the sake of this example that only a single damaged component is repaired at each t), then for 50 damaged components and 10 unit of resources, $S_\alpha \approx 10^{280}$. In practice, J_α in is replaced by an approximation denoted by $\tilde{J}_\alpha$, called a *scoring function* or *approximate cost-to-go* function. One way to calculate $\tilde{J}_\alpha$ is with the aid of a heuristic; however, there are several ways to approximate J_α that do not utilize heuristic algorithms. All such approximation methods fall under the category of approximate dynamic programming.

3.5. ROLLOUT ALGORITHM[3]

Although obtaining a strict optimal policy is often quite difficult due to the curse of dimensionality, a heuristic policy can be easily designed in many cases. The idea of the rollout approach is to improve a heuristic policy via simulation. Suppose that a heuristic *H* is used to approximate the optimization, and let $H_\alpha(x_1, ..., x_\alpha)$ denote the corresponding approximate optimal value; then rollout yields the suboptimal solution by replacing J_α with H_α in Equation 3-10:

$$\tilde{x}_\alpha \in \arg\min_{x_\alpha} H_\alpha(\tilde{x}_1, ..., \tilde{x}_{\alpha-1}, x_\alpha) \qquad \textit{Equation 3-14}$$

In many practical problems, rollout results in a significant improvement over the underlying base heuristic (Bertsekas et al., 1997).

It is possible to identify the base heuristic *H* in several ways:

i. The current recovery policy of regionally responsible public and private entities;
ii. The importance analyses that prioritize the importance of components based on the considered importance factors;
iii. The greedy algorithm[4] that computes the greedy heuristic;
iv. A random policy without any pre-assumption;
v. A pre-defined empirical policy; e.g., base heuristic based on the maximum node and link betweenness (shortest path).

---

[3] On a historical note, the term rollout was first coined by Tesauro in reference to creating computer programs that play backgammon (Tesauro and Galperin, 1997). An approach similar to rollout was also shown much earlier in (Abramson, 1990).

[4] A greedy algorithm, as the name suggests, always makes the choice that seems to be the best at that moment. A greedy algorithm makes greedy choices at each step to ensure that the objective function is optimized. It has only one shot to compute the optimal solution so that it never goes back and reverses the decision. Analyzing the run time for greedy algorithms will generally be much easier.

The rollout method, described above for a discrete, deterministic, and sequential optimization problem using first principles and string-action formulation, can be interpreted in terms of the policy iteration algorithm in dynamic programming. The policy iteration algorithm (see Howard (1960) for further details, including the definition of policy in the dynamic programming sense) computes an improved policy (policy improvement step), given a base policy (stationary), by evaluating the performance of the base policy. The policy evaluation step is typically performed through simulations. A rollout policy can be viewed as the improved policy calculated using the policy iteration algorithm after a single iteration of the policy improvement step. For a discrete and deterministic optimization problem, the base policy used in the policy iteration algorithm is equivalent to the base heuristic, and the rollout policy consists of the repeated application of this heuristic. This approach was used by Bertsekas et al., (1997) to provide performance guarantees on the basic rollout approach and to discuss variations to the rollout algorithm. Henceforth, base policy and base heuristic will be considered indistinguishable terms.

Ideally, we would like the rollout method to never perform worse than the underlying base heuristic (guaranteed performance). This is possible under each of the following three cases (Bertsekas et al., 1997):

1. The rollout method is terminating (optimized rollout).
2. The rollout method utilizes a base heuristic that is sequentially consistent.
3. The rollout method is terminating and utilizes a base heuristic that is sequentially improving (extended rollout and fortified rollout).

A sequentially consistent heuristic guarantees that the rollout method is terminating. It also guarantees that the base heuristic is sequentially improving. Therefore, 3 and 1 are special cases of 2 with a less restrictive property imposed on the base heuristic (that of sequential improvement or termination). When the base heuristic is sequentially consistent, the fortified and extended rollout methods are the same as the rollout method.

A heuristic must possess the property of termination to be used as a base heuristic in the rollout method. Even if the base heuristic is terminating, the rollout method need not be terminating. Apart from the sequential consistency of the base heuristic, the rollout method is guaranteed to be terminating if it is applied to problems that exhibit special structure. The problem considered herein exhibits such a structure because the finite number of damaged components is equivalent to the finite node set in Bertsekas et al. (1997). Therefore, the rollout method in this study is terminating. In such a scenario, the optimized rollout algorithm could be used to guarantee performance without putting any restriction on the base heuristic to be used in the proposed formulation; however, a better base heuristic can potentially enhance further the computed rollout policy. Nevertheless, the problem herein does not require any special structure on the base heuristic for the rollout method to be sequentially improving, which is justified later in this section.

A base heuristic that admits sequential consistency in dynamic programming is analogous to the Markov or stationary policy. Similarly, the terminating rollout method defines a rollout policy that is stationary.

Two different base heuristics are considered in this study. The first base heuristic is a *random* heuristic denoted by *H*. The idea behind consideration of this heuristic is that in actuality there are cases where there is no thought-out strategy or the computation of such a scheme is difficult or impossible. It will be shown through simulations that the rollout formulation can accept a random base policy at the community level from a decision maker and improve it significantly. The second base heuristic is called a *smart* heuristic because it is based on the importance of components and expert judgment, denoted by $\hat{H}$. The importance factors used in prioritizing the components can accommodate the contribution of each component in the network. This base heuristic is similar in spirit the items (ii) and (v) listed above. Let H be a random heuristic; the state of this algorithm at the first decision epoch is $\tilde{j}_1$ where, $\tilde{j}_1 = (\tilde{x}_1)$. Similarly, the state of the algorithm at the α^{th} decision epoch is the α-solution given by $\tilde{j}_\alpha = (\tilde{x}_1, ..., \tilde{x}_\alpha)$, i.e., the algorithm generates the path of the states $(\tilde{j}_1, ..., \tilde{j}_\alpha)$. Note that $\tilde{j}_0$ is the dummy initial state of the algorithm H. The algorithm H terminates when $\alpha = i$ for objective 1, and $\alpha = t_{end}$ for objective 2. Henceforth, in this section, only objective 1 is considered without any loss of generality. Let $H_\alpha\left(\tilde{j}_\alpha\right)$ denote the cost-to-go starting from the α-solution, generated by applying H (i.e., H is used to evaluate the cost-to-go). The cost-to-go associated with the algorithm H is equal to the terminal reward, i.e., $\tilde{H}_\alpha\left(\tilde{j}_\alpha\right) = F_1(X_1)$. Therefore, $\tilde{H}_1\left(\tilde{j}_1\right) = \tilde{H}_2\left(\tilde{j}_2\right) = \ldots = \tilde{H}_i\left(\tilde{j}_i\right)$. This heuristic cost-to-go is used in Equation 3-10 to find an approximate solution. This approximation algorithm is termed "*Rollout on H*" (*RH*) owing to its structure, which is similar to the approximate dynamic programming approach rollout. The *RH* algorithm generates the path of the states $(j_1, j_2, ..., j_i)$ as follows:

$$j_\alpha = arg \min_{\delta \in N(j_{\alpha-1})} \tilde{J}(\delta),\ \alpha = 1, \ldots, i \qquad \textit{Equation 3-15}$$

where, $j_{\alpha-1} = (x_1, ..., x_{\alpha-1})$, and

$$N(j_{\alpha-1}) = \{(x_1, \ldots, x_{\alpha-1}, x) |\ x \in P_N(D_\alpha)\} \qquad \textit{Equation 3-16}$$

The *RH* algorithm improves sequentially with respect to H and ultimately outperforms H (see Ragi et al. (2015) for the details of the proof).

The *RH* algorithm described above is known as a *one-step lookahead* approach because the repair action at any decision epoch t (current step) is optimized by minimizing the cost-to-go given the repair action at t. It is possible to generalize this approach to incorporate multi-step lookahead. Suppose that we optimize the repair actions at any decision epoch t and $t + 1$ (current and the next step combined) by minimizing the cost-to-go given the repair actions for the current and next steps. This can be viewed as a two-step lookahead approach. Note that a two-step lookahead approach is computationally more intensive than the one-step approach. In principle, it is possible to extend it to step size λ, where $1 \leq \lambda \leq i$. However, as λ increases, the computational complexity of the algorithm increases exponentially. Particularly, when λ is selected equal to i at the first decision epoch, the *RH* algorithm finds the exact optimal solution by exhaustively searching through all possible combinations of repair action at each t, with computational complexity $O(S_i)$. Also, note that *RH* provides a tighter upper bound on the optimal objective value compared to the bound obtained from the original heuristic (either smart or random) approach.

3.5.1. Case 1: Repair Action Optimization of EPN for Household Units

The search space $P_N(D_t)$ undergoes a combinatorial explosion for modest values of N and D_t, at each t, until few decision epochs until moving into the trivial assignment problem, where the value of β_t is small. Because of the combinatorial nature of the assignment problem, it is desirable to reduce the search space for the rollout algorithm, at each t, without sacrificing on the performance. Because the EPN is considered only for household units in this section, it is possible to illustrate techniques to reduce the size of the search space for the above rollout algorithm that provide insight into formulating such methods for other similar problems.

Two representative methods to deal with the combinatorial explosion of the search space are considered, namely, 1-step heuristic and N-step heuristic. Note that these heuristics are not the same as the base heuristic H or $\hat{H}$. Before describing the 1-step and N-step heuristic, a discussion of H and $\hat{H}$ is necessary. Both H and $\hat{H}$, have a preordained method of assigning units of resources to the damaged locations. This order of assignment remains fixed at each t. In H, this order is decided randomly; while in $\hat{H}$, it is decided based on importance factors. This order can be illustrated further with the help of an example. Suppose that each of the components of the EPN is identified with serial numbers 1 to 327 as shown partially in Figure 3-1; the assignment of these numbers to the EPN components is based on $\hat{H}$ and remains fixed at each t. A damaged component with a lower number is always assigned a resource unit before a damaged component with a higher number, based on the availability of resource units. Therefore, the serial numbers depict the preordained priority assigned to components which is decided before initiating the decision-making. For example, if components 21 and 22 are both damaged, the decision maker will assign one unit of resource to component 21 first and then schedule repair of component 22, contingent on availability of resources. Such a fixed pre-decided assignment of unit of resource by heuristic algorithm H and $\hat{H}$ matches the definition of a consistent path generation in Bertsekas et al. (1997). Therefore, H and $\hat{H}$ are sequentially consistent. Note that the assignment of numbers 1 to 327 in Figure 3-1 is assumed only for illustration purposes; the rollout method can incorporate a different preordained order defined by H and $\hat{H}$.

Figure 3-1. The Labeled Electrical Power Network

Now consider the 1-step and N-step heuristics. In Figure 3-1, note that each successive EPN component (labeled 1-327), is dependent upon the prior EPN component for electricity; component 227 is dependent upon component 50, component 55 is dependent upon component 50, components in the branch 53-57 and 225-231 depend upon the component 52 for electricity, and so forth. This serial nature of an EPN can be exploited by representing it as a tree structure, as shown in Figure 3-2. Each number in the EPN tree represents an EPN component; each node represents a group of components determined by the label of the node, and the arcs of the tree capture the dependence of the nodes. If the number of damaged components in the root node of the EPN tree is greater than *N*, then it would be unwise to assign a unit of resource at the first decision epoch to the fringe nodes of the EPN tree because no benefit is derived until the damaged components in the root node are repaired. As soon as the number of damaged components in the root node of the EPN tree becomes less than *N*, only then is the assignment problem at other levels of the EPN tree explored.

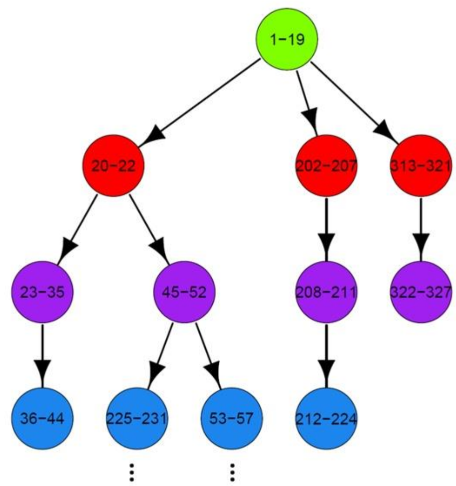

Figure 3-2. Electrical Power Network Tree

1-step Heuristic: Now increase the pool of candidate damaged components, where the assignment of units of resources must be considered, to all the damaged components of the next level of the EPN tree if and only if the number of damaged components at the current level of the EPN tree is less than *N*. Even after considering the next level of the EPN tree, if the number of damaged components is less than *N*, one additional step is taken to account for all damaged components two levels below the current level. This process is repeated until the pool of candidate damaged components is greater than or equal to *N*, or the levels of EPN tree are exhausted.

N-step Heuristic: It might be possible to ignore a few nodes at each level of the EPN tree and assign units of resources to only the most promising nodes. This is achieved in the N-step heuristic (here *N* in N-step is not same as N-number of workers). Specifically, if the number of damaged components at the current level of the EPN tree is less than *N*, then the algorithm searches for a node at the next level that has the least number of damaged components, adds these damaged components to the pool of damaged components, and checks if the total number of damaged components at all explored levels is less than *N*. If the total number of candidate damaged components is still less than *N*, the previous process is repeated at unexplored nodes until either the pool of damaged components is greater than or equal to N or the levels of the EPN tree are exhausted. In other words, rather than to consider the set (D_t) of all damaged components at each t, only a subset of D_t denoted by $\tilde{D}_t^1$ (1-step heuristic) and $\tilde{D}_t^N$ (N-step heuristic), are considered.

The performance of random H is illustrated in Figure 3-3. The faint lines depict plots of EPN recovery for multiple scenarios when H is used for decision making. Here the objective pursued by the decision maker is objective 2. The black line shows the mean of all the recovery trajectories, and the red lines show the standard deviation. Henceforth, in various plots, instead of plotting the recovery trajectories for all the scenarios, only the means of the different trajectories are compared.

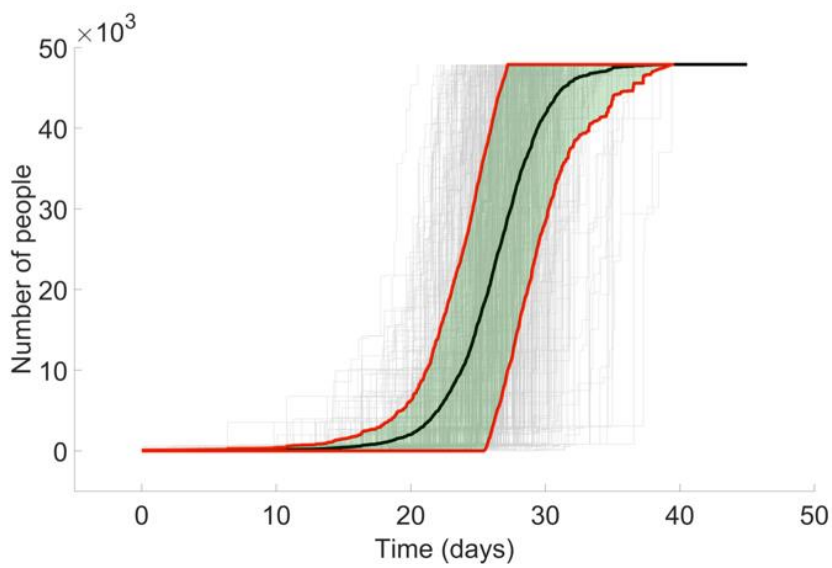

Figure 3-3. Electrical Power Network Recovery Due to Base Heuristic H with One Standard Deviation Band

Figure 3-4 shows the performance of the *RH* algorithm described above with respect to *H*. The simulation results demonstrate significant improvement over algorithm *H* when *RH* is used, for both the 1-step case and the N-step case. Another result is the performance shown by the 1-step heuristic with respect to the N-step heuristic. Even though the N-step heuristic skips some of the nodes at each level in EPN tree to accommodate more promising nodes into the search process, the performance improvement shown is minimal. Even though all the damaged components are not used to define the search space of the rollout algorithm and only a small subset is chosen with the use of either 1-step and N-step heuristic (limited EPN tree search), the improvement shown by *RH* over *H* is significant. This is because pruning the search space of the rollout algorithm using a subset of D_t (restricting an exhaustive search) is only a small part of the entire rollout algorithm.

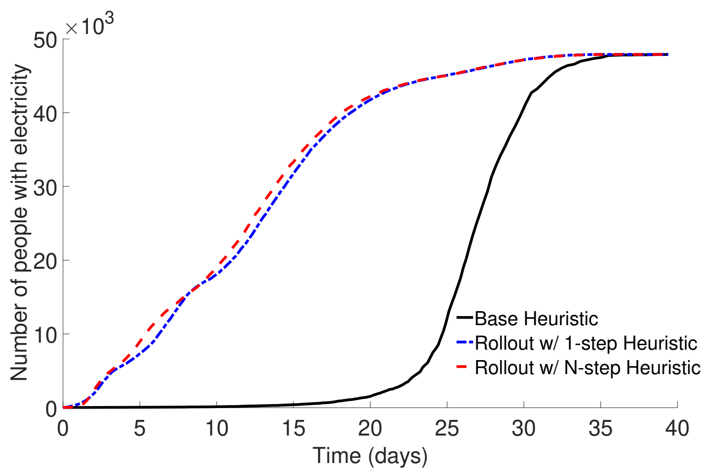

Figure 3-4. Comparison of Base Heuristic vs. Rollout Algorithm with 1-step vs. with N-step Heuristic for Objective 2

Figure 3-5 shows the histogram of values of $F_2(X)$ for multiple scenarios as a result of application of string-actions computed using *H* and *RH* (1-step and N-step heuristic). The rollout algorithms show substantial improvement over *H*, for the EPN restoration optimization.

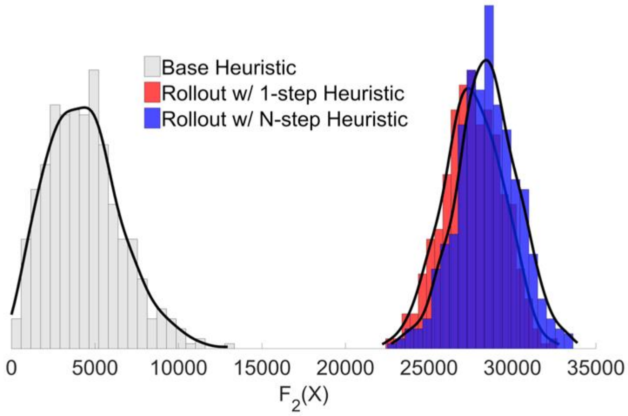

Figure 3-5. Histogram of $F_2(X)$ with Base (H), Rollout with 1-step and N-step Heuristic

Figure 3-6 shows simulation results for multiple scenarios when objective 2 is optimized, but when $\hat{H}$ is considered instead of H. This simulation study highlights some interesting characteristics of the rollout algorithm. In the initial phase of decision making, the algorithm $\hat{H}$ competes with the rollout algorithm $R\hat{H}$, and in fact slightly outperforms the rollout algorithm in many instances. However, after a period of 10 days, rollout (both 1-step and N-step heuristic) outperforms $\hat{H}$ significantly Because rollout has the lookahead property, it suggests conservative repair decisions initially (despite staying competitive with $\hat{H}$) in anticipation of overcoming the loss suffered due to initial conservative decisions. Optimizing with foresight is an emergent behavior exhibited by the optimization methodology presented herein, which can offer significant advantages in critical decision- making scenarios.

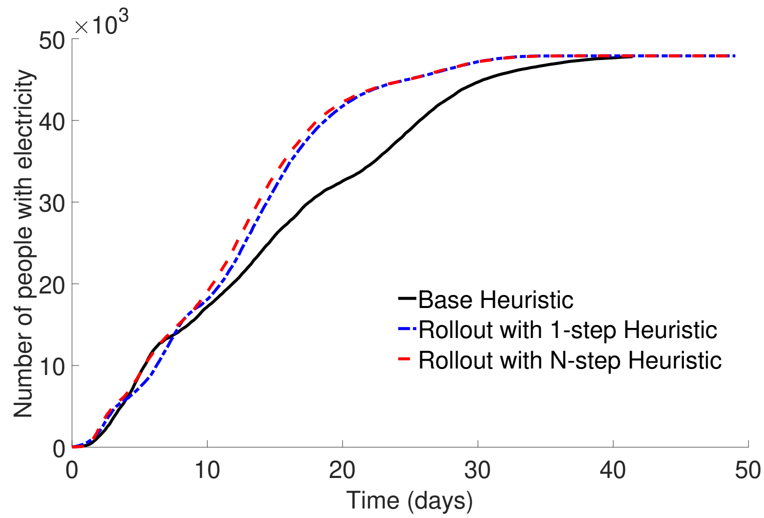

Figure 3-6. Comparison of Base Heuristic ($\hat{H}$) vs. Rollout with 1-step vs. N-step Heuristic for Objective 2

3.5.2. Case 2: Repair Action Optimization of EPN for Household Units & Retailers

It is difficult to come up with techniques similar to the 1-step and N-step heuristics to reduce the size of the search space $P_N(D_t)$ for objective 1 and objective 2, when multiple networks are considered simultaneously in the analysis. This is because any such technique must simultaneously balance the pruning of candidate damaged components in Figure 3-2 (to form subsets like $\tilde{D}_t^1$ and $\tilde{D}_t^N$), serving both food retailers and household units. There is no natural/simple way of achieving this as in the case of the 1-step and N-step heuristics where only household units were considered. When the decision process involves complex objective functions and interaction between networks, it is difficult to prune the action space in a physically meaningful way just by applying heuristics. Any such heuristic must incorporate the gravity model, explained in Chapter 2, and consider the network topology and actual physical position of important EPN components within the network. As shown above, methodology described above works well even if only a small subset of D_t ($\tilde{D}_t^1$ and $\tilde{D}_t^N$) is selected to construct

$P_N(D_t)$ to avoid huge computational costs. This is because the methodology leverages the use of the one-step lookahead property, with consistent and sequential improvement over algorithm H or $\hat{H}$, to overcome any degradation in performance as a result of choosing $\tilde{D}_t \ll D_t$. This is further justified in the simulation results shown in Figures 3-7 to 3-10.

In Figures 3-7 and 3-8, H is used as the base heuristic. This base heuristic is the same as the one used in the simulations shown in Case 1, which is not particularly well tuned for Case 2. Despite this, *RH* shows a stark improvement over H. Figure 3-7 shows that the rollout algorithm, with the random selection of candidate damaged components ($\tilde{D}_t$), significantly outperforms H for objective 1. When candidate damaged locations are selected randomly, in addition to the randomly selected damaged components, we the damaged components selected by $\hat{H}$ at each t are added to the set $P_N(D_t)$. Using the rollout algorithm, the mean number of days, over multiple damage scenarios, to provide electricity to γ times the total number of people is approximately 8 days, whereas for the base heuristic it is approximately 30. Similarly, Figure 3-8 shows that for objective 2 the benefit of EPN recovery per unit of time with rollout is significantly better than with H.

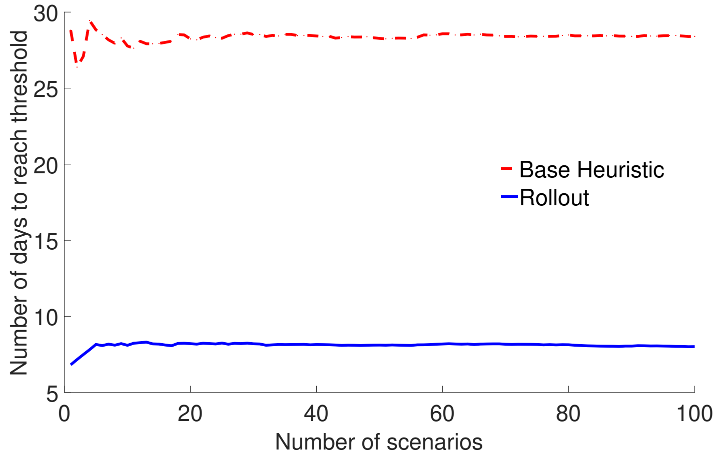

Figure 3-7. Cumulative Moving Average Plot for Objective 1 where γ=0.8 with Base Heuristic (H) and Rollout

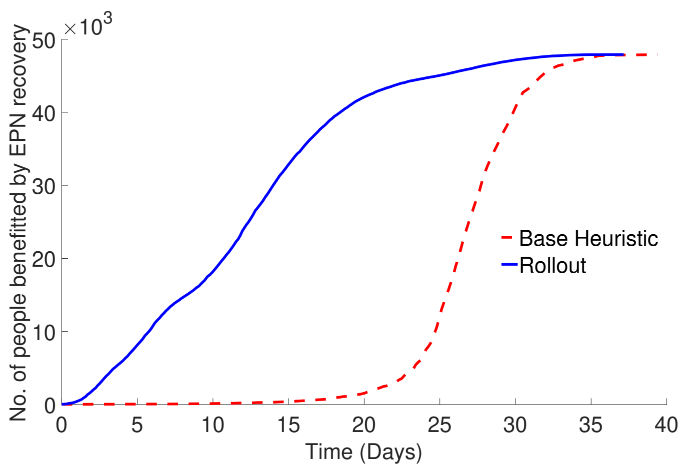

Figure 3-8. Comparison of Base Heuristic (H) vs. Rollout Algorithm

Figures 3-9 and 3-10 summarize the results for both the objectives when $\hat{H}$ is considered. In Figure 3-9, the number of days to reach a threshold γ = 0.8 as a result of $\hat{H}$ algorithm is better than H. However, the number of days to achieve objective 1 is still fewer using the rollout algorithm. The key inference from this observation is that rollout might not always significantly outperform the base heuristic but will never perform worse than the underlying heuristic

(Bertsekas et al., 1997). For simulations in Figures 3-9 and 3-10, the candidate damaged locations in defining the search space for the rollout algorithm are again chosen randomly and are a subset of D_t. As in the case of the simulations presented in Figure 3-7, damaged components selected by $\hat{H}$ are added to the set $P_N(\tilde{D}_t)$. The number of days required to restore electricity to 80% of the population in Figure 3-7 is a day less than that required in Figure 3-9. Despite performing rollout using a random base heuristic instead of the smart base heuristic used in the later. This can be attributed to three reasons: a) The damaged components in the set $(\tilde{D}_t)$ are chosen randomly for each simulation case; b) $\hat{H}$ was designed for the simulations in the past section and is not particularly well tuned for simulations when both household units and retailers are considered simultaneously; and c) $\hat{H}$ is used in simulations in Figure 3-9 to approximate the cost-to-go function whereas H is used in simulations in Figure 3-7 for the approximation of the scoring function.

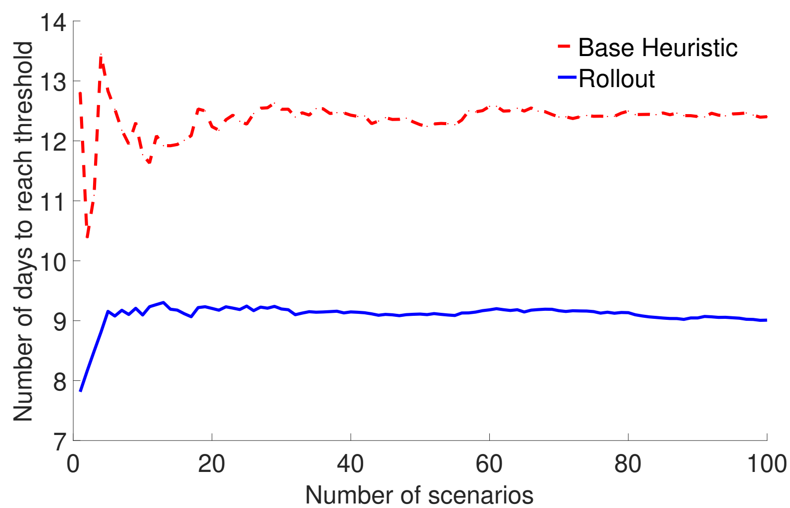

Figure 3-9. Comparison of Base Heuristic ($\hat{H}$) vs. Rollout for Objective 1

Figure 3-10 shows a behavior similar to Figure 3-6 where $\hat{H}$ might outperform rollout in the short-term (as a result of myopic decision making on the part of the heuristic); in the long run, however, rollout improves upon the string-actions provided by algorithm $\hat{H}$ significantly.

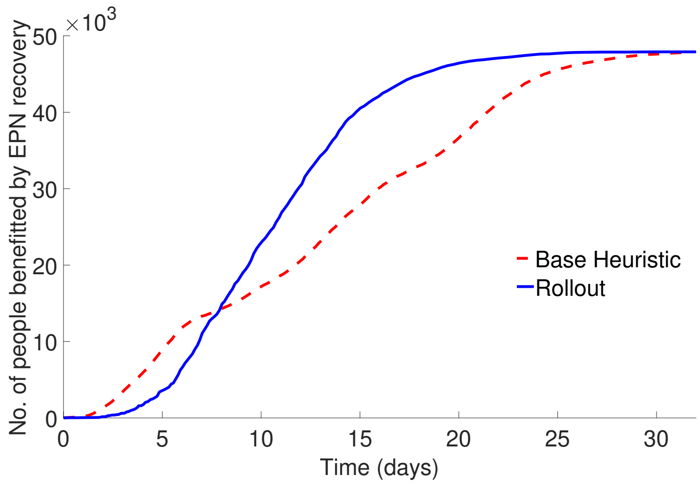

Figure 3-10. Comparison of Base Heuristic ($\hat{H}$) vs. Rollout for Objective 2

CHAPTER 4: OPTIMAL STOCHASTIC DYNAMIC SCHEDULING USING MARKOV DECISION PROCESSES

— *Uncertainty is an uncomfortable position. But certainty is an absurd one.”*

Voltaire

4.1. INTRODUCTION

Following the occurrence of an extreme natural or man-made event, community recovery management should aim at providing optimal restoration policies for a community over a planning horizon. Calculating such optimal restoration policies in the presence of uncertainty poses significant challenges for community leaders. Stochastic scheduling for several interdependent infrastructure systems is a difficult control problem with huge decision spaces. The Markov decision process (MDP)-based optimization approach proposed in this chapter incorporates different sources of uncertainties to identify suitable restoration policies. Efficient tools of MDPs are utilized to obtain optimal sequential actions. The application of approximate dynamic programming (ADP) and rollout algorithms along with the MDP formulation not only provides a robust and stochastic computationally tractable approach but also provides sufficient flexibility in the framework to consider any organizational recovery policies in an *on-line* manner. Combining these two decision-theoretic methods enables different sources of uncertainty in recovery management at the community level to be treated appropriately and efficiently.

In Chapter 4, the MDP formulation will be utilized, along with ADP techniques, to provide a comprehensive risk-informed decision-making framework that possesses the paramount properties, mentioned in Chapter 1.

The proposed method will treat the community as a complex system that embeds a collection of task-oriented systems. Therefore, the framework will compute the near-optimal recovery strategies for a complex system with respect to different objective functions. The role of risk-aversion on the part of decision makers will also be examined.

4.2. Technical Preliminaries

In dynamic programming DP and in MDP, a decision maker (also called an *agent*) interacts with a community (environment), by means of three signals: a state signal, which defines the state of the community, an action signal, which allows the decision maker to control the community, and a scalar reward signal, which provides the decision maker with feedback on his/her immediate performance. At each discrete time step, the decision maker takes the state measurement and makes a decision, which causes the community to transition into a new state. A reward is produced that assesses the quality of this transition. The decision maker receives information on the new state, and the whole cycle repeats until the end of recovery. State transitions can be deterministic or stochastic. The community dynamics and the reward function, together with the set of possible states and the set of possible actions (respectively called state space and action space), establish an MDP. Figure 4-1 depicts the interaction between a decision maker and the community.

In this section, we present the mathematical setting for a MDP. Powell (2007) provides a detailed treatment of the subject.

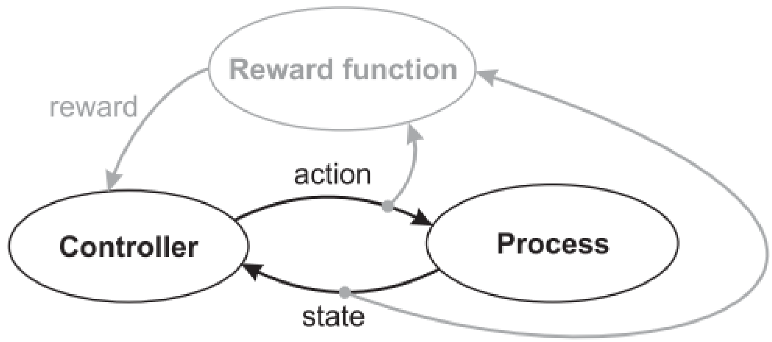

Figure 4-1. The Flow of Interaction in Markov Decision Process, Adopted from Busoniu et al. (2010)

4.2.1. MDP Framework

A Markov decision process (MDP) is defined by the six-tuple (*X, A, A(.), P, R, γ*), where *X* denotes the state space, *A* denotes the action space, $A(x) \subseteq A$ is the set of admissible actions in state *x*, $P(y|\ x, a)$ is the probability of transitioning from state $x \in X$ to state $y \in X$ when action $a \in A(x)$ is taken, $R(x, a)$ is the reward obtained when action $a \in A(x)$ is taken in state $x \in X$, and γ is the discount factor. Let Π be the set of Markovian policies (π), where $\pi: X \rightarrow A$ is a function such that $\pi(x) \in A(x)$ for each $x \in X$. The goal is to compute a policy π that optimizes the *expected total discounted reward* given by

$$V^{\pi}(x) := E\left[\sum_{t=0}^{\infty} \gamma^{t} R(x_t,\ \pi(x_t)) \middle| x_0 = x\right] \qquad \textit{Equation 4-1}$$

The *optimal value function* for a given state $x \in X$ is connoted as $V^{\pi^*} : X \rightarrow \mathbb{R}$ given by

$$V^{\pi^*}(x) = \sup_{\pi \in \Pi} V^{\pi}(x) \qquad \textit{Equation 4-2}$$

The optimal policy is given by

$$\pi^* = \arg\sup_{\pi \in \Pi} V^{\pi}(x) \qquad \textit{Equation 4-3}$$

Note that the optimal policy is independent of the initial state x_0. Also, the maximization takes place over policies π, where at each time t the action taken is $a_t = \pi(x_t)$.

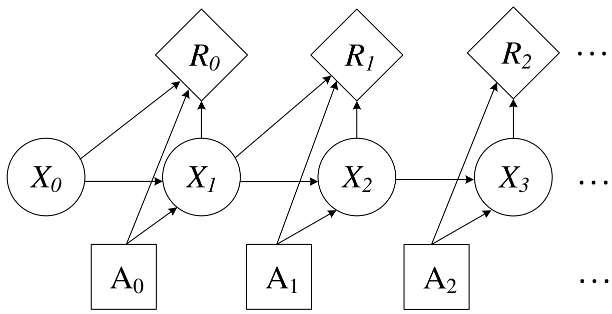

Figure 4-2. Decision Graph of a Markov Decision Process

The optimal policy, π^*, can be determined using different methods, including linear programming and dynamic programing. The methods of value iteration, policy iteration, policy search, etc. can find a strict optimal policy. Bellman's optimality principle (Chang et al., 2013) is especially useful for defining the Q-value function (described subsequently) , which plays a pivotal role in the description of the rollout algorithm. Bellman's optimality principle states that $V^{\pi^*}(x)$ satisfies

$$V^{\pi^*}(x) := \sup_{a \in A(x)} \left\{ R(x,a) + \gamma \sum_{y \in X} P(y \mid x,a) V^{\pi^*}(y) \right\} \qquad \textit{Equation 4-4}$$

in which the term within the braces in Equation 4-4 is denoted the Q-value function associated with the optimal policy π^*:

$$Q^{\pi^*}(x,a) := R(x,a) + \gamma \sum_{y \in X} P(y \mid x,a) V^{\pi^*}(y) \qquad \textit{Equation 4-5}$$

The $Q^{\pi}(x,a)$ value function associated with any policy, π, can be defined similarly.

4.2.2. Simulation-based MDP

For large-scale problems, the state, action or outcome space in the framework defined in the previous section must be represented in a compact form for a simulation-based representation (Fern et al., 2006). A simulation-based representation of a MDP is a 7-tuple ($X, A, A(.), P, R, \gamma, I$), where $|X|$ or $|A|$ ($|\cdot|$ = the cardinality of the argument set "·") is usually large, and the matrix representation of P and R is infeasible because the large dimensions of a typical community recovery problem. The function R returns a real-valued reward, given the current state, current action, and future state (R: $X \times A \times X \rightarrow \mathbb{R}$). Function I is a stochastic function that provides state according to the initial state distribution, while P is a function that returns the new state given the current state and action. Essentially, the underlying MDP model is implemented as a simulator.

4.2.3. Approximate Dynamic Programming in the MDP Context

Calculating an optimal policy using the methods above is usually infeasible for community resilience analysis due to the dimensions of the state and/or action spaces. The size of the state/action space grows exponentially with the number of *state/action variables*, a phenomenon referred to by Bellman as the *curse of dimensionality*. The computational costs of running a single iteration of the value iteration and policy iteration algorithm for the MDPs defined in the past section are $O(|X|^2|A|)$ and $O(|X|^2|A| + |X|^3)$, respectively. The computational cost of finding the optimal policy by directly solving the linear system provided by the Bellman equation is

O($|X|^3$ $|A|^3$) (Chang et al., 2013). Finally, the computational cost of an exhaustive direct policy search algorithm for a single trajectory consisting of K simulation steps is $3\left(\sum_{k=1}^{K} |X|^k\right) |A|^{|X|} |X|$, which is prohibitive for even small-sized problems (Busoniu et al., 2010).

Thus, these algorithms described above are computationally intractable for large problems involving resilience assessment or recovery of a real-size community and approximate solutions are necessary. To this end, several algorithms have been developed in the realm of Approximate Dynamic Programming (ADP) that enable near-optimal restoration policies to be identified. One popular class of algorithms involves approximating the Q-value function in Equation 4-5. However, it often is difficult in practice to identify a suitable approximation to the Q-value function for practical, large-scale problems. Thus, in the following, a promising class of ADP algorithms based on the *rollout* algorithms introduced in Chapter 3 are utilized that sidesteps these difficulties by avoiding an explicit representation of the Q-value function.

4.2.4. Rollout in the MDP Context

While computing an optimal policy for an MDP is often quite difficult because of the curse of dimensionality, policies based on heuristics (termed as *base policies*) can be readily identified in many cases. As noted in Chapter 3, the principal idea behind the rollout technique is to improve upon the performance of the base policy through various means. Therefore, the base policy does not have to be close to optimal. In this study, we focus on improvement of the base policy through simulation. This idea was first proposed for stochastic scheduling problems by Bertsekas and Castanon (1999). Instead of the classical DP scheme (Bertsekas, 2017), the agent "rolls out" or simulates the available policy over a selected finite horizon $H< \infty$; thereafter, the agent implements the most "promising" action in an *on-line* fashion. In *on-line* methods, unlike classical *off-line* techniques, optimal actions are calculated only for the states realized in the real-world (reachable states); the idea is to conserve computational effort on the unreachable states. Conversely, in *off-line* computations the policy is pre-computed for all the states and stored; then, the agent selects an optimal action from the stored policy corresponding to the observed evolution of the system (Chang et al., 2013).

Monte Carlo (MC) simulations assess the Q-value function on demand. To estimate the Q-value function ($\hat{Q}^{\pi}(x,a)$ represents the estimate) of a given state-action pair (x, a), N_{MC} number of trajectories are simulated, where each trajectory is generated using the policy π, with length H, and starting from the pair (x, a). The assessed Q-value function is typically taken as the average of the sample returns obtained along these trajectories:

$$\hat{Q}^{\pi}(x,a)=\frac{1}{N_{\mathrm{MC}}}\sum_{i_0=1}^{N_{\mathrm{MC}}}\left[R(x,a,x_{i_0,1})+\sum_{k=1}^{H}\gamma^{k}\,R(x_{i_0,k},\pi(\mathrm{x}_{i_0,k}),x_{i_0,k+1})\right] \qquad \textit{Equation 4-6}$$

For each trajectory i_0, the first state-action pair to (x, a) is fixed; the simulator provides the next state $x_{i_0,1}$ when the current action a in state x is completed. Thereafter, actions are chosen using the base policy. Note that if the simulator is deterministic, a single trajectory suffices, while in the stochastic case, a sufficient number of trajectories (N_{MC}) must be pursued to approximate the Q-value function. This study focuses on the rollout policy computed with single-step look-ahead. An agent can consider multistep look-ahead, at an added computational cost, to extract maximum performance out of the solution technique. The number of look-ahead steps mainly depends on the scale of the problem, computational budget, real-time constraints, and agent's preferences. An important property of the rollout algorithm, as noted previously, is that it improves upon the performance of the underlying base policy, if the base policy is not *strictly* optimal. The rollout policy computed using this method is not necessarily strict-optimal, but it is guaranteed that it will never perform worse than the underlying base policy.

4.3. POST-HAZARD RECOVERY FORMULATION

Following an earthquake, the EPN and WN systems and components either remain undamaged or exhibit a level of damage which is determined from the seismic fragility curves. Suppose that an agent must restore a community that includes several networks, which function as a System of Systems (SoS). Let M be the total number of damaged components at time t, and let t_c denote the decision time at which all the damaged components are repaired (M=0). The agent has only a limited number of RUs that can be assigned, which is usually much less than M, especially in severe disasters that impact large communities. The RUs differ from network to network because of the skill of repair crews and qualities of the required tools. The problem is to assign the available RUs to M damaged components in a manner that best achieves the community objectives and policymakers' preferences.

The following assumptions are made: (1) The agent has access to all the damaged component for repair purposes; (2) A damaged component only needs one RU to be repaired and assigning more than one RU would not reduce the repair time (Ouyang et al., 2012); (3) The agent has limited RUs for each network and cannot assign a RU of one network to another (e.g., a WN RU cannot be assigned to the EPN); (4) The agent can preempt the assigned RUs from completing their work and reassign them at different locations to maximize the beneficial outcomes. (5) Once a damaged component is repaired, all assigned RUs are available for re-assignment even if their assigned components are not fully repaired. It is also possible to let the RU continue the repair work at the same location in the next time slot according to the objectives of the agent. Such assignment is referred to as *preemptive scheduling*, which allows the agent to be flexible in planning and is particularly useful when a central stakeholder manages an infrastructure system; see (Nozhati et al., 2018b) for a discussion on *non-preemptive scheduling*. (6) The agent can deal with stochastic scheduling, where the outcome of the repair actions is not fully predictable and can be quantified probabilistically. The unpredictability arises mainly from the randomness in the repair times (see Table 4-1). The MDP simulator exhibits stochastic behavior owing to the random repair times. On the other hand, the alternative perspective, where the outcome of actions is fully predictable (Chapter 3), is also an active research topic (Nozhati et al., 2019b).

The proposed MDP methodology is applied to the modeled EPN and WN described in Chapter 2. Restoration times are synthesized based on exponential distributions (Nozhati et al., 2018a, 2018b; Sarkale et al., 2018; FEMA, 2003), as summarized in Table 4-1. The proposed framework, nevertheless, allows one to use any arbitrary distribution. The pipe-restoration time in the WN is based on repair rate or number of repairs per kilometer (Adachi and Ellingwood, 2009).

Table 4-1. The Expected Repair Times (Unit: Days)

	Damage states			
Component	Minor	Moderate	Extensive	Complete
Electric sub-station	1	3	7	30
Transmission line component	0.5	1	1	2
Distribution line component	0.5	1	1	1
Water tanks	1.2	3.1	93	155
Wells	0.8	1.5	10.5	26
Pumping plants	0.9	3.1	13.5	35

4.4. MARKOV DECISION PROCESS FORMULATION

Suppose that x_t^E and x_t^W represent the damage states of the EPN and WN at time, *t,* respectively. x_t^E is a vector of length L_t^E, where L_t^E is the number of damaged components in EPN. Each element of the vector x_t^E is in one of the five damaged states (counting no damage as one possible state) in Table 4-1. Similarly, define x_t^W ($\left|x_t^W\right| = L_t^W$), where L_t^W is the number of damaged components in the WN at time slot *t*. Let N_E and N_w denote available RUs for the EPN and WN, respectively: $N_{\mathrm{E}} \le L_{\mathrm{t}}^{\mathrm{E}}$ and $N_W \le L_{\mathrm{t}}^W$. The tuples of the MDP framework are defined as follows:

- *States X*: x_t denotes the state of the damaged components in the community at time *t* as the stack of two vectors, x_t^E and x_t^W, :

$$x_t := \left(x_t^E, x_t^W\right) \quad s.t. \quad |x_t| = L_t^E + L_t^W \qquad \textit{Equation 4-7}$$

- *Actions A*: a_t denotes the repair actions to be carried out on the damaged components at time *t*, as the stack of two vectors, a_t^E and a_t^W ,

$$a_t := \left(a_t^E, a_t^W\right) \quad s.t. \quad |a_t| = L_t^E + L_t^W \qquad \textit{Equation 4-8}$$

  where both, a_t^E and a_t^W , are binary vectors of length L_t^E and L_t^W, respectively, where values of zero and unity mean no repair and conduct repair, respectively. a_t^E and a_t^W represent the actions (no repair, repair) to be performed on the damaged components of the EPN and WN.

- *Set of Admissible Actions A (x_t)*: The set of admissible repair actions *A* (x_t) for the state x_t is the set of all possible binary combinations of integers one and zero such that each element of this set is of size $L_t^E + L_t^W$ and each element has N_E number of ones in the first L_t^E locations and N_w number of ones at the remaining locations. The interdependence between networks causes the size of the set of admissible actions to increase, as follows:

Let D_t^E be the set of all damaged components of the EPN before a repair action a_t is performed. $P\left(D_t^E\right)$ denotes the powerset of D_t^E;

$$P_{N_E}\left(D_t^E\right) := \left\{C \in P\left(D_t^E\right) : |C| = N_E\right\} \qquad \textit{Equation 4-9}$$

where $\left|P_{N_E}\left(D_t^E\right)\right|$ represents the size of the set of admissible actions for the EPN. $P_{N_W}\left(D_t^W\right)$ can be defined similarly. The size of the set of admissible actions, at any time *t*, is the product of the size of set of admissible actions for EPN and WN:

$$|A(x_t)| := \left|P_{N_E}\left(D_t^E\right)\right| \times \left|P_{N_W}\left(D_t^W\right)\right| \qquad \textit{Equation 4-10}$$

Therefore, when multiple networks are considered simultaneously, the size of $A\ (x_t)$ grows very fast. Searching exhaustively over the entire set $A\ (x_t)$ for calculating the optimal solution is not possible.

- *Simulator P*: Given x_t and a_t, the simulator *P* provides the new state x_{t+1}. *P* is a *generative model* that can be implemented as a simulator without any explicit knowledge of the actual transitions. It considers the interconnectedness within and between networks to compute the cascading effects of a_t through the whole community and recovery process. As stated previously, a compact representation of *P* is important for large-scale problems.

It is assumed that as soon as at least one of the damaged components is repaired, the repair action a_t is considered complete. Define this completion time at every *t* by $\hat{t}_t$. Recall that the repair time is exponentially distributed. The completion time is the minimum of the repair times at one or more damaged locations, where repair action is being performed. The minimum of exponential random variables is exponentially distributed; therefore, the completion time is also exponentially distributed (Aslett, 2012). The sojourn time (a.k.a. the holding time) is the amount of time that the system spends in a specific state. For an MDP, the sojourn time, t_s, is exponentially distributed (Bertsekas, 2017; Aslett, 2012; Ibe, 2013). Note that for the MDP formulation, $\hat{t}_t$ is equal to t_s.

A natural question that arises is "does this formulation work when the repair times are non-exponential?" In that case, the completion time is not exponentially distributed. However, in the present problem formulation, the completion time is the same as the sojourn time. Thus, the sojourn time would not be exponentially distributed, which is inconsistent with the Markovian assumption. This can be remedied simply by incorporating the lifetime of the damaged component into the state definition. The lifetime of the damaged component is the time required for the damaged component to be repaired after the occurrence of hazard. With this new definition of the state space, the sojourn time is not the same as the completion time $\hat{t}_t$, and the sojourn time is exponentially distributed. Here the completion time $\hat{t}_t$ is still the minimum of the repair time at one or more damaged locations but with any underlying distribution of the repair times. Thus, the framework is sufficiently flexible to accommodate repair times with any underlying distribution.

- *Rewards R*: Two different objectives are pursued for the agent:

  The first objective (hereinafter Obj. 1) is to optimally plan decisions so that a certain percentage of the total inhabitants (denoted by threshold α) *benefit by the recovery of utilities* in the shortest period of time, implying that household units not only have electricity and water by also have access to a functional retailer that has electricity and water. Conversely, even if a household unit has electricity and water and has access to a retailer that has electricity but not water, the household unit does not benefit from the recovery actions. The mapping of people in the gridded rectangle to a food retailer is determined by the gravity model. The aim here is to optimally plan the repair actions to minimize the time it takes to achieve the benefit from utilities to α percent of people. The reward function for the first objective is defined as:

$$R_1(x_t, a_t, x_{t+1}) = \hat{t}_t \qquad \textit{Equation 4-11}$$

The second objective (hereinafter Obj. 2) is to optimally plan decisions so that the maximum number of inhabitants are *benefited from recovery of utilities* per unit of time (days, in the present case). Therefore, in the second case, there are two objectives embedded in the reward as follows:

$$R_2(x_t, a_t, x_{t+1}) = \frac{r}{t_{rep}} \qquad \textit{Equation 4-12}$$

where r is the number of people deriving benefit from utilities after the completion of a_t, and t_{rep} is the total repair time to reach x_{t+1} from any initial state x_0 (i.e., $t_{rep} = \sum \hat{t}_t$). Note that the reward function is stochastic because the outcomes of the repair action are stochastic.

- Initial State *I*: As mentioned in Section 3, the stochastic damage model of the EPN and WN components can be obtained by the fragility curves. The initial damage states associated with the components will be provided by these models.

Discount factor γ: In this study, the discount factor is set equal to 0.99 (Howard, 1960). A measure of how "far-sighted" the agent is in considering its decisions. The discount factor weighs the future stochastic rewards at each discrete time *t*.

4.5. Results and Discussion

The simulation results are divided into two sections. The first section caters to risk-neutral decision makers, and the second section caters to risk-averse decision makers (Cha and Ellingwood, 2014; Tversky and Kahneman, 1992). Each of these sections is further divided into two sub-sections to demonstrate the performance of the method developed in the preceding section on two separate objectives functions. When *Objective 1* is considered, the reward function in the MDP is given by Equation 4-11, while for *Objective 2*, the reward function is given by Equation 4-12. For all the simulation results presented henceforth, N_{MC} in Equation 4-6 and Equation 4-13 was selected so that the standard deviation of the estimated Q-value $\hat{Q}^{\pi}(x,a)$ is below 0.05.

As mentioned in Chapter 3, the most feasible base policy for community recovery planning often is the current recovery strategy of regional responsible companies or organizations. However, there is no restriction on the selection of a policy as a base policy. We proposed the alternatives for the definition of base policies for recovery management problems in Nozhati et al. (2019b) and Chapter 3. In this study, the base policy is defined based on expert judgment and importance analyses that prioritize the importance of components owing to their contribution to the overall risk. Specifically, the restoration sequence defined by our base policy for EPN is transmission line, power substation, and distribution lines to downtown and water pumps; similarly, the base policy for WN involves water wells, water tanks, BPS, and pipelines to downtown and food retailers.

4.6. Mean-based Stochastic Optimization

The mean-based optimization is suited to risk-neutral decision makers (Meidani and Ghanem, 2015). In this approach, the optimal policy is determined based on the optimization of the Q-value function, where the estimate of the Q-value function $\hat{Q}^{\pi}(x,a)$ is based on the mean of N_{MC} trajectories, as demonstrated in Equation 4-6. Calculating the Q-value based on the expected Q-value of N_{MC} trajectories may not always be appropriate, especially in the case of risk-averse decision makers. However, it has been shown that the mean-based stochastic optimization approach can be appropriate when the objective function properly encodes the risk preferences of policymakers (Bertsekas, 2017). Nevertheless, we demonstrate the performance of our method when the decision maker has a risk-averse attitude to planning.

4.6.1. Implementation of Rollout Algorithm for Objective 1

The rollout algorithm with respect to Obj. 1 identifies recovery strategies to minimize the time it takes to provide the utilities to α percent of people in the community. In this formulation, the selection of α depends on the preferences of policymakers. For our simulation, we selected α=0.8, implying that we want to provide the benefit of the utility recoveries to 80% of the people in the community in a minimum amount of time.

Figure 4-3 shows the performance of the rollout and base policies for Objective 1. The rollout algorithm optimizes the restoration of two networks, EPN and WN, simultaneously to provide utilities for 80% of people in 19.3 days following the earthquake, while the base policy completes this task in 26.1 days. This 35% improvement over the entire recovery period indicates the performance of rollout at the community level. Figure 4-3 also highlights the look-ahead property of rollout. Although the base policy showed better performance during the first 15 days following the earthquake, the rollout algorithm outperformed the base policy during the recovery period. By selecting conservative repair decisions initially, rollout can balance the desire for low present cost with the undesirability of high future costs.

The performance of rollout on the individual food retailers is summarized in Table 4-2. Note that the base policy restored EPN and WN to Safeway, Nob Hill Foods, and Mi Pueblo Food faster than the rollout policy; however, the base policy is incapable of determining the recovery actions to balance the rewards so that 80% of people benefit from the restoration of utilities (our true objective).

Table 4-2. Performance of Rollout vs. Base Policy for the First Objective Function for the Retailers

Policy	Recovery time	Costco	Walmart	Target	Safeway	Nob Hill Foods	Mi Pueblo Food
Base	26.06	0.31	0.31	21.02	5.91	5.91	2.76
Rollout	19.23	0.31	0.31	15.95	18.33	18.33	8.01

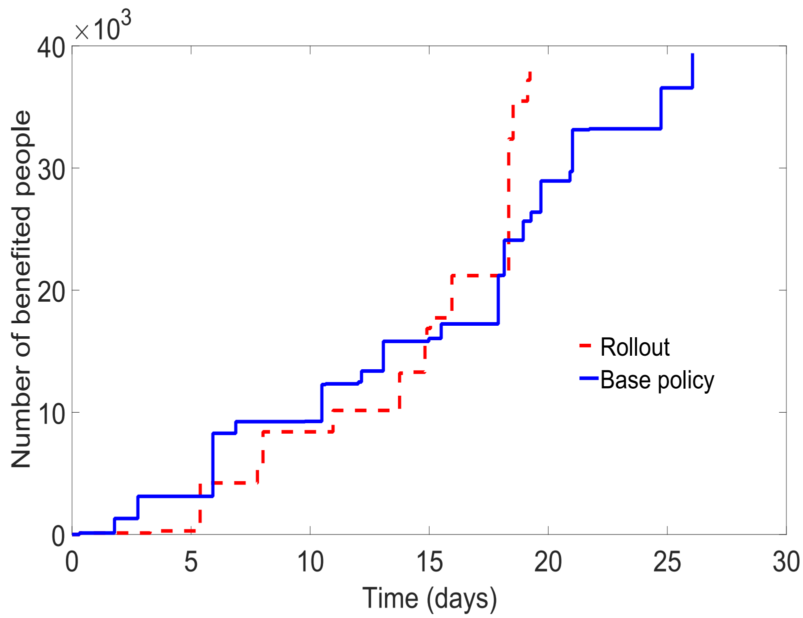

Figure 4-3. Performance of Rollout vs. Base Policy for the First Objective Function

After 80% of the people have benefitted from utility restoration, the progress in restoration of the EPN and WN continues to be evaluated. Even though the objective of providing the benefit of utilities to 80% of the population has been met, 25% of the EPN components remain unrepaired. This interesting result shows the importance of prioritizing the repair of the components of the network so that the objectives of the decision maker are met. Because the objective here was to restore utilities so that 80% of people would benefit from the restoration in a minimum amount of time, the algorithm prioritized repair of only those components that would have the maximum effect on that objective without wasting resources on the repair of the remaining 25% of EPN components.

4.6.2. Implementation of Rollout Algorithm for Objective 2

The rollout algorithm applied to Objective 2 identifies recovery strategies that maximize the number of inhabitants per day that benefit from the strategy selected. In other words, the algorithm must maximize the area under the restoration curve normalized by the total recovery time. This objective function is specifically defined to match the definition of the common resilience index, which is proportional to the area under the restoration curve (Bruneau et al., 2003). Figure 4-4 depicts the performance of base policy and the corresponding rollout policy. It highlights the look-ahead property of the rollout algorithm for Obj. 2.

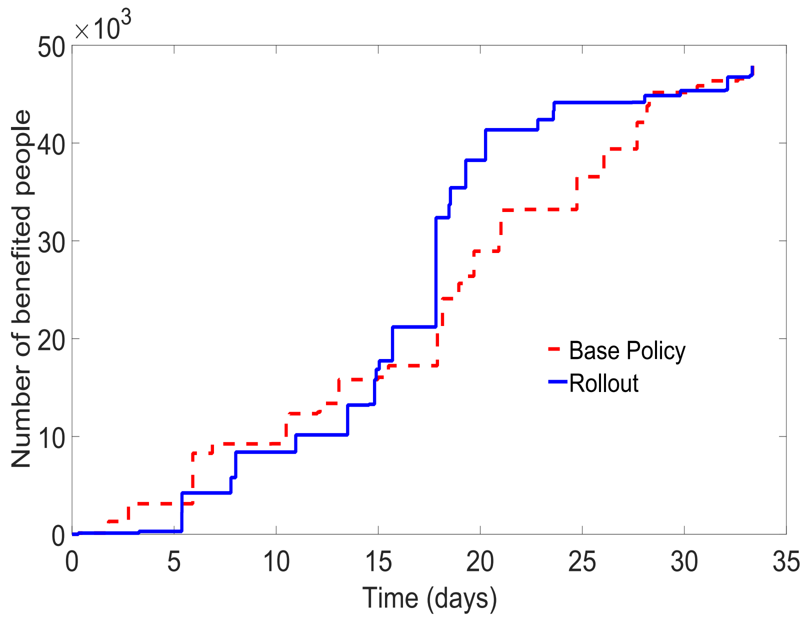

Figure 4-4. Performance of Rollout vs. Base Policy for the Second Objective Function

The performance of the rollout algorithm was analyzed for the individual networks. One of the main reasons for this analysis is that these networks are restored and maintained by different public or private entities who would like to know how rollout would perform for their individual systems. The recovery actions a_t, were determined using the rollout policy for the combined network that considers all the interdependencies (for Obj. 2), and the performance of these repair actions on individual networks was subsequently checked.

First, we check the performance of the repair actions on the EPN network, calculating the effect of EPN restoration on only the household units. The results are depicted in Figure 4-5. The base policy leads to EPN recovery so that the mean number of people provided with electricity is 24,229 per day, while the rollout policy provides electricity for 27,689 people on average. Second, the performance of the repair actions on the EPN is checked, but the effect of EPN restoration on both household units and retailers is considered. In this analysis, summarized in Figure 4-6, people derive benefit of EPN recovery when their household unit has electricity and they go to a retailer that has electricity. In this case, the mean number of people who benefit from the EPN recovery owing to the base policy is 23,155/day, whereas that owing to the rollout policy is 25,906/day. Third, the performance of the repair actions on the WN is checked, calculating the effect of WN restoration on only the household units, as illustrated in Figure 4-7. In this case, the mean number of people with potable water under the base and rollout policies is 31,346/day and 25,688/day, respectively. Finally, the performance of the repair action on the WN is checked, but where the effect of WN restoration on both household units and retailers is considered. In this case, people benefit from WN recovery when their household unit has water, and they go to a retailer that has water. In this case, the mean number of people with potable water under the base and rollout policies is 31,346/day and 25,688/day, as shown in Figure 4-8.

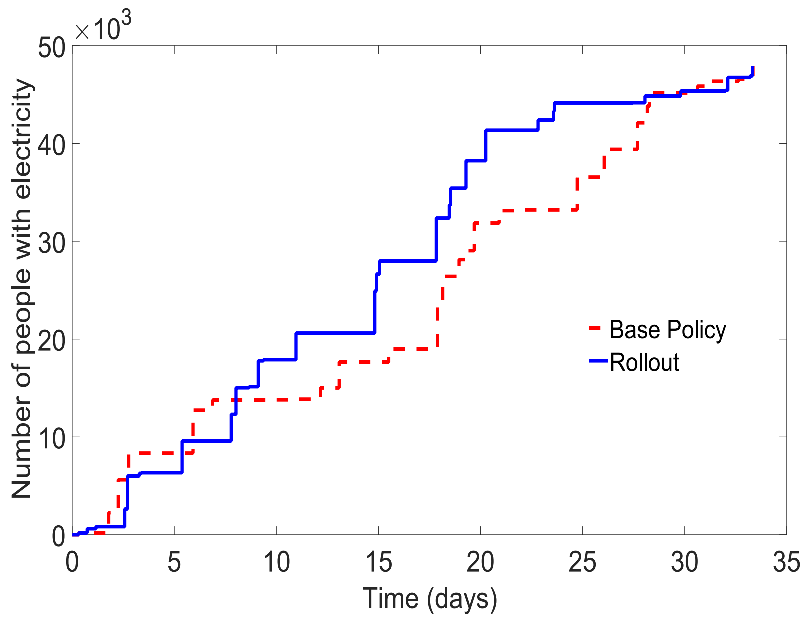

Figure 4-5. The Performance of Policies to Provide Electricity for Household Units

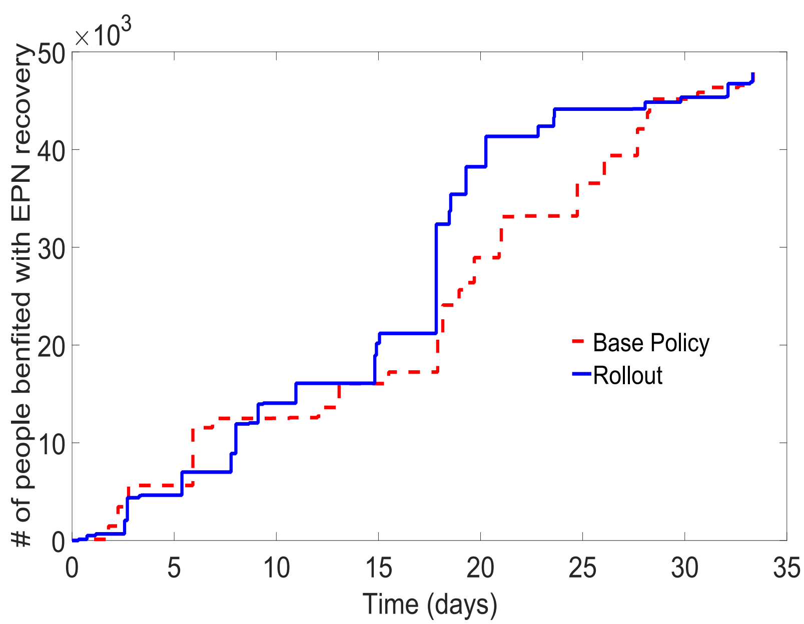

Figure 4-6. The Performance of Policies to Provide Electricity for Household Units and Retailers

It is interesting to note that the rollout policy need not outperform the individual base policy when the recovery of each individual network is considered separately because in our framework, the calculation of recovery actions due to rollout considers the *combined* network and corresponding *interdependencies* that outperforms the base policy as shown in Figure 4-3 to 4-6. Our objective considers two networks as one complex system (or SoS), which is captured in the definition of the benefit, and is not reflected in the restoration of a single network alone. Figures 4-7 and 4-8 indicate that the concerns of individual stakeholders must be alleviated when recovery is performed based on interdependencies in the network. Nozhati et al. 2019b and Sarkale et al. 2018 provide a thorough examination of the performance of rollout when the EPN and WN are considered separately. Furthermore, the number of days required to restore the WN is less than what is required to restore EPN, even when the optimized recovery actions for the combined network are used to evaluate the performance of the individual network restoration (see Figures 4-5 and 4-8). This behavior can be attributed to a lesser number of WN components being restored compared to the number of EPN components.

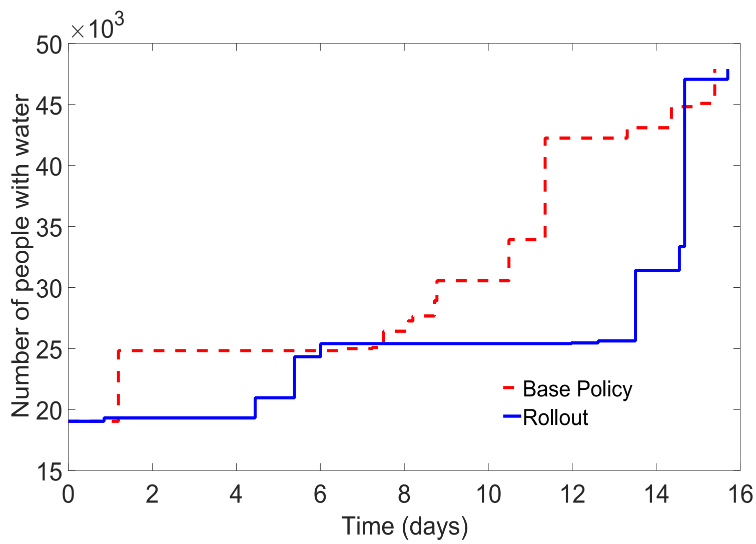

Figure 4-7. The Performance of Policies to Provide Potable Water for Household Units

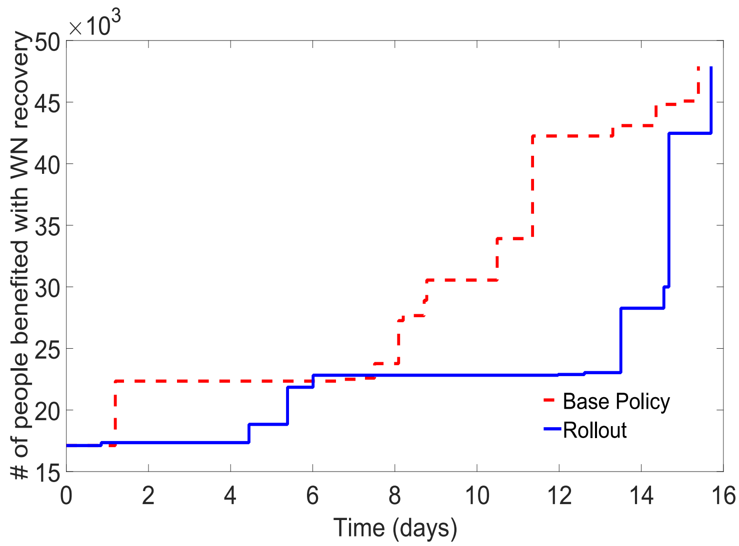

Figure 4-8. The Performance of Policies to Provide Potable Water for Household Units and Retailers

4.7. WORST-CASE STOCHASTIC OPTIMIZATION

Mean-based stochastic optimization seeks to identify the most cost-efficient repair actions in the face of uncertainty under the assumption that the decision maker has a risk-neutral attitude. This assumption has been criticized on several counts (Tversky and Kahneman, 1992; Von Neumann and Morgenstern, 2007). Research on risk attitudes has revealed that most decision makers are not risk-neutral in the face of a low-probability threat or hazard. Moreover, policymakers and community stakeholders are not risk-neutral, especially when considering large systems at the community level that influence public safety (Cha and Ellingwood, 2012). Finally, a stochastic model of uncertainty may not be possible in many practical problems in which only limited data exist and, accordingly, policy-makers tend to be more risk-averse (Bertsekas, 2017). These observations lead us to study the performance of the proposed rollout algorithm for risk-averse policymakers.

Risk-averse policymakers tend to be more worried about extrema than expected consequences of uncertainty. Worst-case optimization (a.k.a. robust optimization) is employed for MDPs to allow for risk-averse behavior (Iyengar, 2005; Meidani and Ghanem, 2015; Nilim and Ghaoui, 2005). Note that Obj. 1 involves a minimization problem, while Obj. 2 addresses a maximization problem. Both Objs. 1 and 2 require the use of N_{MC} trajectories. However, unlike in Equation 4-6, the mean of the N_{MC} estimated Q-values is not used to approximate the original Q-value function in Equations 4-4 and 4-5; rather, depending on whether Obj. 1 or Obj. 2 is considered, the maximum or minimum value among the N_{MC} trajectories is used to represent worst-case behavior. If i_0^* maximizes Equation 4-6, where $i_0^* \in \{1,\ldots,N_{MC}\}$, the worst-case *Q-value* estimation for Obj. 1 is represented in Equation 4-13 and is used in Equation 4-4. Conversely, for Obj. 2, i_0^* minimizes Equation 4-6, where $i_0^* \in \{1,\ldots,N_{MC}\}$,

$$\hat{Q}^{\pi}(x,a) = R(x,a,x_{i_0^*,1}) + \sum_{k=1}^{H} \gamma^k R(x_{i_0^*,k}, \pi(\mathrm{x}_{i_0^*,k}), x_{i_0^*,k+1}) \qquad \textit{Equation 4-13}$$

When Obj. 1 is considered, the number of days required to reach the threshold of α=0.8 under the base policy under worst-case optimization is 26.1 days, whereas under rollout, it is 19.7 days, a 32% improvement that signifies a desirable performance of the proposed methodology for the risk-averse policymakers. Figure 4-9 shows the performance of rollout for Obj. 2, where the number of people deriving benefit from utilities per day because of recovery actions under the base and rollout policies is 22,395/day and 24,478/day. Figure 4-9 also illustrates the look-ahead property, which is characteristic of the rollout algorithms. Finally, the performance of rollout for the individual networks is summarized in Table 4-3 and Figure 4-10. The results indicate that risk-averse policymakers should not presume that rollout will outperform the base policy when the EPN and WN are considered separately.

Table 4-3. The Performance of Policies in Different Cases for the Worse-case Optimization

Case	Base policy	Rollout policy
EPN restoration for household units	24229	27897
EPN restoration for household units and retailers	23155	26159
WN restoration for household units	31346	25966
WN restoration for household units and retailers	30099	23535

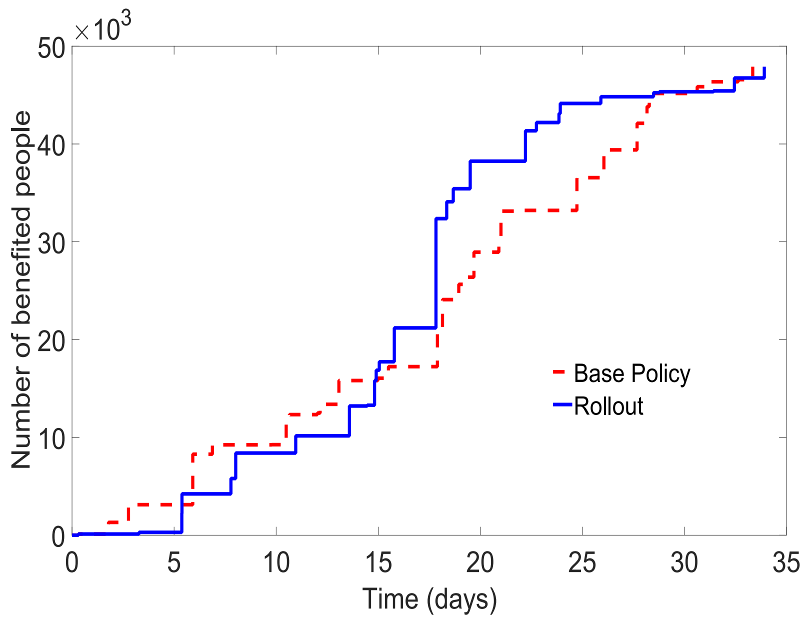

Figure 4-9. Performance of Rollout vs. Base Policy in the Worst-case Optimization for the Second Objective Function

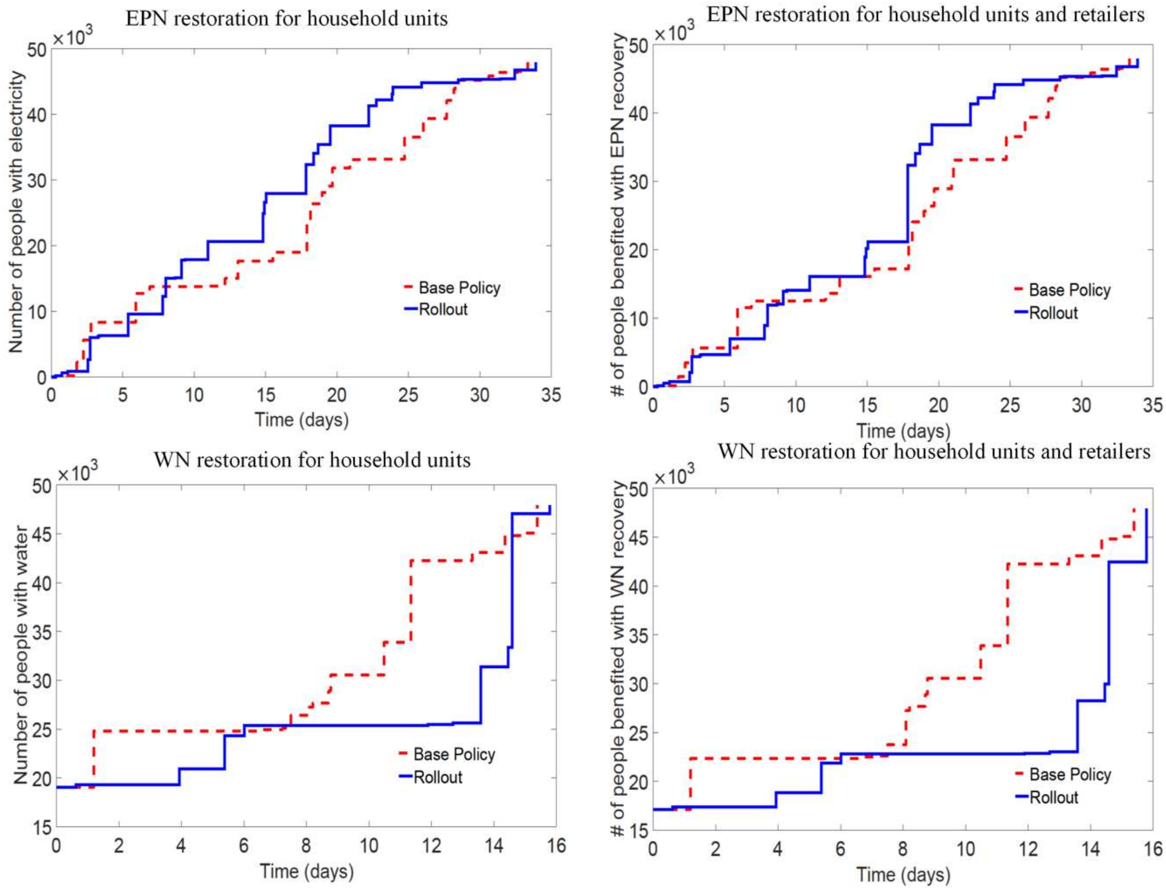

Figure 4-10. The Performance of Policies in Different Cases for the Worse-case Optimization

In summary, the results presented in this section illustrate the desirable performance of the rollout algorithm when a decision-maker is risk-averse. The individual attitudes toward risk can be dependent on the personalities of policymakers and stakeholders of a community and be influenced by many factors, such as the community properties, type of hazard, available resources and time, existing information about the uncertainties and prior experience with similar hazards, to name but a few. Lastly, because of the stochastic approximation involved in the computation of the estimated *Q*-values, it is not possible to compare the performance of the mean-based and worst-case optimization methods proposed above.

CHAPTER 5: ADDRESSING LARGE-SCALE COMMUNITIES' RECOVERY

—*Risk is just an expensive substitute for information.*"

Adrian Slywotzky and Karl Weber

5.1. Introduction

Optimal recovery decisions for community resilience assurance post-hazard involve a combinatorial decision-making problem under uncertainty. The last remaining major bottleneck with the rollout solution proposed above is that for the current state, the Q values must be determined for all possible actions. This large-scale computation can be costly and impractical for large-scale communities and metropolitan areas. This chapter proposes different methods to enhance the efficiency of the rollout algorithm for large-scale communities to provide near-optimal recovery strategies in a timely fashion.

Rollout can be implemented regardless of the size of the state space. However, the execution of rollout algorithm that exhaustively searches the entire action space is potentially computationally expensive. In the case of exhaustive search, the rollout algorithm linearly depends on the action space. There are several more efficient optimization techniques than exhaustive search so that the estimation of the most promising actions can be accelerated.

5.2. SIMULATED ANNEALING[5]

One of the most common techniques in the realm of optimization is the employment of metaheuristic algorithms. Metaheuristics provide an adequate approximate solution to an optimization problem, especially with a limited computational budget. Simulated annealing (SA) has been used in many combinatorial optimization problems since its introduction by Kirkpatrick et al. (1983). While there is no guarantee that a globally optimal solution can be found by all metaheuristics, it has been proved that SA converges to its global optimum under general conditions (Yang, 2008).

The cornerstone of the SA algorithm is the utilization of a random search in terms of a Markov chain that not only accepts changes that improve the objective function but also some that are not ideal; thereby avoiding being trapped in local minima. The difference in objective values is proportional to the likelihood of accepting a worse solution. The transition probability of accepting a worse solution is:

$$P = e^{-\frac{\Delta f}{k_B T}} \qquad \textit{Equation 5-1}$$

where Δf *is* the change in objective function, T is a positive real number representing the current temperature, and K_B is the Boltzmann's constant (K_B=1 in this study). The search process would be a greedy search, provided that $T \rightarrow 0, P \rightarrow 0$ because it only accepts better solutions. On the other hand, the search process would be tantamount to a random selection process provided that $T \rightarrow \infty, P \rightarrow 1,$ because it accepts any solution.

[5] This method mimics the annealing process in material processing when a metal cools and freezes into a crystalline state with minimum energy and larger crystal size so as to decrease the defects in metallic structures. The annealing process includes the well-defined control of temperature and cooling rate (often called annealing schedule) (Yang, 2008).

Thus, if T is too high, the system is at a high energy position and cannot easily land at the minima. If T is too low, the system can be trapped in a local minimum and there is not adequate energy to escape the local minimum. This study uses the common approach of geometric cooling (Yang, 2008). The advantage of this method is that when $T \rightarrow 0$ and $t \rightarrow \infty$, there is no need to determine the maximum number of iterations t_f. The cooling process should be slow enough to allow the system to stabilize efficiently.

The SA algorithm is employed to search in the subset of the action space $|A|$, denoted as $|\tilde{A}|$, where $|\tilde{A}| < |A|$. This avoids searching over the entire set $|A|$ exhaustively. A fixed number of iterations is provided to the SA algorithm to repopulate $|\tilde{A}|$ at each iteration. Such a restriction on the number of iterations captures the constraints on the amount of time to be expended in calculating the optimal recovery actions at every t, and the solution accuracy warranted of each candidate recovery action at t. Despite this restriction, the simulation results show how the combined approach leads to a significant improvement over the recovery actions calculated in Chapter 3 using H.

In this study, H is chosen to be a random base restoration policy without any pre-assumption to show the effectiveness of the proposed method. Thereafter, the recovery actions are calculated using the fused method (Rollout w/ SA) explained previously. The rollout algorithm sequentially and consistently improves the underlying H, and the SA algorithm guides the rollout search to find the optimum actions at each stage non-exhaustively. Figure 5-1 shows the application of the proposed fused algorithm (Rollout w/ SA) in the restoration of the defined community. As mentioned in Chapter 4, *the number of benefited people* (ordinate of Figure 5-1) is defined as people who have functional main utilities of electricity, potable water, and available food retailers.

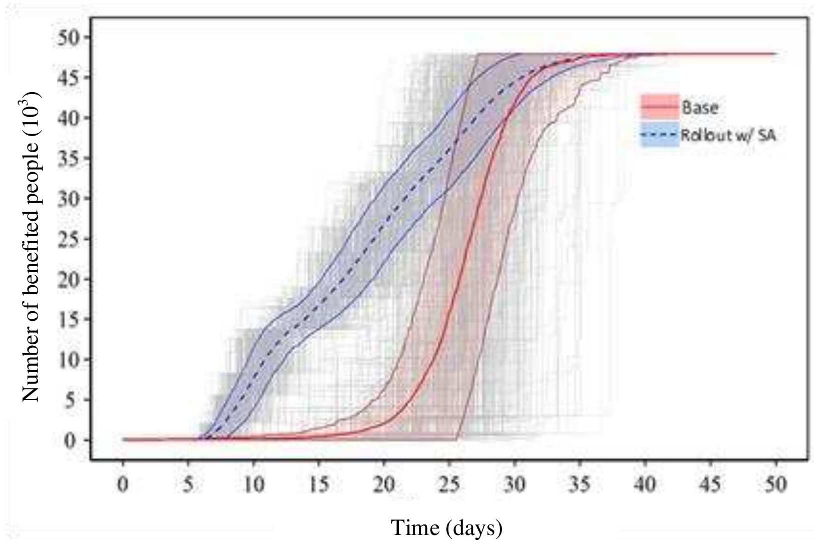

Figure 5-1. Comparison of Base and Rollout with SA Policies

5.3. Optimal Computing Budget Allocation

When applying uniform rollout for solving an MDP problem, a fixed rollout sampling budget α is allocated to each action, yielding α rollout samples per candidate action to estimate the Q value associated with that action. In the literature on simulation methods for optimization, this is analogous to total equal allocation (TEA) with a fixed budget α for each simulation experiment (a single simulation experiment is equivalent to one rollout sample). In practice, the best possible action is of primary interest, and the search should be directed towards the most promising candidates. Also, for large real-world problems, the simulation budget available is insufficient to allocate α number of rollout samples per action. Oftentimes, one would like to get a rough estimate of the performance of each action and spend the remaining simulation budget in refining the accuracy of the best estimates. This is the classic *exploration vs. exploitation* problem faced in optimal learning and simulation-based optimization studies.

Instead of a uniform allocation α for each action, non-uniform allocation methods also have been explored in the literature pertaining to the rollout algorithm; such methods are often referred to as *adaptive rollout* methods (Dimitrakakis and Lagoudakis, 2008). An analysis of performance guarantees for adaptive rollout remains an active area of research (Dimitrakakis and Lagoudakis, 2008; Lazaric et al., 2016)). These non-uniform allocation methods guarantee performance without a constraint on the budget of rollouts. Hence, we explore an alternative non-uniform allocation method that would not only fuse well into our solutions (adaptively guiding the stochastic search) but would also incorporate the constraint of simulation budget in its allocation procedure. Numerous techniques have been proposed in the simulation optimization community to solve this problem. We draw upon one of the best performers (Branke et al., 2007) that naturally fits into our solution framework— Optimal Computing Budget Allocation (OCBA). Moreover, the probability of correct selection P{CS} of an alternative in OCBA mimics finding the best candidate action at each stage in the rollout algorithm.

Formally, the OCBA problem (Chen et al., 2000) can be stated as:

$$\max_{N_1,\ldots,N_n} P\{CS\} \;\; s.t. \;\; \sum_{i=1}^{n} N_i = B \qquad \textit{Equation 5-2}$$

where B represents the simulation budget for determining optimal a_t for x_t at any t, and N_i is the simulation budget for the i^{th} action at a particular t. At each OCBA allocation step (for the definition of the allocation step (see Chen et al. (2000)), barring the best alternative, the OCBA solution assigns an allocation that is directly proportional to the variance of each alternative and inversely proportional to the squared difference between the mean of that alternative and the best alternative. Here, only information required to initialize the OCBA algorithm is provided. For a detailed description of OCBA, see Chen et al. (2000). In the next section, the proposed fused algorithm is applied to the WN of Gilroy, with the objective of performing repair actions in such a way that the maximum number of people will have water in minimum amount of time.

5.3.1. Simulation Results

Two different simulation plots of rollout fused with OCBA are presented in Figures 5-2 and 5-3, termed rollout with OCBA1 and rollout with OCBA2. The basic method is the same for both cases; only the per-stage simulation budget is different. A per-stage budget (budget at each decision time t) of $B = 5 \cdot n+5000$ is assigned for rollout with OCBA1 and $B = 5 \cdot n+10000$ for rollout with OCBA2. Figure 5-2 compares the performance of rollout fused with OCBA and base policy. The "look-ahead property" that is characteristic of the rollout algorithm is evident in the results in Figure 5-2, where the base policy initially outperforms the rollout policy; however, after about six days the former steadily outperforms the later. The area under the curve of the plots represents the product of the number of people who have water and the number of days for which they have water, and is a measure of the performance of the proposed method in meeting the objective. A larger area represents that greater number of people were benefitted as a result of the recovery actions. The area under the curve for recovery with rollout (blue and red plots) is more than its base counterpart (black). A per-stage budget increase of 5,000 simulations in rollout with OCBA2 with respect to rollout with OCBA1 shows improvements in the recovery process.

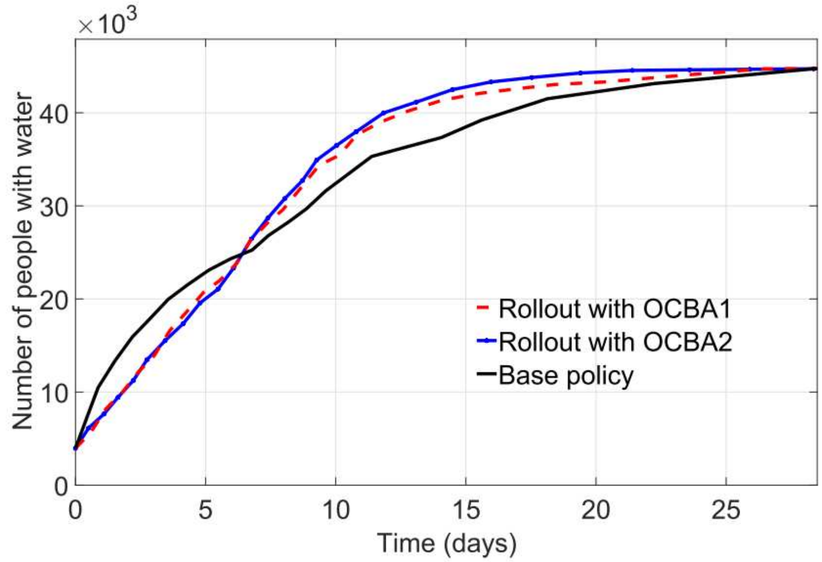

Figure 5-2. Performance Comparison of Rollout vs. Base Policy for Three Units of Resources

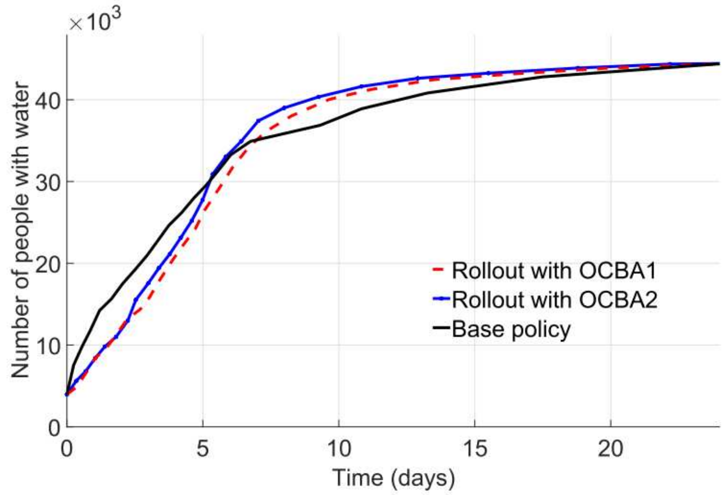

Figure 5-3. Performance Comparison of Rollout vs. Base Policy for Five Unit of Resources

For the rollout with OCBA in Figure 5-4, $B = 5 \cdot n$+20000, whereas $\alpha = 200$ for the uniform rollout simulations. The recovery as a result of these algorithms outperforms the base policy recovery in all cases. Also, the performance of rollout with OCBA is comparable to uniform rollout despite a meagre simulation budget of 10% of uniform rollout. The area under the recovery process in Figure 5-4, as a result of uniform rollout, is only marginally greater than that due to rollout with OCBA. Note that after six days, OCBA slightly outperforms uniform rollout because it prioritizes the simulation budget on the most promising actions per-stage. Rollout exploits this behavior in each stage and gives a set of sequential recovery decisions that further enhances the outcome of the recovery decisions. Note that such an improvement is being achieved at a significantly low simulation budget with respect to uniform rollout. Therefore, these two algorithms form a powerful combination together, where each algorithm consistently and sequentially reinforces the performance of the other. Such synergistic behavior of the combined approach is appealing. Lastly, these simulation studies show that increments in the simulation budget of rollout results in only marginal performance improvement for each increment. Beyond a certain increment in the simulation budget, the gain in performance might not scale with the simulation budget expended. A possible explanation is that a small simulation budget increase might not dramatically change the approximation of the Q - value function associated with a state-action pair in the MDP.

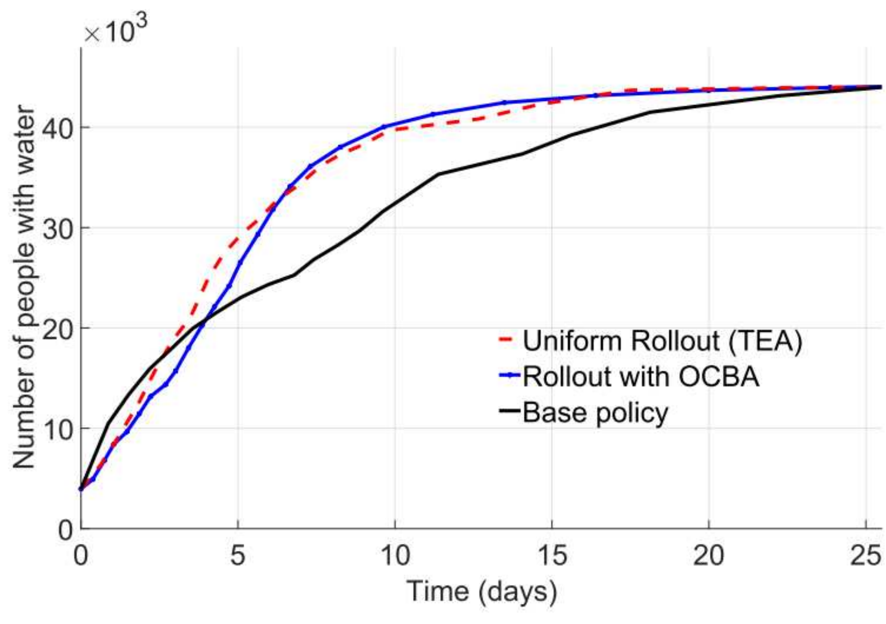

Figure 5-4. Performance Comparison of Uniform Rollout (TEA), Rollout with OCBA and Base Policy for Three Units of Resources

CHAPTER 6: EVALUATING FOOD SECURITY HOUSEHOLDS IN THE AFTERMATH OF DISASTERS

—Innovations that are guided by smallholder farmers, adapted to local circumstances, and sustainable for the economy and environment will be necessary to ensure food security in the future."

Bill Gates

6.1. INTRODUCTION

Resilience-related research during the past decade has led to recommendations of goals and metrics to describe the performance of independent and, indeed, interdependent civil infrastructure systems (ICIS) (Bruneau et al., 2003; Applied Technology Council, 2016). These metrics have been investigated for different systems, such as Electrical Power Networks (EPN) (Ouyang, et al., 2012), Water Networks (WN) (Adachi and Ellingwood, 2009), residential buildings (Lin & Wang, 2017), health-care facilities (Cimellaro et al., 2013), and transportation systems (Pant et al., 2014). However, there has been very little effort connecting disruption in civil infrastructure to failures in food distribution and food retail infrastructure, despite that fact that food security depends on these critical infrastructure systems that have been identified in the Presidential Policy Directive 21 (PPD, 2013).

The food security of households within a community is, in part, a function of the pre-event spatial configuration and distribution of businesses and organizations comprising the food distribution network, the vulnerability of households to disruptions, and the vulnerabilities and resilience of these businesses and organizations. The vulnerabilities of these entities are shaped, in part, by the vulnerabilities of the individual infrastructural systems (electricity, natural gas, water, wastewater/sewer, etc.) upon which they depend and the characteristics of infrastructure system interdependencies. Unfortunately, there is little systematic data on the consequences of direct damage and disruption to infrastructure systems for the businesses and organizations within the food distribution network in local communities that can inform an understanding of how ICIS interdependencies impact community food security in the context of natural hazards.

The United States Department of Agriculture (USDA) identifies a household as food secure if it has "access, at all times, to enough food for an active, healthy life for all household members" (Coleman-Jensen et al., 2015). The degrees of food security are characterized by four levels: (1) high food security, when there are no reported food access problems or limitations; (2) marginal food security, when there is concern about not having enough food; (3) low food security (food insecure without hunger), when the quality, variety or desirability is reduced, and (4) very low food security (food insecure with hunger), when eating patterns are disrupted and food intake is reduced (United States Department of Agriculture, 2017). According to Coleman-Jensen et al. (2015), the rates of low and very low food security are higher among households with children and minority households.

Food security is not just an issue of the ability of households to purchase or otherwise acquire food from a business or agency. It is also a function of a variety of dimensions of access to providers such as grocery stores, food banks, convenience stores, etc. In this regard, the five A's or dimensions of consumer's access to health care, first conceptualized by Penchansky and Thomas (1981), can be helpful to provide a taxonomic definition of access and improve the measurement science of fit between supply and demand (Biehl et al., 2017). These five (5) dimensions are Accessibility, Availability, Affordability, Accommodation, and Acceptability.

For the purpose of this study, we focus on three of the five dimensions that are particularly germane and relevant for the nexus between civil infrastructure and household food security: *accessibility*, *availability*, and *affordability*. Our primary target is on supply-side issues, with a focus on potential impacts of infrastructure damage and disruption for the retailers that are the direct providers or suppliers of food to households within local communities.

This chapter first studies the impact of interconnectedness among ICISs on the functionality and accessibility of food retailers in the Gilroy community, introduced in Chapter 2, exposed to a severe earthquake on the San Andreas Fault. Food availability, accessibility, and affordability are the basis for the food insecurity metrics, defined subsequently, that quantify the impacts of the disrupted critical systems on the food security of Gilroy inhabitants in the aftermath of the earthquake. The probability distributions of these metrics are developed by simulating spatial and temporal recovery processes that capture various uncertainties following the earthquake. The ADP approach developed in Chapters 2-5 is applied to identify practical policy interventions to hasten the recovery of ICISs and reduce the adverse impacts of food insecurity in Gilroy.

6.2. Probability of Food Security Model

The literature on business disruption after a natural hazard suggests that it is often not direct damage to an establishment's building or inventory that results in disruption and failure, but rather disruption of critical infrastructure (Graham, 2007; Xiao & Van Zandt, 2012). The disruption of business activities and the failure of businesses and other food-related organizations has, in turn, consequences for accessibility, affordability, and availability. In this study, all three conditions must be satisfied to consider a household or an urban grid as a food-secure area in a community (Nozhati et al., 2019c); see Figure 6-1 and Equation 6-1. A brief discussion of each of these dimensions food access and critical infrastructure is presented in the following paragraphs.

$$\mathrm{P}_{\substack{Food\\Security}} = \mathrm{P}\left\{\bigcap_{i=1}^{3}\mathbf{C}_i \,\middle|\, i \in \left\{\underset{1}{\text{availability}}, \underset{2}{\text{accessibility}}, \underset{3}{\text{affordability}}\right\}\right\} \quad \textit{Equation 6-1}$$

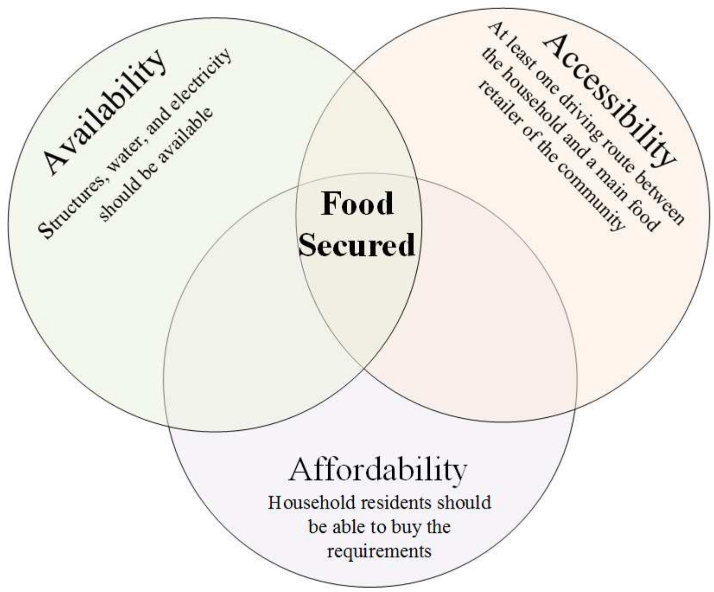

Figure 6-1. Definition of Food Security in This Study

Availability (C_1): The relationship between food supplied and the demand for food. For food to be available, food retailers depend on infrastructure systems to operate such as water, electricity and buildings. Therefore, a household unit and a food retailer both must be functional (F), see Equation 6-2. In this study, a building is considered as functional when it has a safe structure and the potable water and electricity (U) are available, see Equation 6-3.

$$\mathbf{C}_1 := \left\{\bigcap_{j=1}^{2}\mathbf{F}_j \,\middle|\, j \in \left\{\underset{1}{\text{Functionality of household}}, \underset{2}{\text{functionality of food retailer}}\right\}\right\} \quad \textit{Equation 6-2}$$

$$\mathbf{F} := \left\{ \bigcap_{k=1}^{3} \mathbf{U}_k \,\middle|\, k \in \left\{ \underset{1}{\text{Structure}}, \underset{2}{\text{Electricity}}, \underset{3}{\text{Water}} \right\} \right\} \qquad \textit{Equation 6-3}$$

Accessibility (C_2): The relationship of physical access to food retailers, which is a function of the road network. There are several modes of transportation, such as driving, bicycling and walking. This study considered driving as the primary mode of transportation, which includes cars and local buses. *ggmap* by using Google's routing API was called from within R to compute all alternative driving routes between each food retailer and each urban grid center by using the *ggmap* package (Kahle and Wickham, 2018). *ggmap* computes all the alternative routes between a household unit and retailers. Once at least one functional route is found, the accessibility from the origin to the destination is satisfied.

$$\mathbf{C}_2 := \left\{ \bigcup_{r=1}^{N} \mathbf{R}_r \,\middle|\, r \in \left\{ \underset{1,\ldots,N}{\text{All driving routes between household and food retailer}} \right\} \right\} \qquad \textit{Equation 6-4}$$

where N is the total number of driving paths between a household unit and a food retailer. R_r denotes the functionality of the r^{th} path between two points.

Affordability (C_3): The relationship between household income and food retailers. While this dimension of food access is not impacted by critical infrastructure, it is an important factor to capture pre-event levels of food security. Food security within a community depends on many factors and the likelihood that a household unit is in a state of food insecurity immediately following a severe hazard event can be substantial. Availability and accessibility are dominant factors in food insecurity following a hazard, while affordability is the most significant factor prior to a hazard. The role of availability along with accessibility is assessed in the next section.

6.3. THE ROLE OF AVAILABILITY AND ACCESSIBILITY

There are several factors that affect the recovery trajectory of a network, among which the number of recovery crews that can be allocated, network age, event area, and event type are most important (Barabadi and Ayele, 2018). The dominant factors of Gilroy's recovery have been discussed in Chapters 2-4. In this section, the EPN recovery policy is generally as follows: the transmission line, the power sub-station, the distribution line to the water pump or the well that supplies Costco and Walmart, and the distribution lines that supply the downtown. The WN recovery policy is generally as follows: potable water wells, water tanks, pipelines that supply food retailers and residences. We assume that the food retailers as well as bridges can be repaired simultaneously. A random repair time generated based on exponential distributions presented in Table 6-1, is assigned to damages components.

Table 6-1. The Expected Repair Times (Unit: Days)

	Damage State			
Component	Minor	Moderate	Extensive	Complete
Residential buildings	2	30	90	180
Food retailers	5	30	120	240
Highway bridges	0.6	2.5	75	230
Electric sub-station	1	3	7	30
Transmission line component	0.5	1	1	2
Distribution line component	0.5	1	1	1
Water tank	1.2	3.1	93	155
Wells	0.8	1.5	10.5	26
Pumping station	0.9	3.1	13.5	35

Figure 6-2 shows the percent of available EPN components with one and two standard deviation bands over time. This figure is important for decision-support algorithms and policymakers, in that the number of damaged components determines the dimension of the decision-making problem and the number of required RUs for the EPN or any other network in time. The times to full recovery of the EPN, $T_{\varphi(\mathrm{x}(t))(\mathrm{e})}$, and time to 75% recovery, $T_{0.75}(e)$, are also represented in Figure 6-2b. The times required to restore electric power and water for each food retailer are presented in Figure 6-3, which indicates the vulnerability of each food retailer due to the unavailability of utilities and informs the periods of time that reliable backup utility systems should be provided.

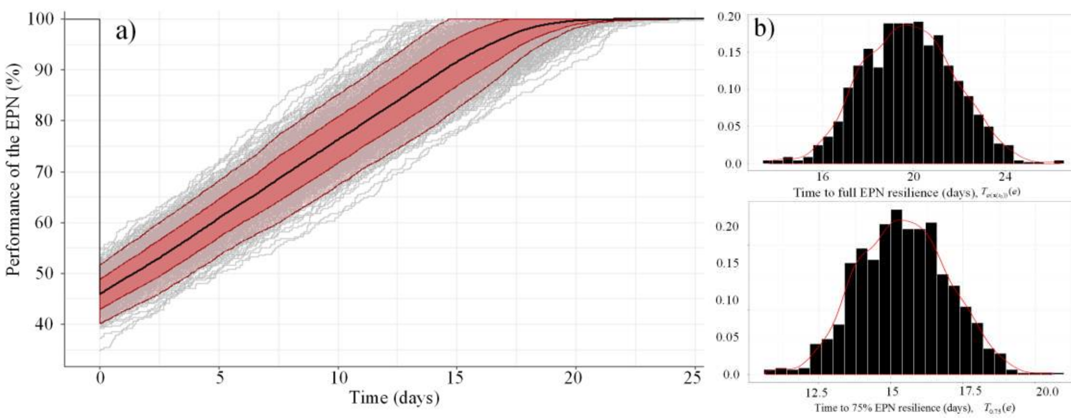

Figure 6-2. a) The Percent of Available the EPN Components Over Time b) Times to Full and 75% Recovery

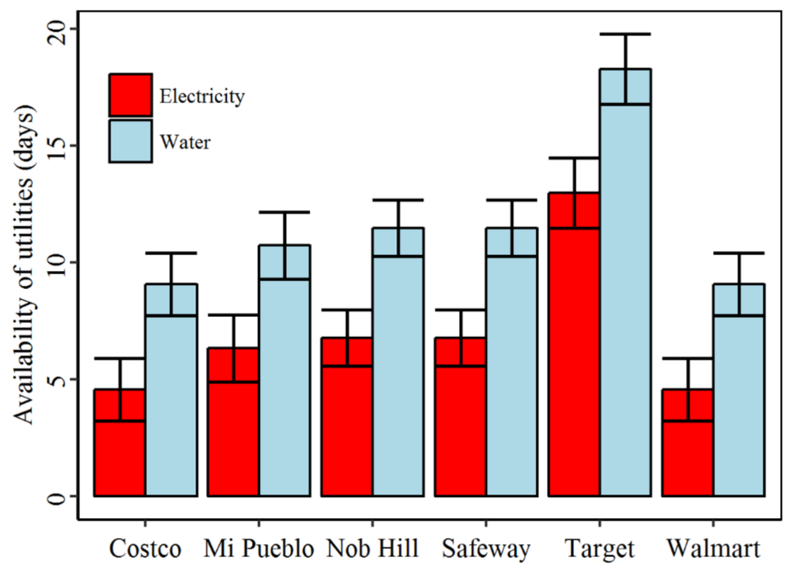

Figure 6-3. Time to Availability of Electricity and Water for Each Main Food Retailer

The shape of the recovery trajectories and availability of utilities for each retailer depend on the location of each retailer in the community and, more importantly, to the recovery strategies. For instance, Walmart and Costco are next to each other and pretty close to the power substation; thus, they have the shortest time to regain electricity. Safeway, Nob Hill Foods, and Mi Pueblo, which are close together in downtown Gilroy, have roughly similar recovery times.

As noted in Figure 6-1, food security depends on availability, accessibility, and affordability. With this in mind, the number of food-secure people has been calculated over the 36 urban grids (see Figure 2-3) as well as the community over time with respect to availability and accessibility in this subsection. For the sake of brevity, only three different grids (one in the south, one in the middle, and one in the north of the community), along with the entire community, are presented. Figure 6-4 shows the number of people, adults, children, and seniors that are food-secure in these three grids. Children include those aged 0-17, including those of preschool and school age, as indicated in (Harnish, 2014).

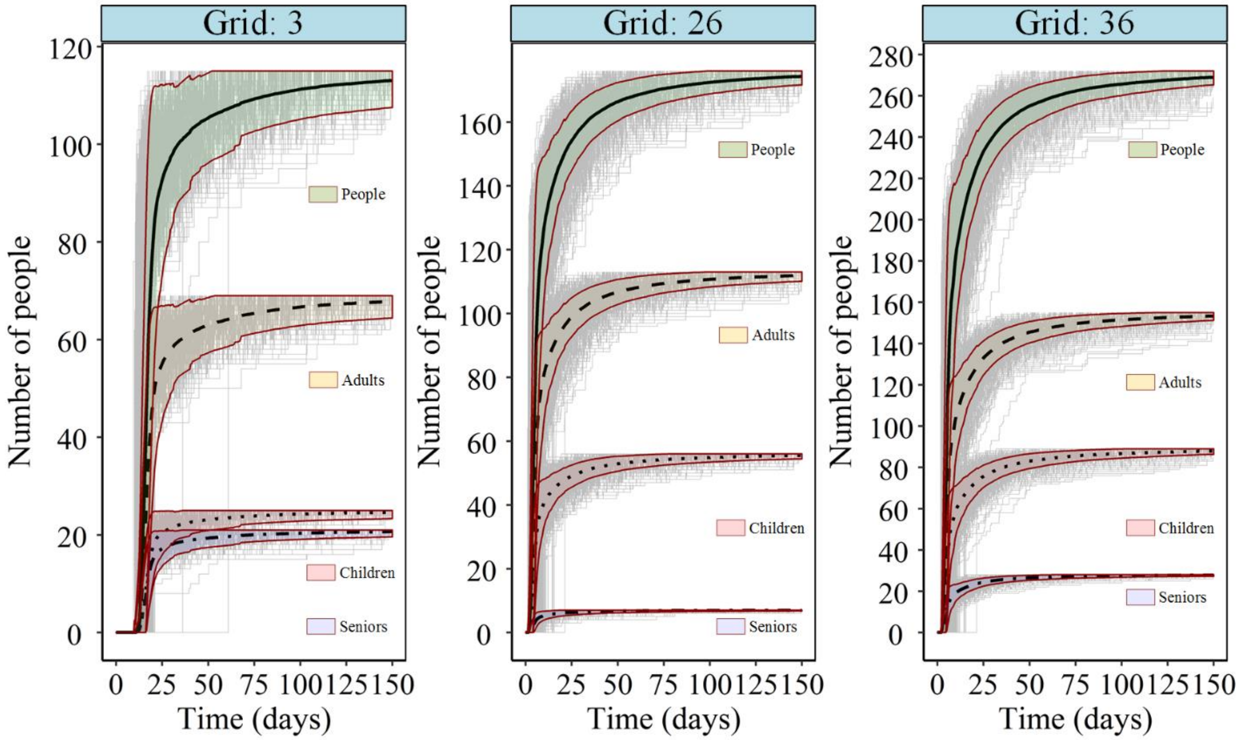

Figure 6-4. The Number of Food-secure People with ±σ Over Three Different Grids

Figure 6-5 represents the number of food-secure people with different age distributions at the community level. Young children are especially vulnerable to food insecurity; policy makers should be conscious of the number of food-insecure children. This figure is important to policymakers in that they can be informed when the community reaches a locally-defined desirable threshold.

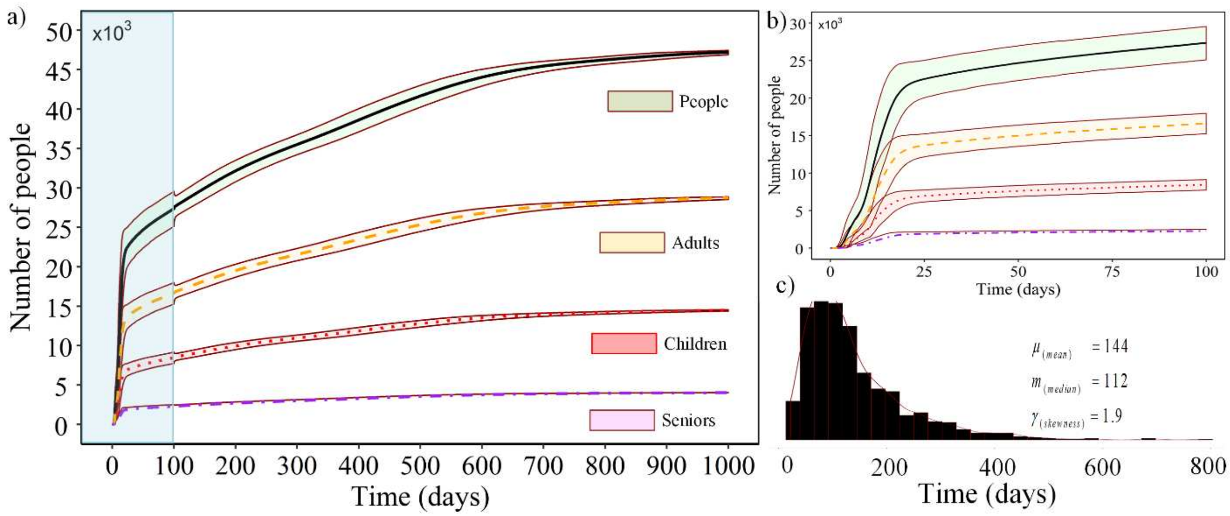

Figure 6-5. Total Number of Food-secure People at the Community Level with ±σ b) Over the First 100 Days c) Times to Full Food Security Recovery

6.4. THE ROLE OF AFFORDABILITY

Affordability measures whether people have sufficient financial resources to purchase essential food items from food retailers. Prior to the occurrence of a severe hazard event when conditions of availability and accessibility are less important, affordability is the most significant issue for vulnerable populations. Affordability has a direct relationship with individual or household income. The annual median family income (MFI) for each area of the country is provided by the Federal Department of Housing and Urban Development (HUD). Gilroy has a lower median family income ($76,060 in 2012) than the median family income ($89,445 in 2012) of the surrounding area, which means that the role of affordability should receive special attention (Harnish, 2014). The State of California categorizes income into five groups based the MFI as follows;

- Extremely Low-Income: 30 percent or less of the median family income;
- Very Low-Income: 31 percent to 50 percent of the median family income;

- Low-Income: 51 percent to 80 percent of the median family income;
- Moderate-Income: 81 percent to 120 percent of the median family income; and
- Above Moderate-Income: Greater than 120 percent of the median family income.

A heat map of food-insecure people based on the poverty rates over the urban grids is shown in Figure 6-6.

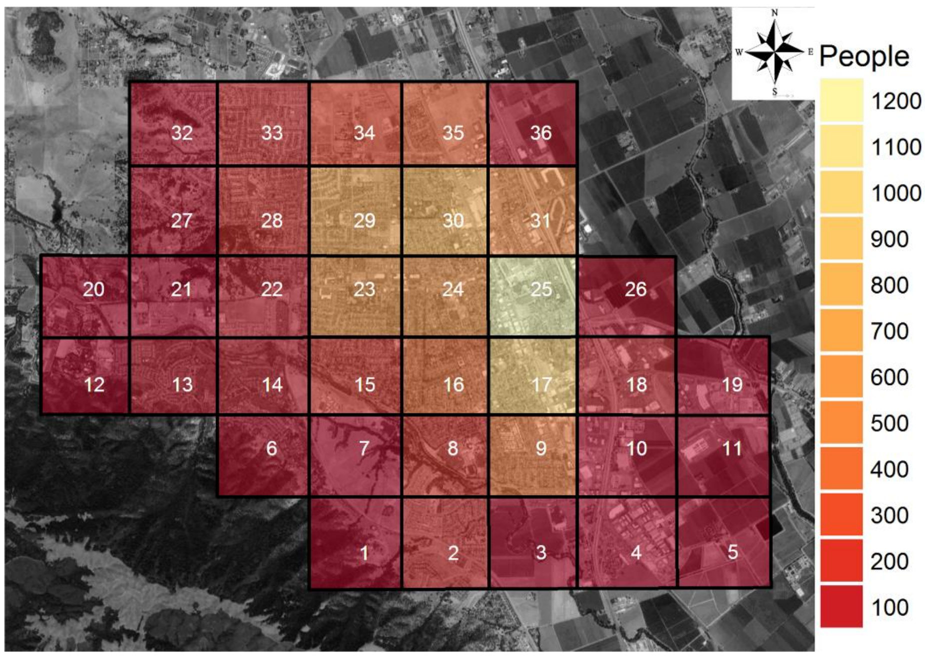

Figure 6-6. The Map of Food-insecure People over the Defined Grids

Figure 6-6 also highlights the fact that, regardless of what happens due to the hazard as well as the recovery activities plans in the aftermath of the hazard, the number of people represented in Figure 6-6 remain in the food insecurity state. In other words, it is assumed that chronic food insecurity issues will return to pre-event levels.

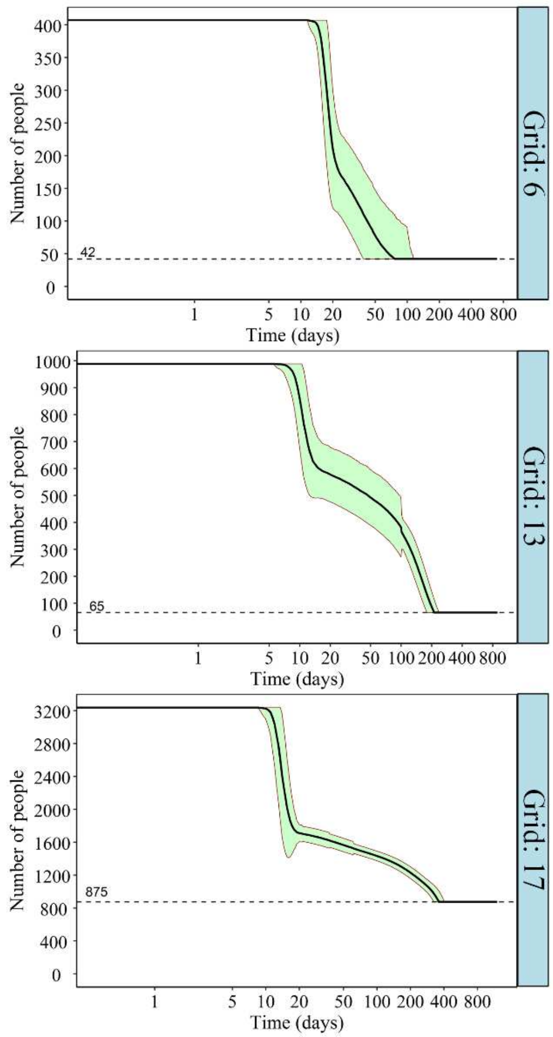

Figure 6-7. The Number of Food-insecure People with ±σ over Three Different Grids

The food insecurity curves of the three different urban grids in terms of initial food-insecure people, along with that for the whole community, are presented in Figures 6-7 and 6-8, respectively. Figure 6-8 can inform policymakers as to when the community reaches the desired percentiles from food securities perspective. Note that the community cannot reach to a complete food security status due to the affordability factor, which considers the food insecurity of the households living in poverty which is represented the level of chronic food insecurity prior to the hazard.

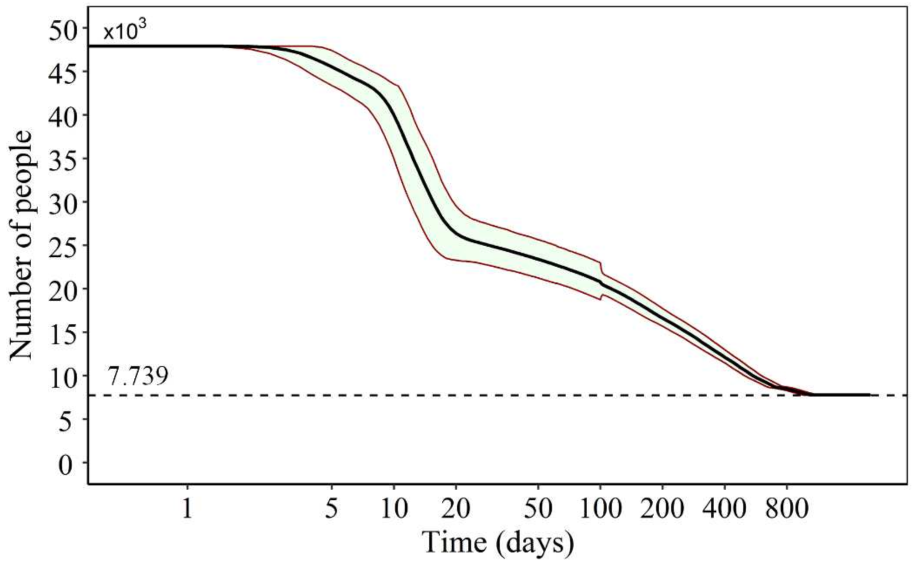

Figure 6-8. Total Number of Food-insecure People at the Community Level with ±σ

6.5. The Application of the Proposed ADP Approach in Food Security of Gilroy Community

In this section, we apply the ADP approach, proposed in Chapters 3-5, to the Gilroy community to illustrate how the approach can be implemented efficiently to find the near-optimal decisions following a severe hazard.

Chapter 4 elaborates the MDP formulation for the community recovery problem. We briefly presents it for the food security problem. Let x_t be the state of the damaged components of the community at time t; x_t is a vector, where each element represents the damage state of each component in Gilroy based on the level of intensity measure and the seismic fragility curves. Let a_t^g denote the repair action to be carried out on the damaged structures in the g^{th} region of the grid at time t. The repair action for the entire community at time t, a_t, is the stack of the repair action a_t^g .differs from grid to grid and depends on the assigned RUs and the number of damaged buildings within grid g. There is a limited number of RUs (defined earlier) available to the decision maker for the repair of the buildings in the community. In this study, we also limited the number of RUs for each urban grid so that the number of available RUs is 20 percent of the number of damaged buildings in each region of the grid. Therefore, the number of RUs varies over the community in proportion to the density of the damaged buildings. The assignment of RUs to damaged locations is *non-preemptive* in the sense that the decision maker cannot preempt the assigned RUs from completing their work and reassign them to different locations at every decision epoch t. This type of scheduling is more suitable when the decision maker deals with non-central stakeholders and private owners, which is the case for a typical building portfolio. Chapter 3 discusses preemptive scheduling and its benefits. We wish to plan decisions optimally so that a maximum number of inhabitants be in food security per unit of time (day in our case). Refer to the definition of food security is in the past section. Therefore, the reward function embeds two objectives as follows:

$$R(x_t, a_t, x_{t+1}) = \frac{r}{t_{rep}} \qquad \textit{Equation 6-5}$$

where r is the *number of food secure people* after the completion of a_t , and t_{rep} is the total repair time to reach x_{t+1} from any initial state x_0. Note that the reward function is stochastic because the outcome of the repair action is stochastic. In this study, we set the discount factor to be 0.99, implying that the decision maker is "farsighted" in the consideration of the future rewards.

We simulated N_{MC} number of trajectories to reach a low (0.1 in this study) dispersion in Equation 4-6. Alluded to previously, Equation 4-6 addresses the mean-based optimization that is suited to risk-neutral decision makers. However, this approach can easily address different risk aversion behaviors with Equation 4-13. Figure 6-9 shows the total number of food secure people over the community. Noted that the ADP approach computes the near-optimal recovery strategies in the *on-line* fashion, described in Chapter 4. We also computed the different numbers of children, adults, and senior citizens that have safe buildings over the recovery. Different age groups have different levels of vulnerability to food insecurity; for example, children are a vulnerable group and must be paid more attention during the recovery process.

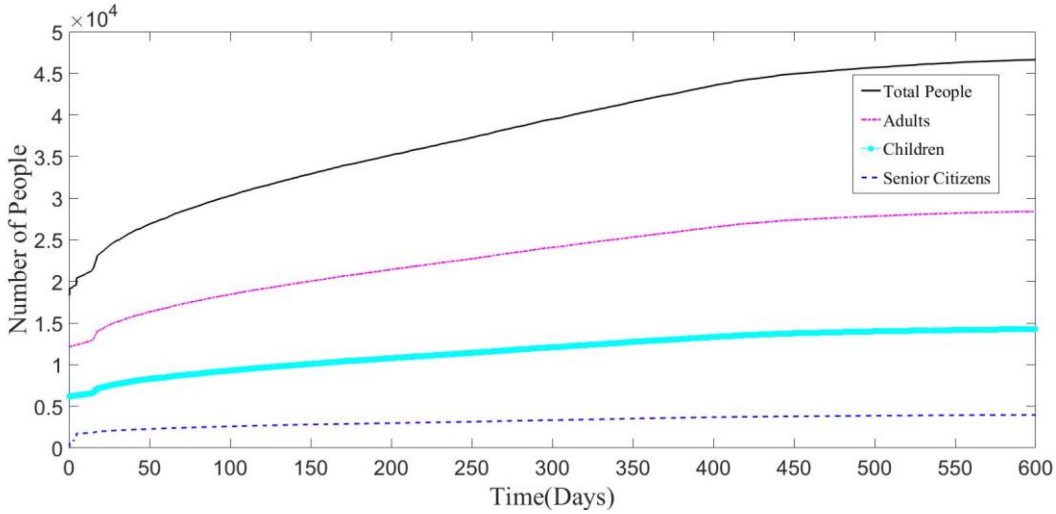

Figure 6-9. Food Secure People over Time

6.6. CONCLUDING REMARKS

This chapter presented a probabilistic framework for evaluating food-security related issues affected by damages to ICISs caused by a severe earthquake. The restoration and functionality of networks are quantified, immediately following the simulated earthquake until full restoration. The case study results also demonstrate the periods of time that each main food retailer suffers from the lack of main utilities of electricity and potable water. Food security metrics based on food availability, accessibility, and affordability are defined and quantified probabilistically either at the grid level or at the community level. However, a more comprehensive definition of food security metrics should be considered. For example, the definition of availability could include the performance and serviceability of the wastewater system and the telecommunication network. Further, a gravity model that can capture the effect of affordability and the income of level households would improve the model.

CHAPTER 7: SUMMARY, CONCLUSIONS AND RECOMMENDATIONS

— There is no single development, in either technology or management technique, which by itself promises even one-order of magnitude improvement within a decade in productivity, in reliability, in simplicity."

Fredrick P. Brooks, Jr., NO SILVER BULLET

7.1. Summary

In this dissertation, a comprehensive risk-informed decision-making methodology for the recovery management of communities with an emphasis on food security issues was proposed. The proposed mathematical approach leveraged approximate dynamic programming along with heuristics for the determination of optimal recovery actions. The methodology overcame the curse of dimensionality which is inherent to large decision spaces and manages multi-state, large-scale infrastructure systems under disasters.

As a basis for the proposed decision-making methodology, a community-level analysis was introduced in Chapter 2 for Gilroy, CA, which was used to provide context to the decision tools introduced in subsequent chapters. Interdependencies within and among various layers of the networks that can potentially produce large-scale cascading effects that make up Gilroy were discussed, along with hazard simulation and the component damage and restoration assessment. Earthquakes emanating from the San Andreas Fault were the prevailing hazard of the Gilroy area. This chapter described how ground motion prediction equations (GMPEs) and fragility curves can simulate a seismic event and determine intensities that can be used to evaluate damage in the aftermath of an earthquake.

Chapter 3 explained the necessity of dynamic optimization in post hazard recovery management. It presented a sequential discrete optimization approach, as a decision-making framework at the community level. This chapter described the requirement of approximate dynamic programming techniques to handle large-scale problems like community recovery management. The methodology introduced not only incorporated recovery policies of responsible public and private entities within the community but also substantially enhanced the performance of their underlying strategies with limited resources. Different base heuristics, used at the community-level recovery, were used in the simulation studies. Chapter 3 showed that rollout technique significantly enhanced the base heuristics. Furthermore, the efficient performance of the rollout formulation in optimizing different common objective functions for community resilience was demonstrated.

Chapter 4 detailed the most important properties (paramount properties) of an exhaustive decision-making framework and introduced Markov decision process (MDP)-based optimization to incorporate different sources of uncertainties in the restoration policies. This chapter also displayed how the rollout algorithm, proposed in Chapter 3, can be employed in stochastic optimization. This chapter ended by studying the applicability of the method to address different risk attitudes of policymakers, which include risk-neutral and risk-averse attitudes in community recovery management.

Stochastic recovery scheduling of large-scale networks in the metropolitan areas following hazards is a difficult stochastic control problem with a huge combinatorial decision space. Chapter 5 proposed different methods to address this issue. While the proposed rollout can be easily implemented regardless of the size of the state space, it heavily depends on the action space with the exhaustive search manner. In this regard, Chapter 5 showed how the fusion of rollout and metaheuristic algorithms can address dimensionality issues. The method is particularly simple to implement and is often surprisingly effective. Furthermore, Chapter 5 offered an optimal learning technique called as optimal computing budget allocation (OCBA) to allocate the computational budget much more effectively. This subclass of adaptive rollout algorithms fused with rollout performs competitively with respect to rollout with total equal allocation (TEA).

This dissertation also introduced a methodology to consider how the interconnectedness among civil infrastructure systems impacts food-security of urban inhabitants. Chapter 6 defined new food security metrics, including food availability, accessibility, and affordability. These metrics are quantified in this chapter to provide risk-informed decision support to community stakeholders in the aftermath of an extreme natural hazard.

7.2. Recommendations for Future Studies

It is believed that the methodology can be extended to other hazards and communities. Several networks like telecommunication, wastewater/sewer, natural gas networks, business and commercial sectors, industrial facilities, schools, emergency services and health care facilities like hospitals have not been included in this study. However, as Figure 4-1 depicts the proposed methodology treats the built environment like a black box which means the simulation and consideration of any arbitrary network and/or sector of a community do not affect the applicability and quality of the framework. Of course, the consideration of a network depends upon the preferences of the policymakers and community stakeholders. These preferences must be included in the reward function thereby considering by the methodology. Furthermore, there are various network/community modeling approaches, such as Bayesian networks, Petri-net based approach, the hierarchical holographic modeling approach, the high-level architecture-based approach, to name but a few. Ouyang (2014) reviewed these modeling approaches and categorized them. The nature of the problem determines the selection of the simulation approach.

To summarize, the proposed methodologies of this study are independent of the type of networks, the community/network modeling approaches, and the considered objectives and policymakers' preferences. Nevertheless, more accurate community simulation and more exhaustive objectives can mimic the environment more realistically, thereby achieving precise recovery strategies, provided by the proposed methods of this study.

This study proposed several methods to overcome the curse of dimensionality that is characteristic of decision problems with large variable spaces. The rollout method can be readily performed independently of the size of the state space as well as the combination with metaheuristics and OCBA was shown to increase the efficiency of the methodology significantly. However, even more powerful methods that can be implemented easily for large state and action spaces is essential if optimal restoration policies for urban areas with millions of inhabitants and built facilities are to be identified. To this end, the methods like neuro-dynamic programming and function approximator are recommended.

Sequential decision problems with state uncertainties that can be modeled as partially observable Markov decision processes (POMDP) can be considered as an extension of this study. A POMDP is an extension to the MDP formulation introduced in Chapter 4. In a POMDP, a model stipulates the probability of making a particular observation given the current state. The state uncertainty in community recovery problems can be produced by inspection errors and the lack of information from the whole of a community, especially immediately following a disaster.

REFERENCES

Abrahamson, N. A., Silva, W. J., and Kamai, R. (2013). Update of the AS08 ground-motion prediction equations based on the NGA-West2 data set. *Pacific Earthquake Engineering Research Center*.

Abramson, B. (1990). Expected-outcome: A general model of static evaluation. *IEEE transactions on pattern analysis and machine intelligence*, *12*(2), 182-193.

Adachi, T., and Ellingwood, B. R. (2009). Serviceability assessment of a municipal water system under spatially correlated seismic intensities. *Computer-Aided Civil and Infrastructure Engineering*, *24(4)*, 237–248.

Adigaa, A., Agashea, A., Arifuzzamana, S., Barretta, C. L., Beckmana, R., Bisseta, K., Chena, J., Chungbaeka, Y., Eubanka, S., Guptaa, E., Khana, M., Kuhlmana C. J., Mortveita, H. S., Nordberga, E., Riversa, C., Stretza, P., Swarupa, S., Wilsona, A., and Xiea, D. (2015). Generating a synthetic population of the United States.

Alexander, D. E. (2013). Resilience and disaster risk reduction: an etymological journey. *Natural Hazards and Earth System Sciences*, 13(11), 2707-2716.

Applied Technology Council. (2016). Critical assessment of lifeline system performance: understanding societal needs in disaster recovery. *US Department of Commerce, National Institute of Standards and Technology*.

Aslett, L. J. (2012). MCMC for inference on phase-type and masked system lifetime models. *Doctoral dissertation, Trinity College Dublin*.

Asteris, P. G., Nozhati, S., Nikoo, M., Cavaleri, L., and Nikoo, M. (2018). Krill herd algorithm-based neural network in structural seismic reliability evaluation. *Mechanics of Advanced Materials and Structures*, 1-8.

Ayyub, B. M. (2014). Systems resilience for multihazard environments: Definition, metrics, and valuation for decision making. *Risk Analysis*, 34(2), 340-355.

Barabadi, A. and Ayele, Y. (2018). Post-disaster infrastructure recovery: Prediction of recovery rate using historical data. *Reliability Engineering & System Safety, 169*, 209–223.

Barker, K., Ramirez-Marquez, J. E., and Rocco, C. M. (2013). Resilience-based network component importance measures. *Reliability Engineering and System Safety*, 117, 89–97.

Bertsekas, D. P., Tsitsiklis, J. N., and Wu, C. (1997). Rollout algorithms for combinatorial optimization. *Journal of Heuristics*, *3*(3), 245-262.

Bertsekas, D. P., and Castanon, D. A. (1999). Rollout algorithms for stochastic scheduling problems. *Journal of Heuristics*, *5*(1), 89-108.

Bertsekas, D. P. (2013). Rollout algorithms for discrete optimization: A survey. *Handbook of combinatorial optimization*, 2989-3013.

Bertsekas, D.P., 2017. Dynamic Programming and Optimal Control. 4th Edition, Volume I. *Athena Scientific*.

Biehl, E., Buzogany, S., Huang, A., Chodur, G., and Neff, R. (2017). Baltimore Food System Resilience Advisory Report. *Johns Hopkins Center for Livable Future.*

Boctor, F. F. (1996). Resource-constrained project scheduling by simulated annealing. *International Journal of Production Research*, *34*(8), 2335–2351.

Bouleimen, K., and Lecocq, H. (2003). A new efficient simulated annealing algorithm for the resource-constrained project scheduling problem and its multiple mode version. *European Journal of Operational Research*, *149*(2), 268–281.

Branke, J., Chick, S. E., and Schmidt, C. (2007). Selecting a selection procedure. *Management Science*, *53*(12), 1916-1932.

Bruneau, M., Chang, S. E., Eguchi, R. T., Lee, G. C., O'Rourke, T. D., Reinhorn, A. M., Shinozuka, M., Tierney, K., Wallace, W. A., and von Winterfeldt, D. (2003) A framework to quantitatively assess and enhance the seismic resilience of communities. *Earthquake spectra*, 19(4), 733-752.

Bruneau, M., and Reinhorn, A. (2007). Exploring the concept of seismic resilience for acute care facilities. *Earthquake Spectra*, 23(1), 41–62.

Busoniu, L., Babuska, R., De Schutter, B., & Ernst, D. (2010). Reinforcement learning and dynamic programming using function approximators. *CRC press*.

Cha, E. J., and Ellingwood, B. R. (2012). Risk-averse decision-making for civil infrastructure exposed to low-probability, high-consequence events. *Reliability Engineering & System Safety*, *104*, 27-35.

Chang, S. E., and Shinozuka, M. (2004). Measuring improvements in the disaster resilience of communities. *Earthquake Spectra*, 20(3), 739-755.

Chang, H. S., Hu, J., Fu, M. C., and Marcus, S. I. (2013). Simulation-based algorithms for Markov decision processes. *Springer Science & Business Media*.

Chen, C. H., Lin, J., Yücesan, E., and Chick, S. E. (2000). Simulation budget allocation for further enhancing the efficiency of ordinal optimization. *Discrete Event Dynamic Systems*, *10*(3), 251-270.

Cimellaro, G. P., Arcidiacono, V., Reinhorn, A. M., and Bruneau, M. (2013). Disaster resilience of hospitals considering emergency ambulance services. *In Structures Congress 2013: Bridging Your Passion with Your Profession*, 2824–2836.

Cimellaro, G. P., Renschler, C., and Bruneau, M. (2015). Introduction to resilience-based design (RBD). In *Computational Methods, Seismic Protection, Hybrid Testing and Resilience in Earthquake Engineering*. 151-183.

Coleman-Jensen, A., Rabbitt, M., Gregory, C., & Singh, A. (2017). Household food security in the United States in 2017. *Washington, DC: Economic Research Service, U.S. Department of Agriculture*.

Corotis, R. B., Hugh Ellis, J., and Jiang, M. (2005). Modeling of risk-based inspection, maintenance and life-cycle cost with partially observable Markov decision processes. *Structure and Infrastructure Engineering*, *1*(1), 75-84.

Dimitrakakis, C. and Lagoudakis, M. G. (2008). Rollout sampling approximate policy iteration. *Machine Learning*, *72*(3), 157-171.

Ellis, H., Jiang, M., and Corotis, R. B. (1995). Inspection, maintenance, and repair with partial observability. *Journal of Infrastructure Systems*, *1*(2), 92-99.

FEMA. (2003). Multi-hazard loss estimation methodology, earthquake model, HAZUS-MH 2.1 Technical Manual. *Department of Homeland Security, FEMA*. Washington, D.C., 1–699.

Food Research and Action Center (2017) An Advocate's Guide to the Disaster Supplemental Nutrition Assistance Program (D-SNAP). *Food Research and Action Center (FRAC)*, 1–40. Retrieved from http://frac.org/wp-content/uploads/d-snap-advocates-guide-1.pdf

Frangopol, D. M., Kallen, M. J., and Noortwijk, J. M. V. (2004). Probabilistic models for life-cycle performance of deteriorating structures: review and future directions. *Progress in structural engineering and Materials*, *6*(4), 197-212.

Gilroy Annex (2011). The Association of Bay Area Governments (CITY OF GILROY ANNEX). Retrieved from http://resilience.abag.ca.gov/wp-content/documents/2010LHMP/Gilroy-Annex-2011.pdf.

Gosavi, A. (2015). Simulation-based optimization. *Berlin: Springer*.

Graham, L. T. (2007). Permanently failing organizations? Small business recovery after September 11, 2001. *Economic Development Quarterly, 21(4),* 299–314.

Harnish, M. (2014). 2015-2023 Housing element policy document and back-ground report. Retrieved from http://www.gilroy2040.com/documents/.

Hemmati, M., and Mahmoud, H. N. (2019). A Framework for Collapse Vulnerability Assessment of Steel Beams Subjected to Increasing Loads and Nonuniform Longitudinal Temperature. *Journal of Structural Engineering*, 145(5), 04019017. DOI: 10.1061/(ASCE)ST.1943-541X.0002287

Henry, D., and Ramirez-Marquez, J. E. (2012). Generic metrics and quantitative approaches for system resilience as a function of time. *Reliability Engineering and System Safety*, 99, 114-122.

Hosseini, S., Barker, K., and Ramirez-Marquez, J. E. (2016). A review of definitions and measures of system resilience. *Reliability Engineering and System Safety*, *145*, 47-61.

Howard, R. A. (1960). Dynamic programming and Markov processes. *MIT Press*, *Cambridge, MA*.

Ibe, O. (2013). Markov processes for stochastic modeling. *Newnes*.

Iyengar, G. N. (2005). Robust dynamic programming. *Mathematics of Operations Research*, *30*(2), 257-280.

Ji, C., Wei, Y., Mei, H., Calzada, J., Carey, M., Church, S., Hayes, T., Nugent, B., Stella, G., Wallace, M., White, J., Wilcox, R. (2016). Large-scale data analysis of power grid resilience across multiple US service regions. *Nature Energy*, *1*(5), 16052

Kahan, J. H., Allen, A. C., and George, J. K. (2009). An operational framework for resilience. *Journal of Homeland Security and Emergency Management*, *6*(1).

Kahle, D. and Wickham, H. (2018). ggmap: Spatial Visualization with ggplot2. *R Journal*, 5(1).

Karami Mohammadi, R. and Hemmati, M. (2013). Alternative method for estimation of IDA curves in single degree of freedom systems. *3rd International Conference on Acoustics and Vibration.* 10.13140/2.1.3781.6967.

Karimi Askarani, K., Stockwell, E. B., Piontek, K. R., and Sale, T. C. (2018). Thermal monitoring of natural source zone depletion. *Groundwater Monitoring & Remediation*, 38(3), 43-52. https://doi.org/10.1111/gwmr.12286

Karimi Askarani, K., and Pakbaz, M. S. (2016). Drained shear strength of over-consolidated compacted soil-cement. *Journal of Materials in Civil Engineering*, 28(5), 04015207. https://doi.org/10.1061/(ASCE)MT.1943-5533.0001510

Keck, M., and Sakdapolrak, P. (2013). What is social resilience? Lessons learned and ways forward. *Erdkunde*, 5-19.

Khaloo, A., Nozhati, S., Masoomi, H., and Faghihmaleki, H. (2016a). Influence of earthquake record truncation on fragility curves of RC frames with different damage indices. *Journal of Building Engineering*, 7, 23-30.

Khaloo, A. R., Masoomi, H., Nozhati, S., and Dehcheshmeh, M. M. (2016b). Influence of diaphragm opening on seismic response of rectangular RC buildings with end shear walls. *Scientia Iranica. Transaction A, Civil Engineering*, 23(4), 1689.

Khayat, M., Poorveis D., Moradi, S., and Hemmati, M. (2016). Buckling of thick deep laminated composite shell of revolution under follower forces. *Struct. Eng. Mech*. 58 (1): 59–91. https://doi.org/10.12989/SEM.2016.58.1.059.

Kirkpatrick, S., Gelatt, C. D., and Vecchi, M. P. (1983). Optimization by simulated annealing. *science*, *220*(4598), 671-680.

Kochenderfer, M. J. (2015). Decision making under uncertainty. *MIT press, Cambridge, MA*.

Koliou, M., van de Lindt, J. W., McAllister, T. P., Ellingwood, B. R., Dillard, M., and Cutler, H. (2018). State of the research in community resilience: progress and challenges. *Sustainable and Resilient Infrastructure*, DOI: 10.1080/23789689.2017.1418547

Lazaric, A., Ghavamzadeh, M., and Munos, R. (2016). Analysis of classification-based policy iteration algorithms. *The Journal of Machine Learning Research*, *17*(1), 583-612.

Lin, P., Wang, N., and Ellingwood, B. R. (2016). A risk de-aggregation framework that relates community resilience goals to building performance objectives. *Sustainable and Resilient Infrastructure*, *1*(1-2), 1-13.

Lin, P., and Wang, N. (2017). Stochastic post-disaster functionality recovery of community building portfolios I: Modeling. *Structural Safety*, *69*, 96-105.

Madanat, S. (1993). Optimal infrastructure management decisions under uncertainty. *Transportation Research Part C: Emerging Technologies*, *1*(1), 77-88.

Martin, R. (2011). Regional economic resilience, hysteresis and recessionary shocks. *Journal of economic geography*, *12*(1), 1-32.

Masoomi, H., and van de Lindt, J. W. (2019). Minimum Performance Targets for the Built Environment based on Community-Resilience Objectives, *13th International Conference on Applications of Statistics and Probability in Civil Engineering (ICASP13), Seoul, South Korea.* https://doi.org/10.22725/ICASP13.051

Masoomi, H. (2018). A resilience-based decision framework to determine performance targets for the built environment (Doctoral dissertation, Colorado State University).

Masoomi, H., and van de Lindt, J. W. (2018a). Restoration and functionality assessment of a community subjected to tornado hazard. *Structure and Infrastructure Engineering*, 14(3), 275-291.

Masoomi, H., and van de Lindt, J. W. (2018b). Community-Resilience-Based Design of the Built Environment. *ASCE-ASME Journal of Risk and Uncertainty in Engineering Systems*, *Part A: Civil Engineering*, 5(1), 04018044.

Masoomi, H., van de Lindt, J. W., and Peek, L. (2018). Quantifying socioeconomic impact of a tornado by estimating population outmigration as a resilience metric at the community level. *J. Struct. Engineering*, 144(5), 04018034.

McAllister, T. (2013). Developing guidelines and standards for disaster resilience of the built environment: A research needs assessment *Gaithersburg, MD: US Department of Commerce, National Institute of Standards and Technology*, 1–142.

Medury, A., and Madanat, S. (2013). Incorporating network considerations into pavement management systems: A case for approximate dynamic programming. *Transportation Research Part C: Emerging Technologies*, *33*, 134-150.

Meidani, H., and Ghanem, R. (2015). Random Markov decision processes for sustainable infrastructure systems. *Structure and Infrastructure Engineering*, *11*(5), 655-667.

Mieler, M., Stojadinovic, B., Budnitz, R., Comerio, M., and Mahin, S. (2015). A framework for linking community-resilience goals to specific performance targets for the built environment. *Earthquake Spectra*, *31*(3), 1267-1283.

Miles, S. B., and Chang, S. E., (2003). Urban Disaster Recovery: A Framework and Simulation Model, MCEER Technical Report 03-0005, *Multidisciplinary Center for Earthquake Engineering Research*, Buffalo, NY.

Miles, S. B., and Chang, S. E. (2004). Foundations for modeling community recovery from earthquake disasters. *In Proceedings of the 13th World Conference on Earthquake Engineering*.

Miles, S. B., and Chang, S. E. (2006). Modeling community recovery from earthquakes. *Earthquake Spectra*, *22*(2), 439-458.

Nachlas, J. A. (2005). Reliability engineering: probabilistic models and maintenance methods. *Crc Press*.

National Research Council (US). Geotechnical Board, and Earthquake Engineering Research Institute. (1994). Practical lessons from the Loma Prieta earthquake: report from a symposium sponsored by the Geotechnical Board and the Board on Natural Disasters of the National Research Council: symposium held in conjunction with the Earthquake Engineering Research Institute...[et al.] *National Academies Press*.

Nilim, A. and El Ghaoui, L. (2005). Robust control of Markov decision processes with uncertain transition matrices. *Operations Research*, *53*(5), 780-798.

Nojima, N., and Kameda, H. (1992). Optimal strategy by use of tree structure for post-earthquake restoration of lifeline network system. *Proceedings of the 10th World Conference on Earthquake Engineering*, Balkema, Rotterdam, 5541–5546.

Nozhati, S., Ellingwood, B. R., and Mahmoud, H. (2019a). Understanding community resilience from a PRA perspective using binary decision diagrams. *Risk analysis*. https://doi.org/10.1111/risa.13321

Nozhati, S., Sarkale, Y., Ellingwood, B. R., Chong, E. K. P., and Mahmoud, H. (2019b). Near-optimal planning using approximate dynamic programming to enhance post-hazard community resilience management. *Reliability Engineering & System Safety*, *181*, 116-126. https://doi.org/10.1016/j.ress.2018.09.011

Nozhati, S., Rosenheim, N., Ellingwood, B. R., Mahmoud, H., and Perez, M. (2019c). Probabilistic framework for evaluating food security of households in the aftermath of a disaster. *Structure and Infrastructure Engineering*, DOI: 10.1080/15732479.2019.1584824

Nozhati, S., Ellingwood, B. R., Mahmoud, H., and van de Lindt, J. W. (2018a). Identifying and analyzing interdependent critical infrastructure in post-earthquake urban reconstruction. *In Proc. of the 11th Natl. Conference in Earthquake Eng. Los Angel., CA.*

Nozhati, S., Sarkale, Y., Chong, E. K. P., and Ellingwood, B. R. (2018b). Optimal Stochastic Dynamic Scheduling for Managing Community Recovery from Natural Hazards. *arXiv preprint arXiv:1812.10194*.

Nozhati, S., Sarkale, Y., Ellingwood, B. R, Chong, E. K. P., and Mahmoud, H. (2018c). A modified approximate dynamic programming algorithm for community-level food security following disasters. *In Proc. 9th Int. Congress Environ. Model. and Software (iEMSs 2018).*

Rinaldi, S. M., Peerenboom, J. P., and Kelly, T. K. (2001). Identifying, understanding, and analyzing critical infrastructure interdependencies. *IEEE Control Systems*, 21(6), 11–25.

O'rourke, T. D., and Jeon, S. S. (2000). Seismic zonation for lifelines and utilities. *In Proceedings of the sixth international conference on seismic zonation*. Palm Springs, CA.

Ouyang, M. (2014). Review on modeling and simulation of interdependent critical infrastructure systems. *Reliability engineering & System safety*, *121*, 43-60.

Ouyang, M., Dueñas-Osorio, L., and Min, X. (2012). A three-stage resilience analysis framework for urban infrastructure systems. *Structural safety*, *36*, 23-31.

Ouyang, M., and Fang, Y. (2017). A mathematical framework to optimize critical infrastructure resilience against intentional attacks. *Computer-Aided Civil and Infrastructure Engineering*, *32*(11), 909–929.

Ozdamar, L. (1999). A genetic algorithm approach to a general category project scheduling problem. *IEEE Transactions on Systems, Man and Cybernetics, Part C*, *29*(1):44–59.

Pant, R., Barker, K., Ramirez-Marquez, J. E., and Rocco, C. M. (2014). Stochastic measures of resilience and their application to container terminals. *Computers and Industrial Engineering*, 70, 183–194.

Papakonstantinou, K. G., and Shinozuka, M. (2014). Planning structural inspection and maintenance policies via dynamic programming and Markov processes. Part I: Theory. *Reliability Engineering and System Safety*, *130*, 202-213.

Penchansky, R. and Thomas, J. W. (1981). The concept of access: definition and relationship to consumer satisfaction. *Medical care, 19(2)*, 127–140.

Pfefferbaum, B. J., Reissman, D. B., Pfefferbaum, R. L., Klomp, R. W., and Gurwitch, R. H. (2008). Building resilience to mass trauma events. *In Handbook of injury and violence prevention*, *Springer, Boston, MA*, 347-358.

Powell, W. B. (2007). Approximate Dynamic Programming: Solving the curses of dimensionality. *John Wiley & Sons*.

Presidential Policy Directive (PPD), (2013). Critical Infrastructure Security and Resilience. PPD-21, Released February 12, 2013. Available at: http://www.whitehouse.gov/the-press-office/2013/02/12/presidential-policy-directive-critical-infrastructure-security-and-resil, Accessed March 07, 2018.

Ragi, S., Mittelmann, H. D., and Chong, E. K. (2015). Directional sensor control: Heuristic approaches. *IEEE Sensors Journal*, *15*(1), 374-381.

Rose, A., and Liao, S. Y. (2005). Modeling regional economic resilience to disasters: A computable general equilibrium analysis of water service disruptions. *Journal of Regional Science*, *45*(1), 75-112.

Sarkale, Y., Nozhati, S., Chong, E. K. P., Ellingwood, B. R., and Mahmoud, H. (2018). Solving Markov decision processes for network-level post-hazard recovery via simulation optimization and rollout. *In 2018 IEEE 14th International Conference on Automation Science and Engineering (CASE)*. 906-912.

Semseler, R. G. and Akel, T. (2010). 2010 Urban water management plan 2010. Retrieved from http://www.ci.gilroy.ca.us/265/Water-Management-Plan.

Seyyed Alangi, S. H., Nozhati, S., and Vazirizade, S. M. (2018). Critical reliability slip surface in soil slope stability analysis using Monte Carlo simulation method. *International Journal of Structural Integrity*, 9(2), 233-240.

Smilowitz, K., and Madanat, S. (2000). Optimal inspection and maintenance policies for infrastructure networks. *Computer‐ Aided Civil and Infrastructure Engineering*, *15*(1), 5-13.

Sun, W., and Zeng, A. (2017). Target recovery in complex networks. *European Physical Journal B*, *90*(1), 10, https://doi. org/10.1140/epjb/e2016-70618-0.

Tesauro, G., and Galperin, G. R. (1997). On-line policy improvement using Monte-Carlo search. *In Advances in Neural Information Processing Systems*. 1068-1074.

Tversky, A., and Kahneman, D. (1992). Advances in prospect theory: Cumulative representation of uncertainty. *Journal of Risk and uncertainty*, *5*(4), 297-323.

Ulusan, A., and Ergun, O. (2018). Restoration of services in disrupted infrastructure systems: A network science approach. *Plos One*, *13*(2), e0192272.

United States Department of Agriculture (2017). Definitions of food Security. Food Security in the U.S. *United States Department of Agriculture*.

United States Department of Agriculture (2010). FNS 2008 and 2009 disaster lessons learned and best practices report. *United States Department of Agriculture*. Retrieved from http://www.fns.usda.gov/sites/default/files.2008-2009-lessons.pdf

U.S. Census 2010 SF1, DP-1 (2010a). *United States Census Bureau*. Retrieved from https://factfinder.census.gov/

U.S. Census 2010 SF1, QT-P2 (2010b). *United States Census Bureau*. Retrieved from https://factfinder.census.gov/

Vale, L. J. (2014). The politics of resilient cities: whose resilience and whose city. *Building Research and Information*, *42(2),* 191–201.

Vlacheas, P., Stavroulaki, V., Demestichas, P., Cadzow, S., Ikonomou, D., and Gorniak, S. (2013). Towards end-to-end network resilience. *International Journal of Critical Infrastructure Protection*, *6*(3), 159-178.

Vogus, T. J., and Sutcliffe, K. M. (2007). Organizational resilience: towards a theory and research agenda. *In 2007 IEEE International Conference on Systems, Man and Cybernetics*, 3418-3422.

Von Neumann, J., and Morgenstern, O. (2007). Theory of games and economic behavior (commemorative edition). *Princeton university press*.

Xiao, Y., and Van Zandt, S. (2012). Building community resiliency: Spatial links between house- hold and business post-disaster return. *Urban Studies, 49(11)*, 2523–2542.

Xie, L., Tang, J., Tang, H., Xie, Q., and Xue, S. (2012). Seismic fragility assessment of transmission towers via performance-based analysis. *In Proceedings of the 15th world conference on earthquake engineering, Lisbon, Portugal*.

Xu, N., Guikema, S. D., Davidson, R. A., Nozick, L. K., Cagnan, Z., and Vaziri, K. (2007). Optimizing scheduling of post-earthquake electric power restoration tasks. *Earthquake Engineering and Structural Dynamics*, *36*(2), 265–284.

Yang, X. (2008). Introduction to mathematical optimization, From Linear Programming to Metaheuristic*s*. *Cambridge International Science Publishing.*

Youn, B. D., Hu, C., and Wang, P. (2011). Resilience-driven system design of complex engineered systems. *Journal of Mechanical Design*, *133*(10), 101011.

Zhang, W., and Wang, N. (2017). Bridge network maintenance prioritization under budget constraint. *Structural safety*, *67*, 96-104.

Zimmerman, R., Zhu, Q., and Dimitri, C. (2016). Societal issues in adopting life-cycle concepts within the political system. *Journal of Environmental Studies and Sciences*, 6(1), 50-61.